# UNIVERSITÉ DE STRASBOURG

UNIVERSITÉ DE STRASBOURG

*ÉCOLE DOCTORALE Physique / Chimie-Physique (ED 182)*

**Institut Charles Sadron**

# THÈSE présentée par :

## LONGO Johan

soutenue le : **25 septembre 2014**

pour obtenir le grade de : **Docteur de l'université de Strasbourg**

Discipline/ Spécialité : Physique / Chimie-Physique

---

Design of biomechanocatalytic surfaces:

Modulations of enzymatic activity through

macromolecular conformational changes

---

**THÈSE dirigée par :**
  M. SCHAAF Pierre                Professeur, université de Strasbourg

**EXAMINATEUR :**
  Mme. BEGIN-COLIN Sylvie         Professeur, université de Strasbourg

**RAPPORTEURS :**
  Mme. AUZELY Rachel              Professeur, université Joseph Fourier Grenoble
  M. FRANCIUS Grégory             Chargé de recherche CNRS

# Elaboration de surfaces biologiquement actives répondant à un stimulus mécanique

## Contexte :

Depuis plusieurs années, une nouvelle génération de matériaux appelés « matériaux intelligents » et définis par leur capacité à s'adapter à leur environnement s'est intensivement développée. Des systèmes sensibles à différents stimuli tel que le pH, la lumière, la force ionique ou encore la température ont été rapportés. Un de ces stimuli peut aussi être un stress mécanique connu pour être impliqué dans une multitude de processus naturels. Ainsi, l'activité des protéines ou des enzymes est fortement dépendante de leurs conformations. Des modifications de leurs structures sont donc capables d'induire des modulations/changements de celle-ci. Un exemple de cette propriété est la perte de fluorescence d'une GFP (Green Fluorescent Protein) lorsque sa structure en « Beta barrel » est déformée. Ce comportement pouvant être expliqué par la modification de l'environnement du chromophore présent qui est directement relié à la réponse en fluorescence de la protéine.

## Présentation :

L'objectif de mon projet de thèse est le développement de surfaces mécano-responsives, c'est-à-dire de surfaces dont les propriétés sont modulées ou induites par l'application d'un stimulus mécanique tel que l'étirement. De telles surfaces transforment un stress mécanique en un signal chimique. Pour ce faire nous essayons de mimer les processus existant dans la nature, le plus souvent basés sur des changements de conformation de protéines. Nous cherchons à atteindre ce but en greffant de façon covalente des protéines ou des enzymes sur un substrat étirable ou en les incorporant à une matrice polymère réticulée. Etirer le substrat ou le réseau polymère devrait induire un changement conformationnel des protéines et dans le cas des enzymes induire un changement d'activité catalytique. Dans le but d'établir une preuve de concept, nous nous sommes d'abord intéressés au greffage d'une protéine en surface d'un matériau. Nous avons utilisé une Green Fluorescent Protein (GFP) modifiée chimiquement afin de pouvoir la coupler à un matériau polymère (projet 1) et d'étudier sa réponse spectrale sous contrainte. Dans un second temps nous nous sommes focalisés sur

l'utilisation d'enzymes à la place des protéines afin d'élaborer un matériau dont l'activité enzymatique peut être modulée par étirement (projet 2 A et B).

**Projet 1 : Modification de la réponse spectrale d'une Green Fluorescent Protein (GFP) sous contrainte mécanique**

Une GFP spécifiquement modifiée par des groupes azides (conçue et synthétisée par génie génétique – par Chunyan Yao de l'équipe du Docteur Schiller de l'université de Freiburg) est utilisée lors de notre étude. Ces modifications permettent l'ancrage covalent en deux endroits définis de la biomacromolécule au réseau polymérique pour conduire à une déformation optimale sous étirement (figure 1).
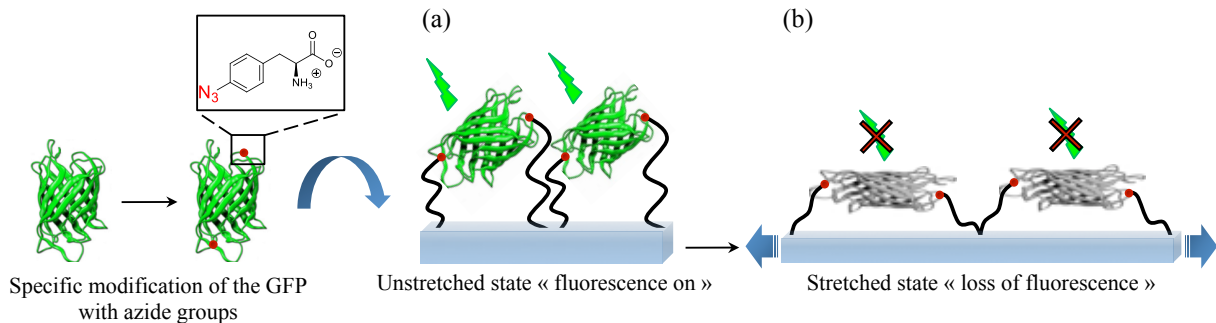


*Figure 1: Représentation schématique de la surface méchano-responsive. Au repos (a), les GFP spécifiquement greffées sur le substrat présentent une fluorescence. Sous contrainte (b), la structure tridimensionnelle des protéines est modifiée engendrant une perte de leur réponse en fluorescence.*

Lors de notre étude nous avons élaboré un substrat étirable, homogène et fonctionnalisé à base de silicone. Nous avons greffé de manière covalente des GFP sur sa surface en respectant des contraintes inhérentes à la manipulation de biomolécules tels qu'une température basse, un pH ajusté et l'utilisation de réactions chimiques préservant l'intégrité des protéines, mais aussi celle du matériau.

**Résultats :**

a) **Fonctionnalisation du substrat PDMS pour le greffage covalent de la GFP**

De part leurs propriétés visco-élastiques, des substrats en silicones ou polydimethylsiloxane (PDMS) ont été préparés et modifiés en surface lors de cette étude. Dans le but de créer différents groupes chimiques à la surface des substrats en PDMS une activation du PDMS basée sur un traitement UV-Ozone à été développée. Cette étape qui permet de rendre la

surface hydrophile grâce à l'introduction de groupements hydroxyles et carboxyliques est suivie d'une fonctionnalisation avec un composé homobifonctionnel de type bis-isocyanate, le methylene diphenyl diisocyanate (MDI). Des chaines de polyéthylène glycols (PEG) présentant un groupe alcyne et une fonction amine à chacune de leurs extrémités, sont ensuite greffées de façon covalente et irréversible sur la surface de PDMS modifiée par les groupements MDI. Ces brosses de PEG en surface confèrent un caractère non-adsorbant au matériau et permettent le couplage des GFP par chimie « click ». La fonctionnalisation du matériau est schématisée en figure 2.
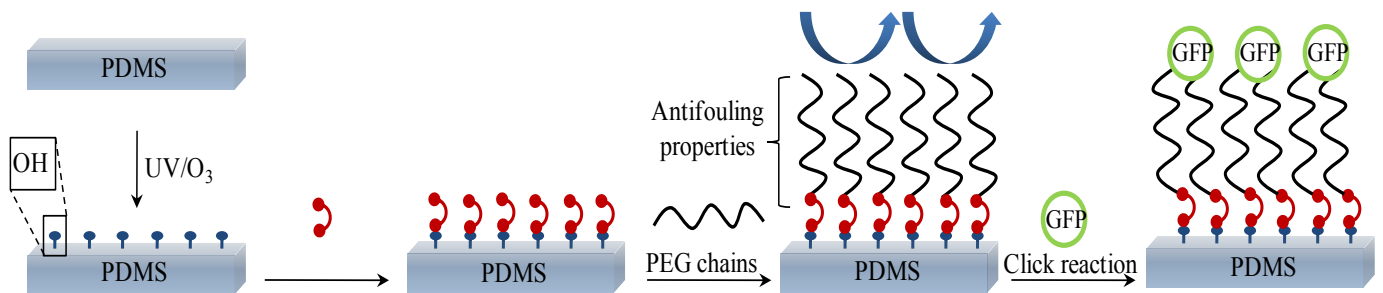


*Figure 2: Représentation schématique de la fonctionnalisation de surface et du couplage de la GFP*

### b) Couplage des GFP par « chimie click »

La GFP modifiée fournie par notre collaboration à Freiburg, possède deux groupements azides placés à des positions opposées sur sa structure tridimensionnelle (figure 3).
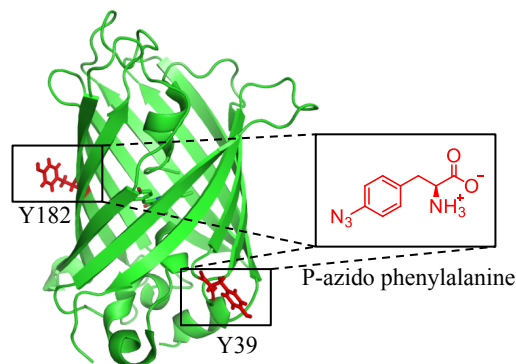


*Figure 3: Green Fluorescent Protein (GFP) spécifiquement modifiée par insertion d'un amino-acide non naturel; la p-azido-phénylalanine contenant un groupement azide.*

Le choix d'un tel groupement chimique est justifié par la possibilité d'utiliser une réaction de couplage « click » telle qu'une cyclo-addition alcyne/azide de Huisgen. En effet, ce type de couplage permet d'être réalisé dans des conditions « douces », qui évitent l'altération de la protéine. Le greffage effectif de la GFP est confirmé par des mesures de fluorescence de la

surface. En effet, en l'absence de groupements azides sur la GFP, nous avons montrés qu'aucune fluorescence n'est mesurée puisqu'il n'y a pas de greffages possibles.

### c) Tests d'étirement mécanique

Afin de discriminer entre la diminution de fluorescence due à la baisse de densité des chromophores sous étirement de celle due à la déformation des protéines, les tests d'étirements ont été réalisés sur deux GFP modifiées différemment: des GFP mono-fonctionnalisées (ne présentant qu'une seule fonction $N_3$), pouvant se lier à la surface sans pouvoir être étirées lors de l'étirement du matériau, ainsi que des GFP bi-fonctionnalisées potentiellement sensibles à l'étirement. Ces protéines ont été greffées sur des surfaces PDMS qui ont ensuite été étirée jusqu'à 30% et leur fluorescence mesurée. La réversibilité des systèmes a été vérifiée en relaxant les surfaces à leur état initial après étirement. Les résultats de ces tests sont résumés dans les figures 4 et 5.
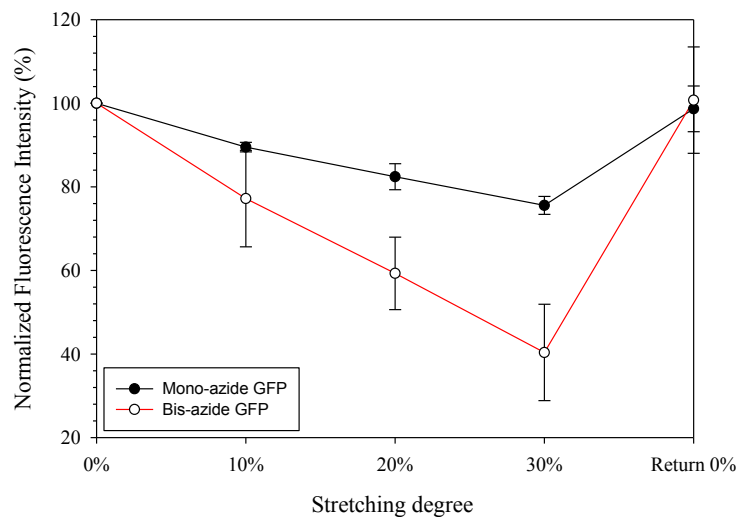


*Figure 4: Mesures de fluorescence à différents degrés d'étirement d'un substrat PDMS fonctionnalisé à l'aide de GFP monofonctionnalisées (courbe noire) et de GFP bifonctionnalisées (courbe rouge).*

Une diminution de fluorescence sous étirement est observée pour les deux types de GFP utilisées. Cependant, lors d'un étirement de 30% de la longueur initiale du matériau, la décroissance de fluorescence de la GFP modifiée en deux points est d'environ 60% par rapport à sa fluorescence initiale tandis que celle de la mono GFP est de 20%. Dans le cas de la GFP modifiée avec un seul groupement azide, cette diminution de fluorescence s'explique par la diminution de la densité de GFP en surface lors de l'étirement. La décroissance importante de la fluorescence mesurée de la GFP bi-fonctionnalisée sous étirement est attribuée à la déformation de sa structure 3D, conduisant à une diminution de sa fluorescence.
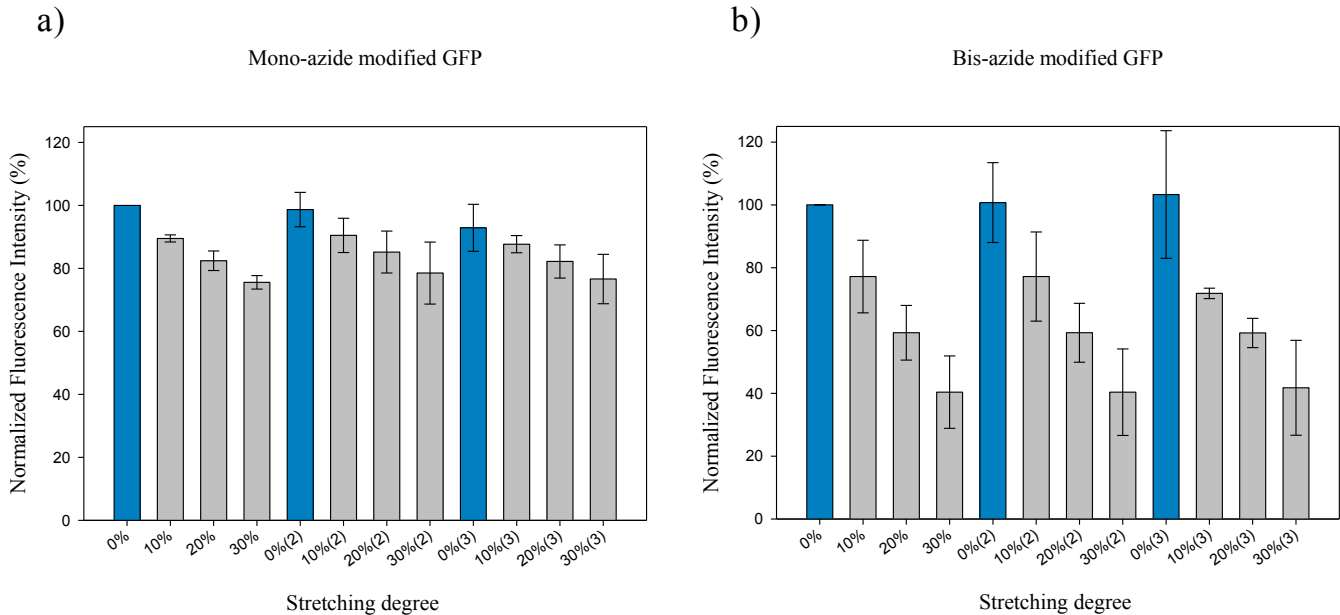
*Figure 5 : Intensité de fluorescence normalisée en fonction du degré d'étirement du substrat pour des GFP monofonctionnalisées a) et bifonctionnalisées b).*

Il est à noter que l'on a observé une réversibilité de ce système lors du retour des échantillons à leur état initial, pour au moins deux cycles d'étirement – relâchements.

## Elaboration de films enzymatiquement actifs méchano-sensibles

Après avoir démontré la possibilité de déformer des macromolécules par étirement de leur substrat, nous nous sommes intéressés à l'élaboration d'un matériau possédant une activité enzymatique modulable par l'application d'un stress mécanique. Dans cette optique, nous nous sommes intéressés à deux stratégies de fonctionnalisation différentes reposant sur le couplage d'une enzyme dans un réseau polymère (figure 6).
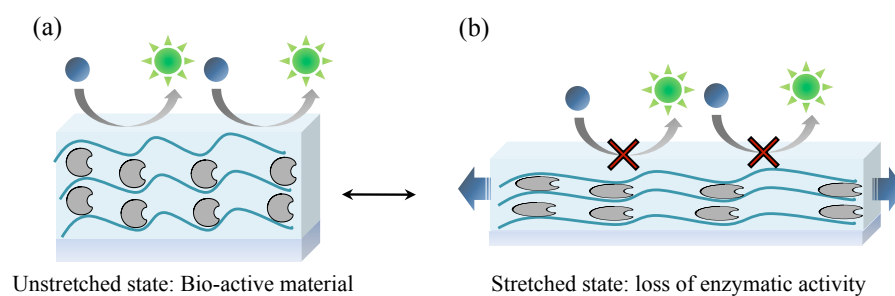


*Figure 6: enzymes couplées à une matrice polymère. (a) état non étiré, matériau catalytique actif et (b) état étiré, déformation de l'enzyme, perte ou diminution de l'activité catalytique*

La première est basée sur l'incorporation d'enzymes en l'occurrence de β-galactosidase à l'intérieur d'une matrice polymère préconstruite. Dans la seconde, un film couche-par-couche alternant un polymère et une enzyme (alkaline phosphatase) a été construit.

# Projet 2 : Incorporation d'enzymes dans une matrice polymère préconstruite

De part ses propriétés visco-élastiques, une matrice réticulée constituée de couches de poly-(L-lysine) (PLL) préalablement modifiées par des groupements thiopyridyls alternant avec des couches d'acide hyaluronique (HA) a dans un premier temps été construite sur un substrat silicone. L'enzyme modifiée par des groupes maléimides est ensuite incorporée à la multicouche et couplée de façon covalente à celle-ci (figure 7).
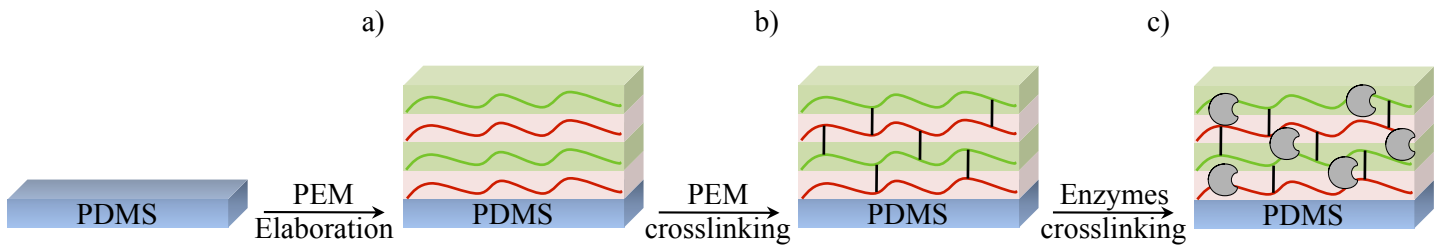


*Figure 7: Représentation schématique de l'élaboration de la matrice polymère: a) élaboration d'une multicouche de PLL/HA. b) Réticulation de la matrice. c) Insertion puis couplage covalent d'enzymes au sein de la matrice polymère*

## Résultats :

### a) Construction de la matrice

La matrice PLL/HA a été construite selon la technique dite de couche-par-couche consistant en un dépôt alterné d'un polycation (PLL) et d'un polyanion (HA) et conduisant à l'élaboration d'un film multicouche (figure 8).
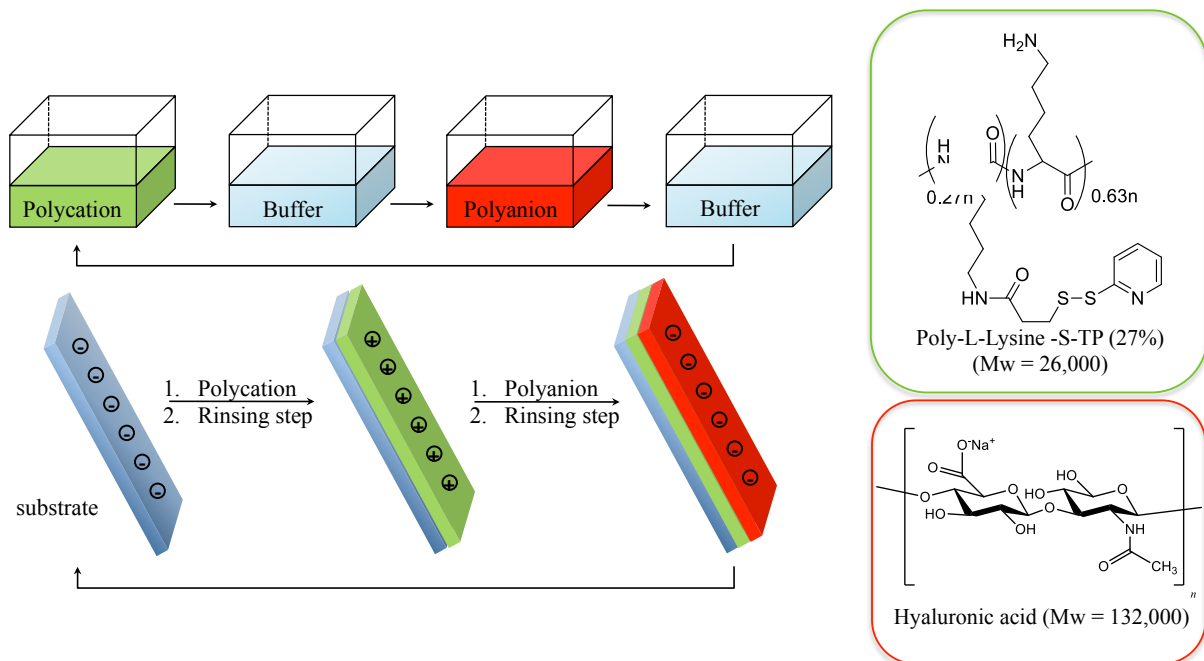


*Figure 8 : Représentation schématique de la préparation d'une multicouche de polyélectrolytes. Le substrat est alternativement immergé dans une solution de polycations (poly-L-lysine) et de polyanions (acide hyaluronique) conduisant à l'élaboration du film.*

Ce film a ensuite été réticulé en utilisant une réaction de couplage entre les groupements amine de la PLL et les fonctions acide carboxylique du HA, formant des liaisons amides. Des réactifs de type carbodiimide ont étés utilisés (figure 9).
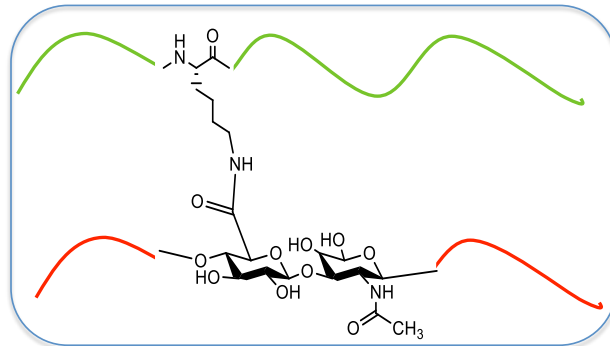


*Figure 9 : Création d'une liaison amide par réaction de l'amine de la poly-L-lysine (en vert) avec un acide carboxylique de l'acide hyaluronique (en rouge) en présence d'EDC/NHS.*

### b) Diffusion et couplage de la β-galactosidase

Une fois réticulée, la matrice polymère est mise en contact avec une solution de β-galactosidase modifiée par des groupements maléimides pour que l'enzyme diffuse dans le film. Un agent réducteur est utilisé pour déprotéger les fonctions thiopyridyl sur la PLL et libérer des groupements thiols. Par réaction dite « click » entre les groupements maléimides de la β-galactosidase et les thiols de la multicouche réticulée, l'enzyme se lie au film (figure 10).
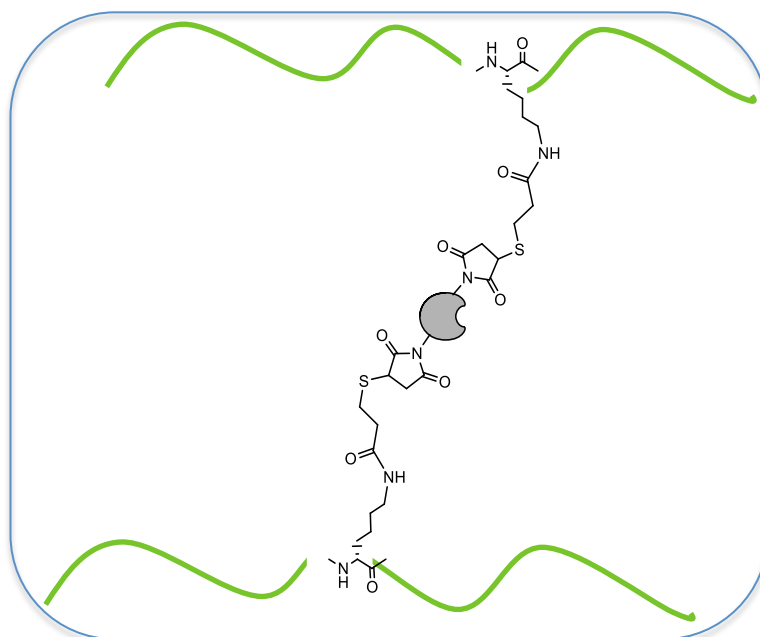


*Figure 10: Réaction de couplage entre la béta-galactosidase fonctionnalisée par des groupements maléimides et les groupements thiopyridines présents sur la poly-L-lysine modifiée en présence de TCEP, un agent réducteurs.*

Le film résultant présente une activité catalytique, ce qui confirme l'intégrité de l'enzyme utilisée.

### c) Tests d'étirement

Les films sont mis en contact avec la fluoresceine di-beta-D-galactopyranoside (FDG), un substrat spécifique de la β-galactosidase et non fluorescent. L'hydrolyse très rapide de la FDG produit de la fluoresceine aisément détectable et mesurable (figure 11).
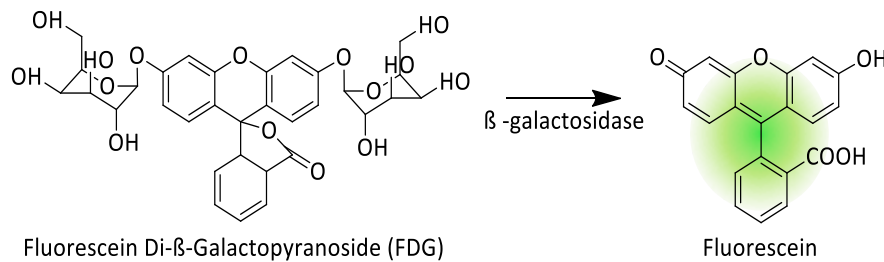


Fluorescein Di-ß-Galactopyranoside (FDG)    ß -galactosidase    Fluorescein

*Figure 11: Transformation de la FDG en fluorescéine sous l'action de la béta-galactosidase*

L'activité des films est suivie par fluorescence pour différents degrés d'étirement (figure 12).
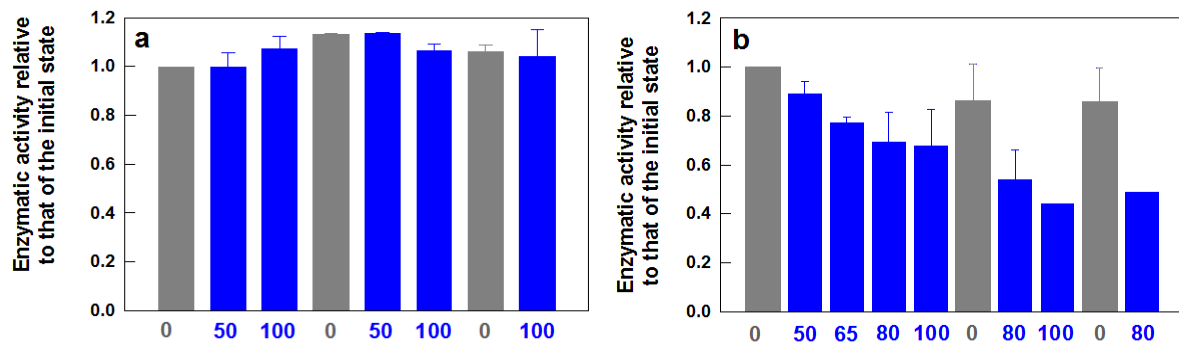


*Figure 12: Suivi de l'activité enzymatique d'une matrice polymère PLL/HA à différents degrés d'étirement pour (a) une enzyme libre non réticulée au réseau et (b) une enzyme couplée covalemment à la matrice.*

Quand l'enzyme est liée au réseau, une décroissance de l'activité enzymatique est mesurée lors de l'étirement des films (figure 12). L'activité du film décroit avec le degré d'étirement appliqué. Par contre, l'utilisation d'une enzyme non modifiée, simplement enfouie dans le film multicouche, ne conduit pas à une diminution de l'activité enzymatique du film lorsque celui-ci est étiré. Le changement de l'activité de le β-galactosidase est attribuée aux contraintes mécaniques appliquées le film.

La seconde stratégie développée consiste en l'élaboration d'un film multicouche à base d'alginate, un polyanion, modifié par des groupements catéchol et d'alkaline phosphatase qui servira de polycation et d'enzyme modèle. Le film ainsi construit et réticulé doit former une matrice de type enzyme/polymère (figure 13).
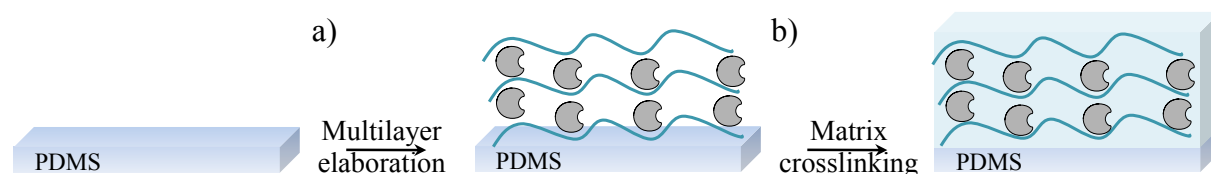


Figure 13: Représentation schématique de l'élaboration de la matrice polymère: a) élaboration d'une multicouche de aginate-catéchol / alkaline phosphatase. b) Réticulation de la matrice.

## Résultats :

### a) Construction du film multicouche

Comme précédemment le film est élaboré selon la technique dite de couche-par-couche consistant en un dépôt alterné d'un polyanion (HA) (figure 14) et d'un polycation, ici l'enzyme chargée négativement.
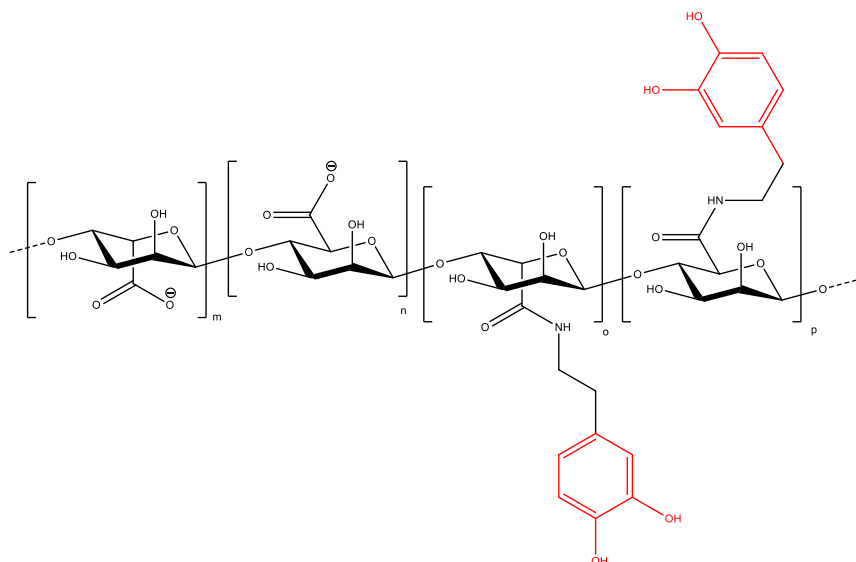


Figure 14: Alginate modifié par des fonctions catéchol (en rouge)

Le film est ensuite réticulé à l'aide d'un oxydant, le periodate de sodium. Les groupements catéchols présents sur l'alginate sont alors oxydées en quinones, ce qui permet aux fonctions amines (nucléophiles) présents sur l'enzyme de s'additionner en 1,4 sur le cycle aromatique pour former une liaison covalente (figure 15).
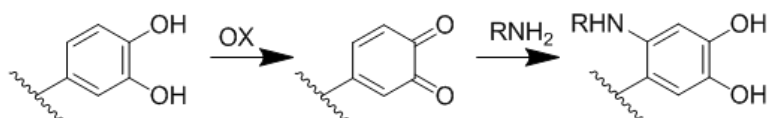


*Figure 15: Réaction d'addition 1,4 de Mickael entre les fonctions quinones de l'alginate modifié et les amines présentes sur l'alkaline phosphatase.*

### b) Tests d'étirement

Les films sont ensuite mis en contact avec de la para-nitrophenylphosphate (PNP), un substrat spécifique de l'alkaline phosphatase devenant jaune après hydrolyse enzymatique (figure 16).



Para-nitrophenylphosphate        Para-nitrophenolate

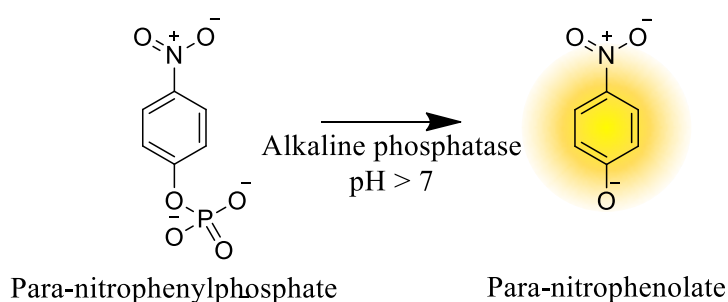*Figure 16: Transformation du para-nitrophenylphosphate (incolore) en para-nitrophénolate (coloré) sous l'action de l'alkaline phosphatase.*

L'activité des films est ainsi suivie par UV pour différents degrés d'étirement. Un contrôle à l'aide d'un film polymère/enzyme non réticulé est réalisé. La réversibilité des systèmes a été vérifiée en relaxant les surfaces à leur état initial après étirement.
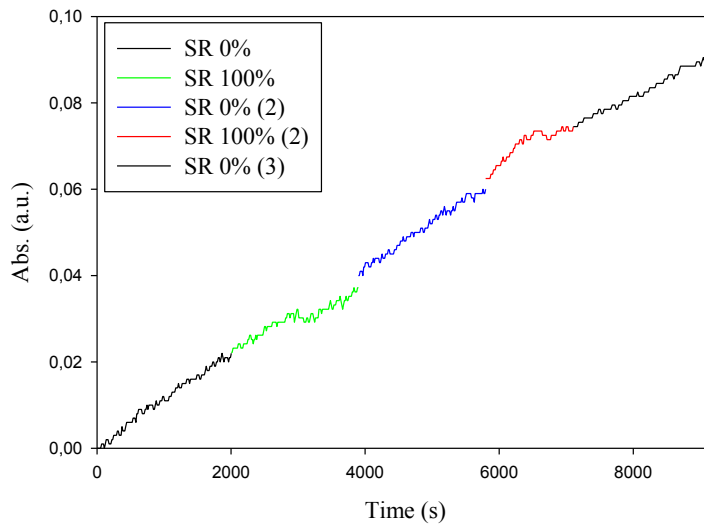
*Figure 17: Suivi de l'activité enzymatique d'une matrice polymère / enzyme pour différents degrés d'étirement (SR = Stretching ratio).*

Aucune différence d'activité des films au repos et à l'état étiré n'a été détectée lors des tests. Ces résultats peuvent s'expliquer par la robustesse structurale de l'alkaline phosphatase. Des tests de vieillissement ont permis de montrer une meilleure stabilité dans le temps de l'alkaline phosphatase présente dans les films polymères par rapport à l'enzyme naturelle en solution. De plus des tests de lyophilisation des films ont été effectués et montre un maintient de l'activité enzymatique après réhydratation de ceux-ci (figure 18).



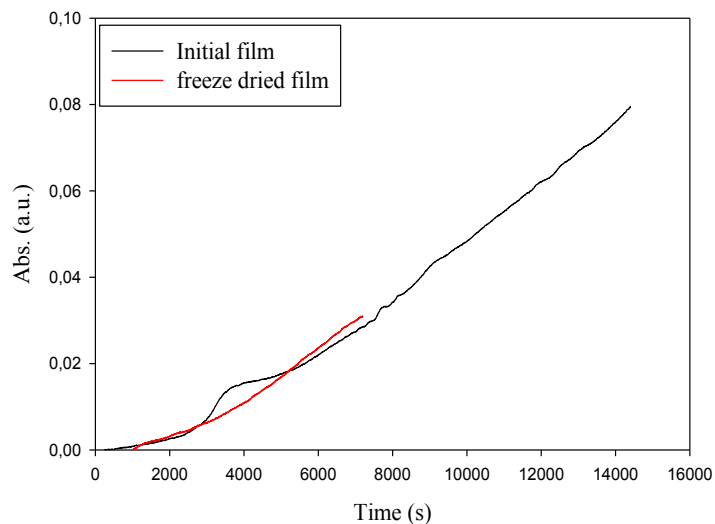*Figure 18: Suivi de l'activité enzymatique d'une matrice polymère / enzyme dans un état initial (t = 0, courbe noire) et après lyophilisation et réhydratation (t = 21 jours, courbe rouge).*

**Conclusion :**

Lors de ces travaux de thèse nous nous sommes focalisés sur la conception de matériaux dit intelligents, et plus précisément de films polymères, fonctionnalisés à l'aide de biomacromolécules, sensibles à une contrainte mécanique. Nous avons ainsi, dans un premier temps, démontré la possibilité d'élaborer des films homogènes possédant une activité biologique. Cette propriété à été obtenue par l'insertion et le couplage covalent d'enzymes ou de protéines au sein de substrats étirables en conditions dites douces afin de préserver leur intégrité. Ainsi, différents types de couplages chimiques en milieu biologique ont été développé et mis en œuvre dans ces travaux. Le caractère mécano-répondant des différents films a ensuite été développé. En effet, il a été possible de moduler l'activité biologique ou enzymatique de différents matériaux en le soumettant à une contrainte mécanique, dans ce cas un étirement longitudinal. Il a de plus été démontré que ces changements de propriétés étaient réversibles lors de la relaxation du matériau, et présents même après plusieurs cycles d'étirement. Durant ces travaux nous avons donc mis en avant une relation directe entre l'application d'une force sur un système et son changement de propriété à l'échelle moléculaire, et plus précisément sur une modification de la structure tridimensionnelle des biomacromolécules le composant.

La suite du projet s'inscrit dans l'extension de ce concept et son adaptation à différents systèmes enzymes/polymères ou à des systèmes complexes tels que multi-enzymes.

# Table of contents

## Chapter 1: Bibliography overview

## Chapter 2: Materials and Methods

## Chapter 3: Modification of the Green Fluorescent Protein spectral response under mechanical constraints

# Chapter 4: Catalytic mechano-responsive polyelectrolyte multilayers based on conformational changes of enzymes

# Chapter 5: Design of mechano-responsive materials based on multilayer films made from alginate-catechol and alkaline phosphatase

## Conclusion and outlook                                                        141

## Annexes

# Abbreviations

*Polyelectrolytes and polymers*

| | |
|---|---|
| AC/ Alg-cat | Alginate modified with catechol moieties |
| HA | Hyaluronic acid |
| PAH | Poly(allylamine) hydrochloride |
| PDADMA | Poly(diallyldimethylammonium) |
| PDMS | Poly(dimethylsiloxane) |
| PEG | Poly(ethylene glycol) |
| PLL | Poly(L-lysine) |
| PLL-FITC | Poly(L-lysine) labeled with fluorescein |
| PLL-S-TP | Poly(L-lysine) modified with pyridyl disulfide |
| PSS | Polystyrene sulfonate |

*Proteins, Enzymes and enzymatic substrates*

| | |
|---|---|
| AP/ALP | Alkaline phosphatase |
| β-Gal | β-Galactosidase |
| β-Gal-FITC | β-Galactosidase labeled with fluorescein |
| β-Gal-mal | β-Galactosidase-maleimide |
| β-Gal-malFITC | β-Galactosidase-maleimide labeled with fluorescein |
| FDG | Fluorescein di(β-D-galactopyranoside) |
| FDP | Fluorescein diphosphate |
| GFP | Green fluorescent protein |
| PNP | Para-nitrophenylphosphate |
| PN | Para-nitrophenolate |

## Molecules, reagents and buffer solutions

| | |
|---|---|
| DIDS | 4,4'-Diisothiocyano 2,2'stilbenedisulfonic acid |
| EDC | N-(3-Dimethylaminopropyl)-N'-ethylcarbodiimide hydrochloride |
| FITC | Fluorescein isothiocyonate |
| L-DOPA | 3,4-dihydroxy-L-phenylalanine |
| MDI | 4,4'Methylenebis(phenyl)isocyanate |
| NHS | N-Hydroxysuccinimide sodium salt |
| PBS | Phosphate buffered saline |
| PDIT | 1,4-Phenylene diisocyanate |
| Strepta-FITC | Streptavidin labeled with fluorescein |
| TCEP | Tris(2-carboxyethyl)phosphine hydrochloride |
| THPTA | Tris(3-hydroxypropyltriazolylmethyl)amine |
| TRIS | Tris(hydroxymethyl)aminomethane |

## Materials and methods

| | |
|---|---|
| AFM | Atomic force microscope |
| CA | Contact angle |
| CLSM | Confocal laser scanning microscope |
| CuAAC | Copper(I)-catalyzed Azide-Alkyne Cycloaddition (CuAAC) |
| FTIR | Fourier transform infrared spectroscopy |
| LbL | Layer by layer |
| NMR | Nuclear magnetic resonance |
| PEM | Polyelectrolyte multilayers |
| QCM-D | Quartz crystal microbalance |
| UVO | Ultraviolet ozone |

# General introduction

Since many years, a new generation of materials called « smart materials » and defined by their capacity to adapt to their environment is intensively developed. Systems sensitive to different stimuli such as pH, light, ionic strength or solvent polarity have been reported. One of these stimuli can also be a mechanical force which is involved in many reactions in nature such as cells adhesion and proliferation, tissues growing or even plants developments.

The aim of my thesis was dedicated to the design and the elaboration of mechano-responsive materials and more precisely, materials that transform a stretching constraint into a chemical signal. For this purpose we try to mimick physical processes used by nature, namely mechanically induced protein conformational changes. We planned to achieve this goal by covalent grafting of proteins or enzymes onto stretchable substrates or incorporating them into cross-linked polymer networks. Stretching the substrate or the network should induce protein conformational changes leading to modifications of their properties. In order to make a proof of concept, we first intended to "visualize" conformational changes of proteins that respond physically to mechanical constraints such as stretching. Thus, we started by grafting green fluorescent proteins (GFP) chemically modified onto a surface (chapter 3). Furthermore, we focused on the use of enzymes instead of proteins to develop materials whose catalytic activity can be modulated by stretching (chapters 4 and 5).

The 1st chapter of my thesis introduces the concept of mechano-transduction and its implementation in mechano-sensitive materials field. A general description of the state of art is presented with the contribution of our team and of external groups using different approaches to elaborate various mechano-responsive materials.

The 2nd chapter reports in details the reagents and methods used during my work. In order to make an easier comprehension of the different projects presented, experimental chapters are treated individually. A specific part is dedicated to the presentation and explanation of the physico-chemical techniques of characterization.

The 3$^{nd}$ chapter presents the elaboration of a mechano-sensitive surface functionalized with green fluorescent proteins (GFP). After explaining the different modification steps of the substrate leading to the binding of specifically modified GFP by click chemistry as a monolayer, fluorescence response of the material was monitored under stretching. This work highlights the possibility to transfer macromolecular forces induced by stretching into changes in the three dimensional structure of a protein.

In the 4$^{th}$ chapter, *beta-galactosidase* was used in order to elaborate a catalytic active material. To increase the number of immobilized enzymes inside the material, and thus increasing its response to the stretching, a new strategy based on the elaboration of a polymeric matrix loaded with the enzymes was developed. This chapter was performed within the collaboration of César Rios a PhD student of our group.

The 5$^{th}$ chapter is dedicated to the development of a new type of material based on a crosslinked multilayer film buildup made of alternated depositions of enzymes and activated polymers modified with catechol moieties. The enzymes representing in this case an integral part of the material structure, this new architecture is elaborated to increase the sensitivity of the material to stretching. The study of the film elaboration and stretching experiments are presented.
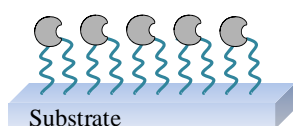
Chapter 3: Elaboration of a mechano-sensitive surface made of proteins
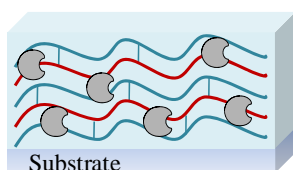
Chapter 4: Mechano-responsive enzymatically active polymeric matrix
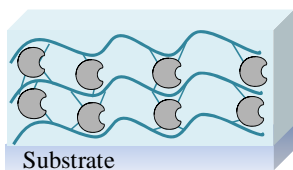
Chapter 5: Enzymatically active PEM structure development

*Schematic representation of the three projects developed in this thesis work.*

<table>
<tr><td>Chapter</td><td>1</td></tr>
</table>

# Bibliography overview

## Contents

## 1.1. Introduction

Mechanotransduction processes are mechanismes in which a mechanical force is transformed into a signal. We are interested in this thesis in developing materials that respond chemically to a mechanical stress. The topic of mechanotransductionis a rapidly growing field of study which covers biology, chemistry and material science. From a chemical point of view there are clearly two possible approaches to tackle this subject: One approach is to investigate the effect of a mechanical force on the behavior of covalent bonds and its possible applications in material science. This approach is the most widely used. It was initiated in particular by the groups of Moore and Sotos[1] who showed that a mechanical force can initiate chemical modifications in molecules, usually resulting in a color change in material regions of high strain.Poly(methyl acrylate) elastomeric matrices copolymerized with methyl methacrylate to form poly(methyl methacrylate) incorporating spiropyrans represent one well-known example of such materials. Recently, using a *gem*-dichlorocyclopropanated indene incorporated into a cross-linked poly(methylacrylate) material, the group of Moore reported a new material which under compression releases protons (mechanogenerated acid)[2]. Many more chemo-mechano-responsive materials have been developed which are, similarly, all based on an intra-molecular reaction usually resulting in a color change of the material. A second approach is to mimic the mechanotransduction processes used by nature to transform a mechanical signal into a chemical one. Such processes are in particular used by cells which sense the mechanical properties of their environment with widespread consequence on their fate. There at least two mechanisms used by cells to transform a mechanical force into a chemical signal : one is based on membrane channels whose properties change when the membrane is under the influence of a mechanical stress and the other is based on conformational changes of proteins that are submitted to a mechanical force[3]. One of the first examples of this type of protein that has been extensively studied is that of fibronectin, an adhesion protein present in the extracellular matrix[4]. It is the approach used by nature that we try to mimic to create chemo-mechano-responsive materials. It is these kinds of processes that our group is trying to mimic for the development of chemo-mechano-transduction materials. In this introduction I will first review the results obtained by our group in this domain in order to present my contribution in this perspective. Because my goal will be to develop systems that are mechanoresponsive by stretched induced conformational changes of

proteins deposited on or incorporated in materials, as it is the case for fibronectin, I will then review the results published so far in this field.

## 1.2. Towards chemo-mechano-responsive materials: contributions from our group

### 1.2.1. Polyelectrolyte multilayers

The group in which I perform my Ph.D. is active since 2000 in the development of polyelectrolyte multilayers. Polyelectrolyte multilayers are films obtained by the alternate deposition of polyanions and polycations on almost any kind of substrate, whatever its chemical nature and its form. First introduced by Decher[5, 6] in 1991, the concept is extremely simple: When a surface is charged, let's assume negatively charged, and when this surface is brought in contact with a solution of polycations, electrostatic interactions will induce the adsorption of the polycations onto the substrate. It comes out that at the end of the adsorption process the surface is not neutral but appears to be positively charged. This is called the charge overcompensation effect and originates from the polymeric nature of the polyelectrolytes. This then allows this film to be brought in contact with a polyanion solution and here again, once the polyanions have interacted with the adsorbed polycations the surface has become negative. This allows this process to be continued and a film to be grown step by step, alternating polyanions and polycations (figure 1.1).
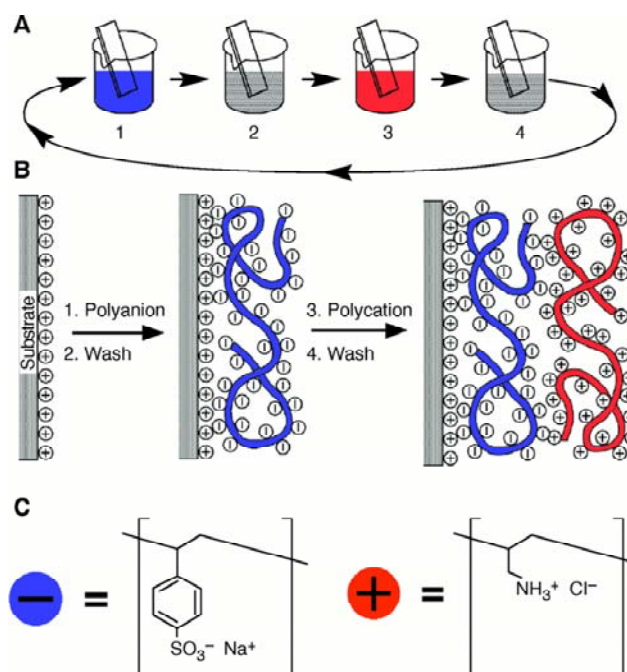
*Figure 1.1 :* *(A) Schematic of the film deposition by dipping process. Steps 1 and 3 represent the adsorption of a polyanion and polycation, respectively, and steps 2 and 4 are washing steps. The four steps are the basic buildup sequence for the simplest film architecture, (A/B)n. (B) Simplified molecular picture of the first two adsorption steps.(C) Chemical structures of two typical polyions, the sodium salt of poly(styrene sulfonate) (PSS) and poly(allylamine hydrochloride) (PAH)[6].*

The first films that were investigated followed all this buildup process leading to films which were structured and whose thickness increased linearly with the number of deposition layers. This type of films are called linearly growing films. PSS/PAH (PSS: Poly(styrene sulfonate); PAH: poly(allylamine)) and PSS/PDADMA (PDADMA: poly(diallyldimethyl ammonium)) represent two prominent examples of this type of multilayer. The structured nature of these films results from the fact that the polyelectrolytes from layer n interact only with the polyelectrolytes of its neighboring layers as shown by Decher et al. by using neutron reflectivity experiments.

Whereas the fact that the alternate deposition of polyanions and polycations should lead to film deposits whose thickness increases linearly with the number of deposition steps became a dogma by the scientific community, in 1999 the group of Hubbelreported that the alternate deposition of alginate and polylysineleads to a deposit whose thickness seems to increase exponentially with the number of deposition steps, reaching of the order of 2 µm for 15 bilayers[7]. Soon later Picart et al. reported a second polyanion/polycation system, hyaluronic acid/polylysine whose thickness increases exponentially with the number of deposition steps. They also explained the buildup mechanism behind this growth process[8,

[9].When the polyanion/polycation complexes that form on the surface are highly hydrated, as it appears to be the case with polysaccharides, during each deposition step the polyelectrolytes from the solution can diffuse into the multilayer instead of just interacting with the outer layer of the multilayer. During the next deposition step, this polyelectrolyte that has diffused into the film is soaked out of the film by the polyeletrolyte of opposite charge present in solution. As it diffused out, it is captured by the polyelectrolytes of opposite charge at the film/solution interface and these polyanion/polycation complexes that form remain bound on the multilayer and form the new additional layer of the film. This mechanism leads to an exponential growth of the film. What is of interest for these films is that they behave as gels and even highly viscous liquids and that the polyelectrolytes constituting the multilayer are usually highly mobile in the film. It also comes out that when incorporating proteins into such multilayers during their buildup they are also mobile as shown by Fluorescence recovery after photobleaching experiments. These films can also incorporate large amount of proteins. All these properties of exponentially growing multilayers were used for the development of chemo-mechanoresponsive films.

### 1.2.2.Mechanotransductive films based on linearly growing polyelectrolyte multilayers: towards cryptic site films

The initial idea to design mechano-responsive materials was to use linearly growing polyelectrolyte multilayers into which are embedded ligands and by stretching to exhibit these ligands and render them accessible to receptors as it is the case for cryptic site proteins. The general idea of the concept is depicted in figure 1.2.
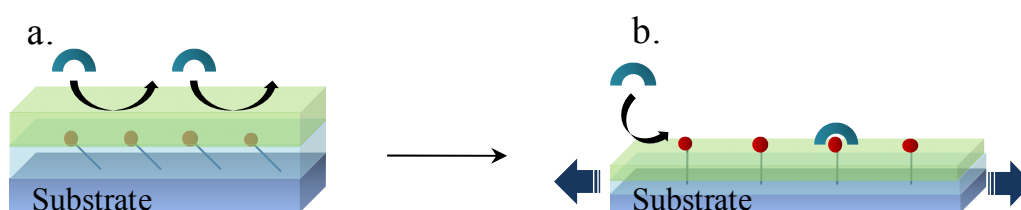


*Figure 1.2: (a) At rest, ligands are embedded inside the polymeric matrix, no interaction occurs. (b) Under stretching constraint, the ligands are exhibited and can interact with specific receptors.*

The first work performed by the group along this line was to develop surfaces that respond to a stretching by changing their hydrophobicity[10]. This was achieved by using

architectures based on two linearly growing multilayers: (PAH/PAA) and (PAH/Naf) (PAA: poly(acrylic acid); Naf : Nafion). Nafion which corresponds to Teflon modified by sulfonate groups is a hydrophobic polyanion. It can be deposited on substrates in alternation with PAH from water/ethanol mixtures. When dried, the contact angle of a (PAH/Naf)$_n$ film terminating by Nafion is 110° with respect to water. On the other hand, (PAH/PAA)$_n$ multilayers present a contact angle of 45°. It was shown (see figure 1.3) that when depositing a (PEI-(Naf/PAH)$_4$-Naf-(PAH/PAA)$_2$ (PEI: poly(ethylene imine))onto a silicone sheet that was first treated by polymer plasma, the contact angle of the substrate switched from 50° in the non-stretched state to 105° when stretched by 120° (2.2 times its initial elongation length). The reversibility of the system is observed during stretching/unstretching cycles.
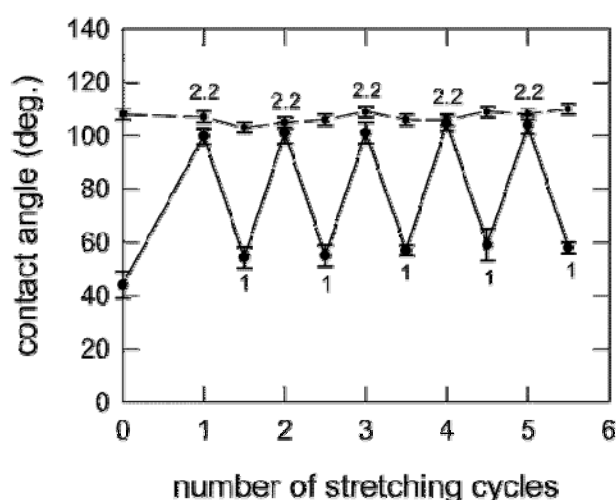


*Figure 1.3*: *evolution of the contact angle with water during elongation/retraction cycles as a function of the number of cycles. The material was stretched up to 2.2 times its initial length. The curve with large amplitude changes corresponds to a PEI-(Naf/PAH)$_4$-Naf-(PAH/PAA)$_2$ multilayer and the curve with small amplitudes corresponds to a (PEI-(Naf/PAH)$_4$-Naf-(PAH/PAA)$_4$-(PAH/Naf)$_2$ multilayer. (image taken from Ref[10])*

The silicone sheet was previously treated by polymer plasma in order to render it negatively charged and allow for a good anchoring of the multilayer. On the other hand when this film was supplemented by a (PAH/PAA)2-(PAH/Naf)$_2$ multilayer, that ending with Nafion layers, almost no contact angle change took place upon stretching. These results were interpreted by a change of the structure of the (PEI-(Naf/PAH)$_4$-Naf-(PAH/PAA)$_2$ multilayer due to stretching with an exhibition of the Nafion, rendering the film hydrophobic. What is particularly interesting is the reversibility of the process.

Based on this first result, namely that stretching a linearly growing multilayer allows to exhibit chemical functions embedded in the film, the group started to develop a strategy to create surfaces which exhibit ligands for receptors. These can be free molecules in solution, and the system that was selected was the biotin/streptavidin system, or they can be cellular receptors and the system that was selected was the standard adhesion arginine-glycine-aspartic acid peptides(RGD)/integrin[11] (peptides). In this case it was the adhesion of cells on the substrate that was investigated as a function of the stretching degree. Yet the development of these systems also required first to render the surfaces non adherent to proteins and cells at rest[12, 13]. To achieve this condition poly(acrylic acid) chains were modified by grafting on them $(EO)_3$-PC moieties where EO represents an ethylene glycol group and PC a phosphorylcholine group (see figure 1.4). These chains will be denoted as PAAPC.
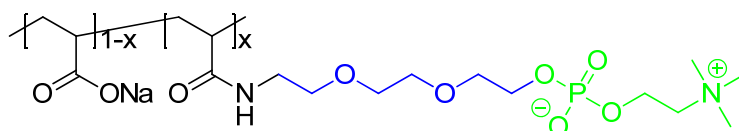


*Figure 1.4: Poly(acrylic acid)-EO$_3$-PC chains.*

Ethylene glycol chains are known to be very hydrophilic and to prevent protein adsorption and cell adhesion. This character was reinforced by using phosphorylcholine groups. These groups are present on the outer membrane of cells and in particular red blood cells and are presented as being in great part responsible for the anti-fouling character of the cell membranes. They also become widely used in biomaterial coatings to confer them an antifouling character[14]. It was then shown that when depositing PEI-(PSS/PAH)n-PAAPC or PEI-(PSS/PAH)n-PAAPC-PAH-PAAPC onto silicone sheets where 25% of the carboxylic groups of the PAA chains were modified by $(EO)_3$-PC moieties, the substrate became antifouling. For example, such a film was brought in contact with an albumin solution at a protein concentration of 0.2mg.mL$^{-1}$,only 2ng.cm$^{-2}$ could be detected on the surface (in the limit of detection of the experiment) whereas on a film where PAAPC was replaced by PAA the adsorbed amount was 390ng.cm$^{-2}$. The decrease of adsorbed amount when PAA was replaced by PAAPC was as spectacular with lysozyme and fibrinogen. When stretched the films remained non-adsorbent to protein up to stretching degrees of 1.5. A slight albumin adsorption was observed when a single PAAPC layer covered the multilayer whereas no protein could be detected on the surface when the multilayer was ended by PAAPC-PAH-

PAAPC. The behaviors of these films were also investigated with respect to cell adhesion (fibroblasts) and fungi (*Candida Albicans*). It was found that the films are non-adherent to cells and fungi at rest and remain non adherent to cells and fungi up to stretching degrees of 1.5 (larger stretching degrees were not investigated) as can be seen in figure 1.5.
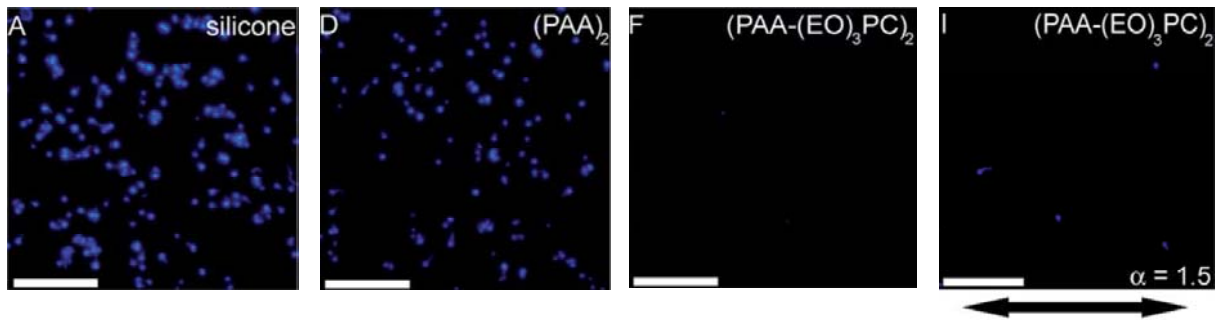


***Figure 1.5***: *Micrographs of Candida Albicans with Calcofluor white after 24h of culture on:  A:  bare silicone; D: (PAH/PSS)2-PAH/PAA/PAH/PAA; F: (PAH/PSS)2-PAH/PAAPC/PAH/PAAPC in the non-stretched state; I: (PAH/PSS)2-PAH/PAAPC/PAH/PAAPC at a stretching degree of 1.5. (White bars corresponding to 100 μm) (images taken from ref [13])*

These results opened the route to the design of a multilayer that exhibits ligands under stretching, a surface that can be considered as a cryptic site surface[15]. The strategy that was used is schematically represented in figure 1.6.
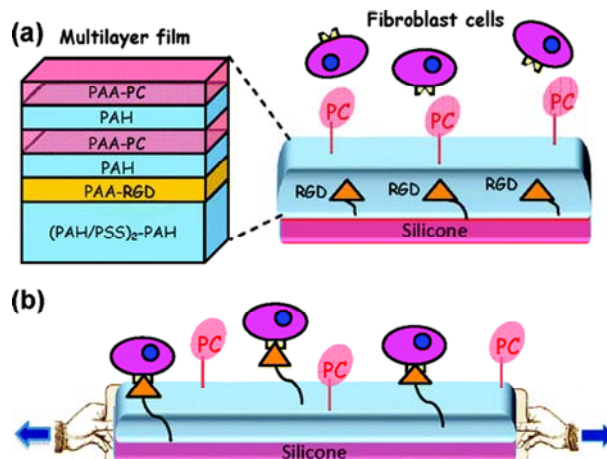


***Figure 1.6***: *Schematic representation of the first cryptic site surface that was developed based on polyelectrolyte multilayers (taken from ref [15]).*

Similar architectures as those used to create anti-fouling surfaces were used with one difference: after the deposition of a precursorPEI-(PAH/PSS)₃-PAH layer, instead of directly adsorbing a PAAPC layer we first deposited a PAA-ligand layer where PAA-ligand

represents PAA chains modified by anchoring a ligand instead of a phosphorylcholinemoietie. The ligand was either a RGD adhesion peptide for cell adhesion or a $(EO)_3$-biotin for interactions with streptavidin. This PAA-ligand layer was then covered by a $(PAH/PAAPC)_2$ multilayer. These multilayers were deposited on silicone sheets. At rest these films proved to be non-cell adhesive and non-protein adsorbent (see figure 1.7 and 1.8) whereas by stretching the film, cell adhesion and protein adsorption both increased when increasing the stretching degree up to 1.5. This thus proved that stretching leads to the exhibition of the embedded ligands which become accessible to their receptors. Unfortunately this system was not reversible. I participated to this work during my master's degree (annexe 1).
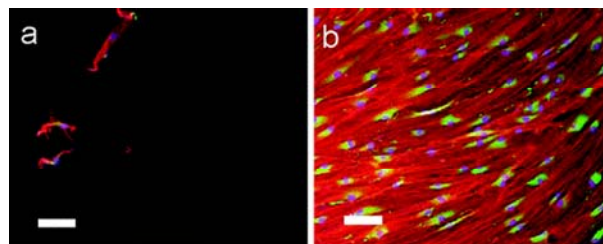


*Figure 1.7: Fluorescence images of fibroblast cells after 1 week of culture on (PEI-(PSS/PAH)$_3$-PAARGD-(PAH/PAAPC)$_2$(a) in the non-streched state and (b) at a surface stretched at a stretching degree of 1.5. (images taken from ref[15]).*
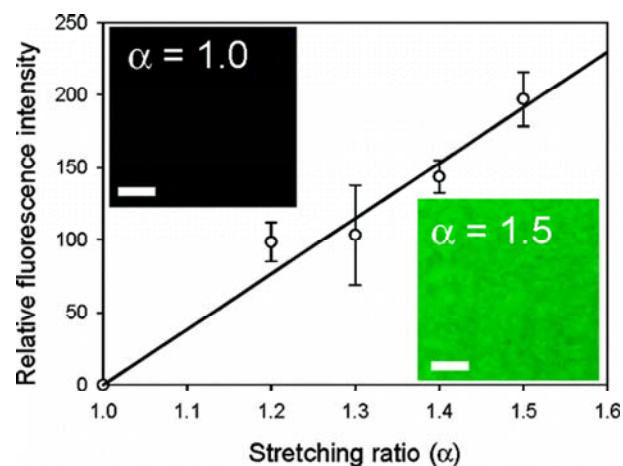


*Figure 1.8: Fluorescence intensity from FITC-Streptavidin adsorbed on a (PAH/PSS)-PAH-PAAbiotin-(PAH/PAAPC)$_2$ film deposited on a silicone sheet at different stretching degrees. (Image taken from ref[15]).*

**1.2.3. Mechano-responsive films based on exponentially growing multilayers capped by a linearly growing film playing the role of barrier: Towards mechano-responsive membranes**

Cells use another way to transduce a mechanical signal into a chemical response, namely by modifying their membrane properties when submitted to a mechanical stress. This can be mimicked by using exponentially growing films playing the role for enzymes or active molecules, covered by a barrier that is provided by linearly growing multilayers which are much denser. A first study by Garza et al. in 2004 showed that one can alternate the deposition exponentially growing HA/PLL films with linearly growing PSS/PAH ones and that the PSS/PAH film then prevents the diffusion of PLL chains from one HA/PLL compartment to the next[16]. This result opened the route to the use of linearly growing films as barriers. Mertz et al. then investigated, in 2007 the behavior under stretching of PSS/PAH and PSS/PDADMA linearly growing films deposited on an HA/PLL multilayer[17]. They first showed that the HA/PLL films directly deposited on silicone sheets remain intact and homogeneous even when stretched up to 110%. This was expected since these films should behave as viscous liquids. When PSS/PAH and PSS/PDADMA were deposited on the HA/PLL films and stretched at 110% cracks appeared in the PSS/PAH films and nanoholes appeared in the PSS/PDADMA films[18]. Moreover, when returning to the non-stretched state, the two lines of the cracks join together and the nanoholes close in the PSS/PDADMA case. These results showed that the PSS/PAH films behave as glassy, brittle films whereas the PSS/PDADMA films are more viscoelastic.

In 2009 Mertz et al. wanted to make use of the properties of the PSS/PDAMA films under stretching to create a mechano-transductive surface that activates an enzymatic reaction under stretching[19]. They embedded an enzyme, alkaline phosphatase, into a PLL/HA multilayer and capped it with a PSS/PDAMA film. Alkaline phosphatase (ALP) is a hydrolase enzyme responsible for the dephosphorylation of many types of molecules including fluoresceine diphosphate (FDP). In this case the reaction leads to the formation of fluorescein which is highly fluorescent and can thus be detected by fluorescence techniques. When this film was brought in contact with the enzyme substrate FDP, no fluorescence appeared in the solution, showing that the PSS/PDADMA multilayer played the role of barrier for the diffusion of FDP. When this film was stretched above 70% a strong increase of the fluorescence could be observed in the solution. Interestingly, the HA/PLL reservoir,

containing the ALP, did not become green indicating that the reaction did not take place in the film. It could be shown that the reaction took place at the film/solution interface. Moreover when returning to the non- stretched state, the film lost its enzymatic activity. It was also shown that the activity of the film under stretching depended upon the number of bilayers constituting the PSS/PDADMA barrier: When the film was constituted of less than 5 barriers it was permeable to FDP even in the non-stretched state; for 6 bilayers a strong fluorescence increase in solution could be observed when stretched at 70%. Almost no fluorescence increase could be observed anymore for 14 bilayers. Figure 1.9 illustrates these results. The results were interpreted as presented schematically in figure 1.10: The PDAMA/PSS film plays the role of barrier. When it is stretched above 70%, it becomes thinner but remains impermeable to FDP, yet ALP enzymes present in the HA/PLL multilayer become exhibited through the barrier and thus accessible to the enzyme substrate. When the film is brought back to the non-stretched state, due to its viscoelastic properties, the PDADMA/PSS film regains its original properties and the enzymes are again buried below the barrier and thus no longer accessible to FDP. A few remarks can be of interest here: 1) the whole stretching/unstreching process appears reversible. Yet it is not fully reversible since a small enzymatic activity was observed when returning to the non-stretched state. When stretched/unstretched a second time this activity increased and so on. 2) One would have expected that under stretching nanoholes forms as it was the case for $(HA/PLL)_n/(PSS/PDAMA)m$ films. It thus appears that the presence of the enzymes modifies the PSS/PDAMA barrier properties. 3) Later studies have shown thatthe formation of barriers is in fact more complicated than expected. Not only the number of bilayers constituting the barrier is an important parameter but also the contact time between the PSS and PDADMA polyelectrolyte solutionsand the film during its buildup process. Long contact times lead to more permeable barriers towards FDP. This made be due to diffusion processes of PSS and PDADMA into the HA/PLL film during contact and eventual exchange processes between PDADMA and PLL in the HA/PLL multilayer.
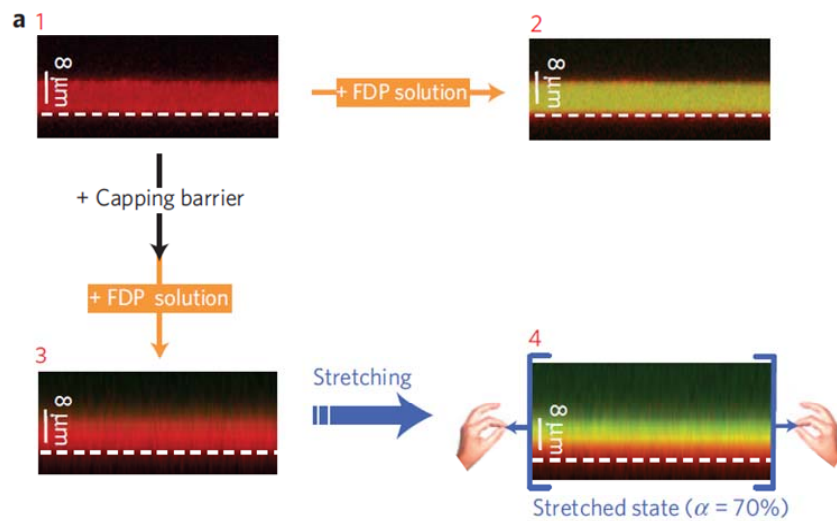
*Figure 1.9*: *Confocal microscope sections of silicone sheets with a (PLL/HA)$_{15}$/PLL/ALP$^{Rho}$/(PLL/HA)$_{15}$ film in a buffer solution (image 1) which is brought in contact with a FDP solution (image 2). This film becomes yellow (red+green) indicating that the ALP enzymes are active in the film. When this film is capped by a (PDAMA/PSS)$_{15}$ film and brought in contact with a FDP solution (image 3), no green fluorescence in observed indicating that PDADMA/PSS film plays the role barrier for FDP. When this film is stretched at 70% (image 4), the solution becomes green, the films remains red and the interface becomes yellow. This indicated that the enzymatic reaction takes place at the interface (image taken from ref [19]).*
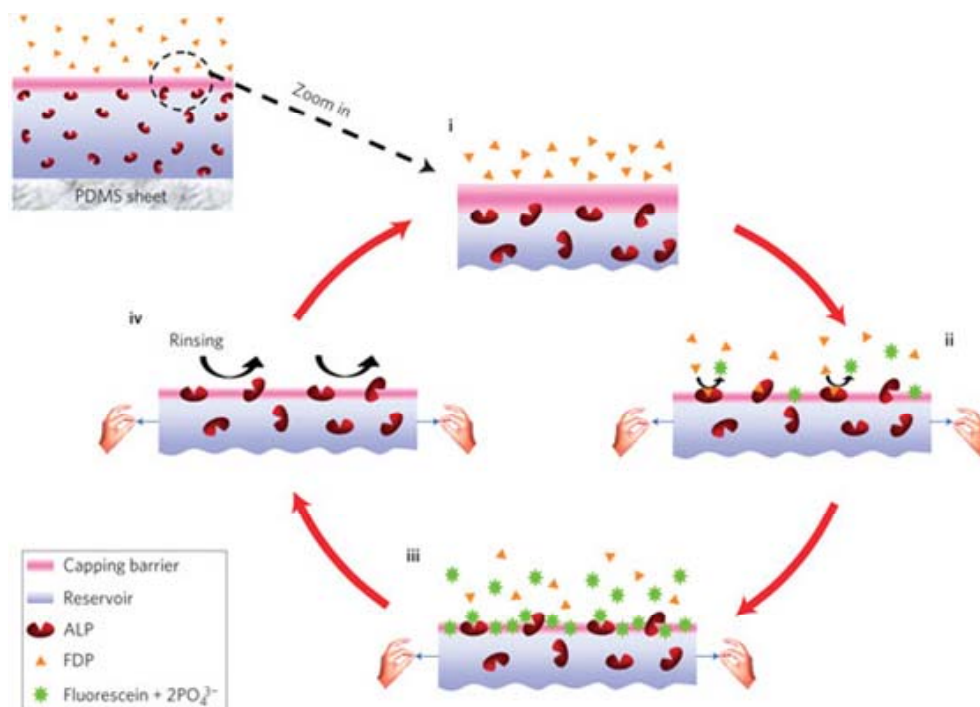


*Figure 1.10*: *Schematic representation of the mechanotransduction process taking place on a (PLL/HA)$_{15}$/PLL/ALP$^{Rho}$/(PLL/HA)$_{15}$(PDAMA/PSS)$_{15}$ as discussed in the text (image taken from ref [19]).*

The same system was used but in another configuration to create chemo-mechano responsive film that was denoted as layer-by-layer enzymatic platform for stretched-induced reactive release[20]. It is schematically represented in figure 1.11. A PLL/HA multilayer was used as reservoir for a compound (in that case FDP). This filled reservoir was capped by the PSS/PDADMA barrier multilayer terminated by a PSS layer. ALP was then adsorbed on top of this multilayer. In this configuration FDP was confined to the HA/PLL reservoir and could not react with the ALP enzymes. When stretching this film above 60% FDP started to diffuse through the barrier, react with ALP to transform into fluorescein which then diffuses into the solution. It was shown that all the FDP that diffused through the film was transformed by the enzymes into fluorescein. This provides a prototypeof a system where a compound in an inactive form would be stored in a reservoir. Upon stretching, it would leach out react at the interface to transform into an active compound. This system was, however, not reversible.
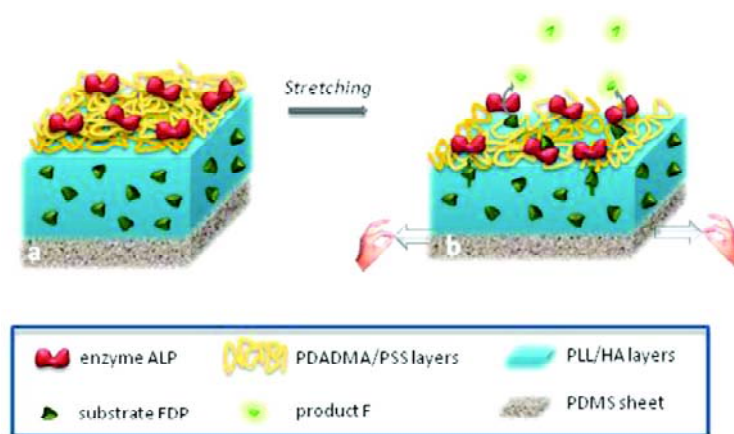


*Figure 1.11*:*Schematic representation of a layer-by-layer enzymatic platform for stretched-induced reactive release (Image taken from [20]).*

Another way to release active compounds upon stretching is by creating, a reservoir into which this compound is stored[21]. The reservoir is capped with a barrier that, under stretching allows enzymes to diffuse through. These enzymes then degrade the reservoir. The validity of this concept was demonstrated by selecting HA/PLL as reservoir, PSS/PAH as barrier and trypsin as enzyme. Trypsin is a serine protease that cleaves the C-terminal side of lysine residues from polypeptides and thus also degrades the polylysine from the film. PSS/PAH acts as a barrier for trypsin. Under stretching, it breaks and allows trypsin to diffuse into the PLL/HA film that is degrades locally.

### 1.2.4. Other cryptic site surfaces

As described above, our group developed cryptic surfaces by embedding ligands into a polyelectrolyte multilayer that was terminated by polyelectrolytes functionalized laterally by anti-fouling $(EO)_3$-PC arms. This idea was even pushed further by proposing to anchor directly the ligands onto a silicone substrate and to cover them by anti-fouling ethylene glycol chains (PEG)[22]. At rest the PEG chains repel the receptors that cannot come in contact with their ligands. Under stretching, the PEG chain density decreases, giving access of the ligands to the receptors. This concept is schematically represented in figure 1.12.
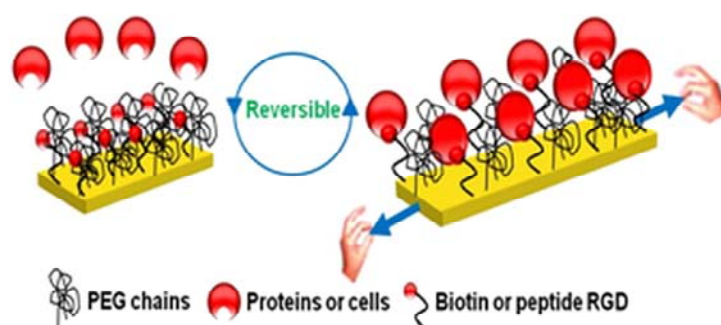


*Figure 1.12*: *schematic representation of a cryptic site surface where ligands are grafted onto a silicone sheet, covered by PEG chains. Under stretching the ligands become accessible to the receptors. This system appears to be fully reversible. (image taken from ref [22]).*

The silicone sheets were first treated by polymer plasma, in order to allow for further functionalization of the substrate. This treatment was performed under stretching. PEG chains of Mw=2000 were then grafter onto this substrate still under stretching. Finally, the ligands were grafted onto this already PEG covered substrate. The ligands, biotin or RDG peptide where coupled to the substrate through a $(EO)_2$ linker. When returning to the non-stretched state, this film proved to be totally non-adsorptive to proteins and non-adhesive to cells. When stretched by 60% the system with biotin became specifically adsorptive to streptavidin (see figure 1.13) or anti-biotin and cell adhesive for RDG ligands (see figure 14). When these systems were returned to their non-stretched starched streptavidin or anti-biotin were totally expelled from the surface and even more spectacular, cells detached from the substrate. This stretching/non-stretching cycle could be repeated similarly several times showing that this systems is fully reversible. Moreover, the amount of adsorbed streptavidin appeared toincrease almost linearly with the stretching degree, allowing to modulate this adsorbed amount.
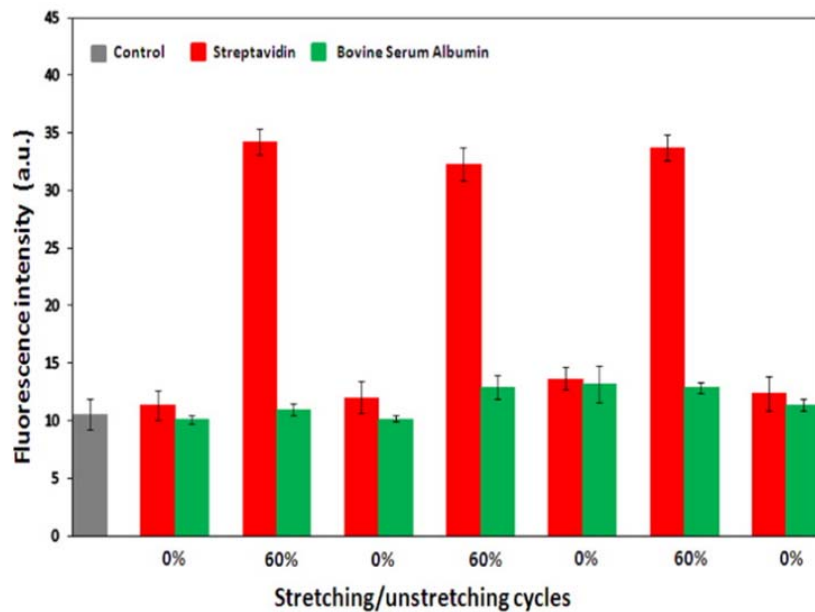
***Figure 1.13****: Fluorescence intensity of a biotin cryptic site substrate where the biotin ligands are shielded at rest by PEG chains. The streptavidin molecules (red) and albumin molecules (green) are brought in in contact with the substrate at rest (0%) then stretched to 60% brought bact to th non-streched state (0%) an so an. At each step, the substrate is brought in contact with the protein solutions (image taken from ref [22])*
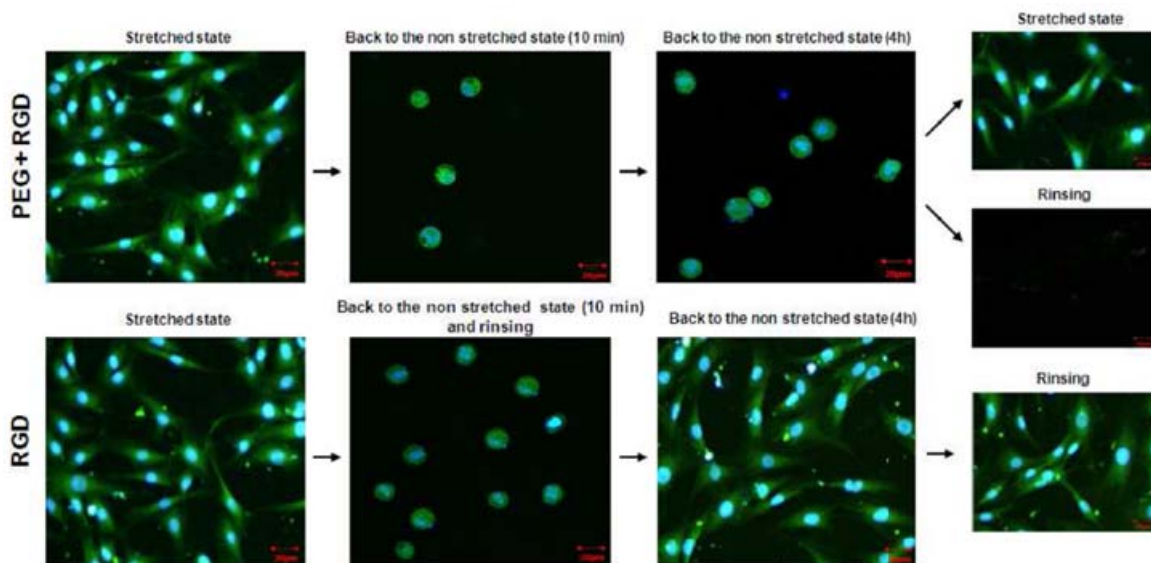


***Figure 1.14****: Optical microscopy images of osteoprogenitor cells deposited on PEG/RGD and RGD functionalized silicone substrates. Column 1: Cells deposited on the substrate and stretched at 60% during 4h. Column 2: The substrates were then suddenly brought back to the non-stretched and rinsed after 10min with buffer. Most of the cells detached from the PEG+RGD substrate. The images were taken after rinsing. Column 3: 4h after the substrate was stretched. Column 4: this substrate was the stretched again (upper image) or rinsed again (lower image of first line). One observes that cell that did not detach can spred again indicating that they remained alive. (images taken from ref [22])*

## 1.3. Towards chemo-mechano-responsive substrates:
## contributions from other groups

### 1.3.1. Chemo-mechano-responsive substrates from biology

Cells use chemo-mechanotransduction on a large basis to guide their fate. It has been shown for example that the Young modulus of a polyacrylamide substrate covered by collagen directs stem cells into various phenotypes : soft substrates (0.1-1 kPa) induce neurogenic phenotype, Youg moduli ranging from 8 to 17 kPa induce a myogenic phenotype whereas on hard substrates (25-40 kPa) stem cells transform into osteoblasts[23]. This implies that cells sense the mechanical properties of their environment using mechano-transduction processes. When cells adhere to a substrate they produce a matrix. This matrix contains various proteins such as collagen and fibronectin. Fibronectin is an adhesion protein known to self-assemble to form fibers (figure 1.15).
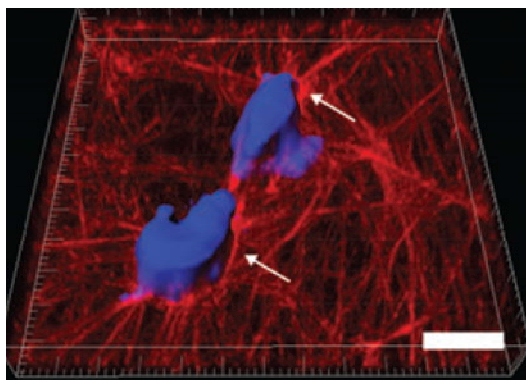


***Figure 1.15***: *Fibroblasts invading a decellularized extracellular matrix. Fibronectin fibers are labeled in red. Image taken from ref [24].*

Cells that interact with these fibers generate tensile forces which change the fibronectin conformation. This leads to a fibronectin unfolding which allows more soluble fibronectin to bind[25]. Sucha matrix thus constitutes a chemo-mechano-responsive substrate. Moreover proteins such as fibronectin are composed of tandem repeat units. These repeat units have different mechanical stability allowing to sense a full range of tensile forces and when unfolding they exhibit various cryptic sites that bind to various receptors[4].

Enzymes constitute another class proteins whose activities are controlled through a precise topology of the residues involved in their active site. Moreover structural dynamics of enzymes play a major role in the enzymatic activity[26]. It is thus expected that when an

enzymes is put under a mechanical constraint that changes its conformation or modifies the dynamics of its structural fluctuations, its activity changes. Using a spring probe (figure 1.16) Choi and Zocchi showed that force induced conformational changes of guanylate kinase, an enzyme that catalyzes the transfer of a phosphate from adenosine triphosphate to guanosine monophosphate, affects its binding affinity towards guanosine monophosphate but not its affinity towards adenosine triphosphate and thus also affect its enzymatic activity[27].
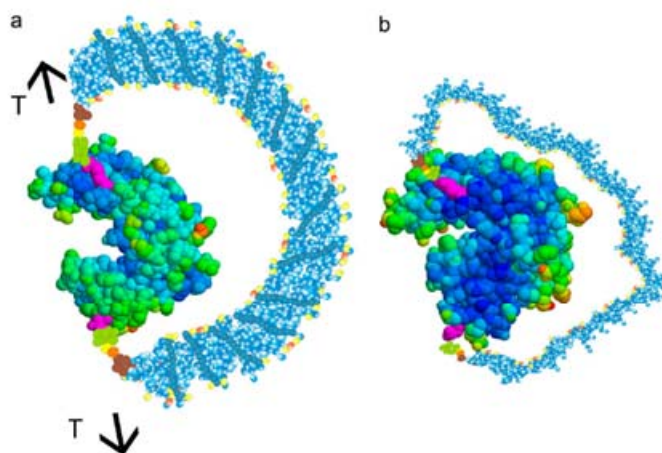


***Figure 1.16****: Representation of a guanylate kinase chimera where (b) a ss DNA is coupled on two cysteins located at opposite positions of the enzyme. When this ss interacts with its complementary stand it induces a mechanical stress on the enzyme that changes its conformation into an open conformation. (image taken from ref [27]).*

Conformational changes of proteins upon stretching can be directly visualized on Green Fluorescent proteins (GFP). These proteins have a typical beta barrel structure, consisting of eleven β-sheets with six alpha helix(s) containing the covalently bonded chromophore 4-(*p*-hydroxybenzylidene)imidazolidin-5-one (HBI) running through the center[28]. Using Steered Molecular Dynamics Simulations of mutant GFPs Saeger et al. showed how application of mechanical forces on specific GFP sites leads to conformational changes in the proteins and how these conformational changes affect their fluorescence properties (figure 1.17)[29].
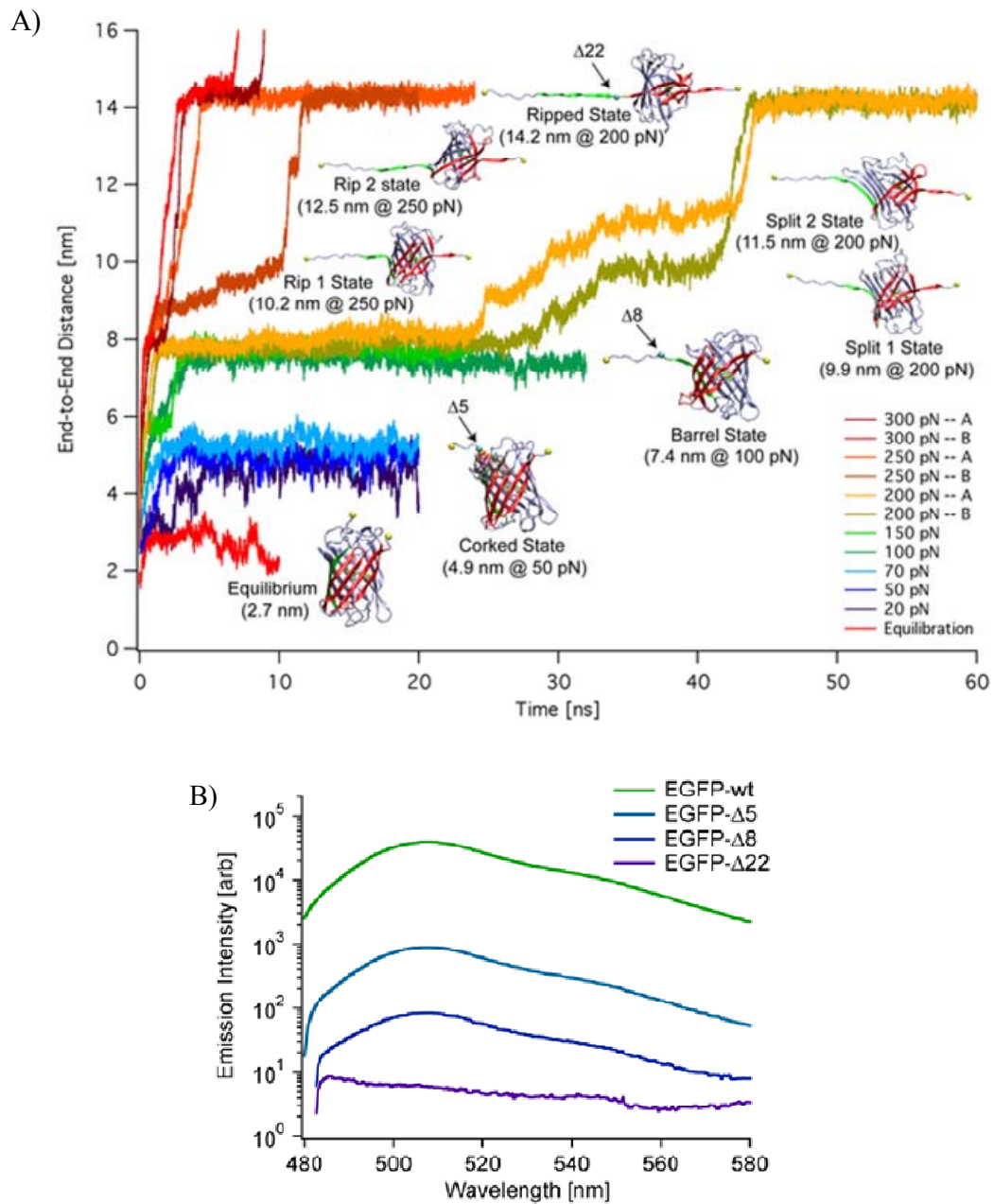
*Figure 1.17*: A)End to end distance of GFP molecules relative to different conformations corresponding to different applied forces as indicated in the figure; B) different emission spectra of GFP molecules for different end to end distances corresponding to different applied forces.

**1.3.2.Other chemo-mechano-responsive systems**

The first to use the use of modulating the enzymatic activity of materials by applying mechanical stresses on enzymes incorporated in the material was Klibanovet al.in 1976[30]. They attached α-chymotrypsin or trypsin on fine elastic polymer fibers, such as Nylon, with glutaradhehyde. This material was then stretched. They found that by stretching this material the activity of the enzymes decreased by almost 70% (see figure 1.18). This decrease was found to be reversible by returning to the non-stretched state. They explained this effect by a conformation change of the enzyme that becomes inactive (see figure 1.19)
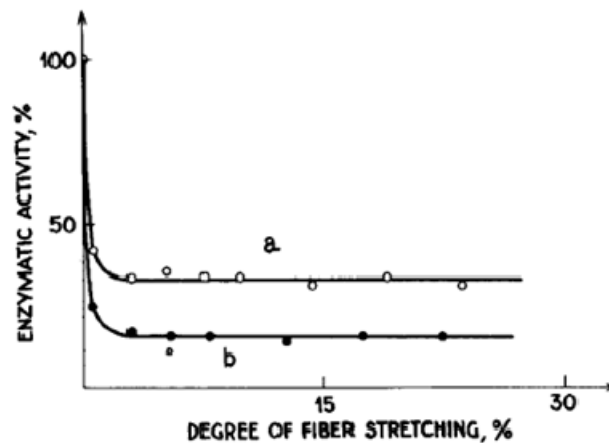


*Figure 1.18: Enzymatic activity of (a) α-chymotrypsin and (b) trypsin covalently bound to nylon fibers as a function of the stretching degree. The enzymatic activity is measured relative to the non-stretched state. (image taken from ref [30]).*
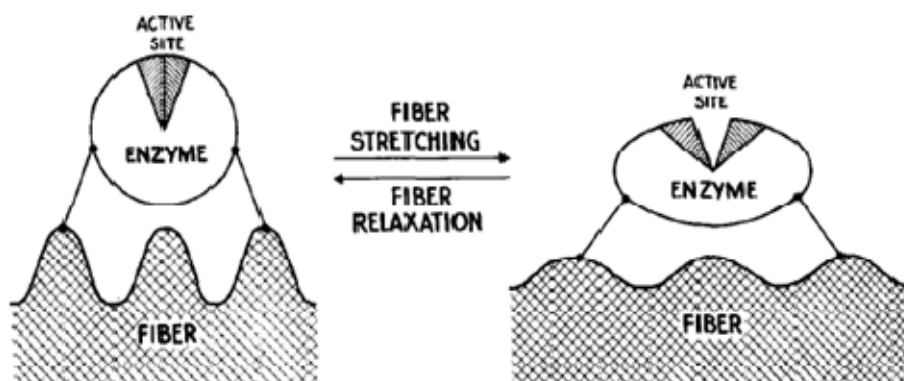


*Figure 1.19:Original drawing for the explanation of the change of the enzymatic activity change under stretching taken from Klibanov's paper [30].*

Interestingly they found that when covalently fixing the enzymes on already stretched fibers and relaxing the whole material, the enzymatic activity increased upon relaxation. The explanation of this mechanism was based on the deposition of the enzymes in two conformations: one that is active and one that is denatured and inactive. They assume that by relaxing the material to a non-stretched state of the fibers, the molecules in the active conformation becomes inactive and that in the inactive conformation become active.They extended their result later to myosin whose activity also depended upon the stretching of nylon fibers[31].This idea, proposed by Klibanov et al. was then applied to control the activity of glucose oxidase adsorbed onto a porous poly(vinyl chloride) membrane[32, 33]. Yet, in this case they found an increase in the enzymatic activity by stretching the material. In fact this effect proved to be due to an increase of the diffusivity and accessibility of the enzymes for the substrates. Agarwal and Bhattacharya similarly attached covalently restriction endonucleases onto nylon and polyethylene membranes[34.] These membranes were then put under a mechanical stress and a decrease of the enzymatic activity was observed by increasing the applied stress. This system appeared to be partially reversible. Yet no mechanism explaining the change in the enzymatic activity under stress was given.

In 2009 Bruns et al. introduced the concept mechanical sensor based on FRET (Fluorescence resonance energy transfer) within a thermosome[35]. The sensor corresponds of two proteins coencapsulated onto the two cavities of a thermosome (see figure 1.20). The two proteins were enhanced cyan fluorescent protein (eCFP) and enhan,ced yellow fluorescent protein (eYFP) which constitute the most commonly used donor-acceptor FRET pair in molecular biology. These thermosomes were then incorporated into a polymeric matrix. When this matrix was put under a high mechanical stress, the induced strain leads to a structural deformation of the whole protein with a separation of the two cavities of the thermosome. This changes the fluorescence properties by reducing FRET. When cracks take place, the relaxation of the matrix leads to a recovery of FRET. These materials can thus be used as damage-reporting materials. Similar molecules were later used by this group for reporting mechanical damage in glass-fiber-reinforced polymer composites[36].

Recently, Bielawski's group reported the design of a mechanically sensitive biocomposite comprised of fluorescent proteins that report local stresses present in the material. They incorporated eYFP which exhibits hypsochromic shifts inits fluorescence emission maxima following compression and a modified green fluorescent protein (GFPuv)

which exhibit fluorescence quenching under the action of mechanical force. This later molecule is covalently linked to the polymer matrix and is denatured (conformational change) under compression [37].
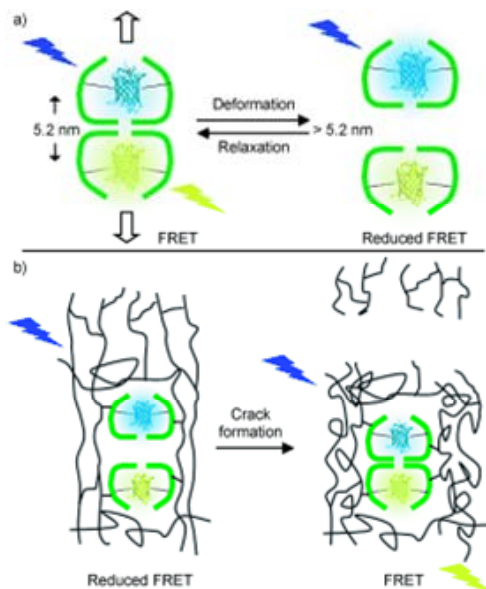


**Figure 1.20**: schematic representation of a mechanical nanosensor based on FRET within a thermosome for damage reporting polymeric materials (image taken from reference [35]).

## 1.4. References

1.      D.A. Davis, A. Hamilton, J.L. Yang, L.D. Cremar, D. Van Gough, S.L. Potisek, M.T. Ong, P.V. Braun, T.J. Martinez, S.R. White, J.S. Moore, and N.R. Sottos, *Force-induced activation of covalent bonds in mechanoresponsive polymeric materials.* Nature, 2009. **459**(7243): p. 68-72.

2.      C.E. Diesendruck, B.D. Steinberg, N. Sugai, M.N. Silberstein, N.R. Sottos, S.R. White, P.V. Braun, and J.S. Moore, *Proton-coupled mechanochemical transduction: A mechanogenerated add.* Journal of the American Chemical Society, 2012. **134**(30): p. 12446-12449.

3.      V. Vogel and M. Sheetz, *Local force and geometry sensing regulate cell functions.* Nature Reviews Molecular Cell Biology, 2006. **7**(4): p. 265-275.

4.      V. Vogel, *Mechanotransduction involving multimodular proteins: Converting force into biochemical signals*, in *Annual review of biophysics and biomolecular structure*. 2006, Annual Reviews: Palo Alto. p. 459-488.

5.      G. Decher and J.D. Hong, *Buildup of ultrathin multilayer films by a self-assembly process .2. Consecutive adsorption of anionic and cationic bipolar amphiphiles and polyelectrolytes on charged surfaces.* Berichte Der Bunsen-Gesellschaft-Physical Chemistry Chemical Physics, 1991. **95**(11): p. 1430-1434.

6.      G. Decher, *Fuzzy nanoassemblies: Toward layered polymeric multicomposites.* Science, 1997. **277**(5330): p. 1232-1237.

7.      D.L. Elbert, C.B. Herbert, and J.A. Hubbell, *Thin polymer layers formed by polyelectrolyte multilayer techniques on biological surfaces.* Langmuir, 1999. **15**(16): p. 5355-5362.

8.      C. Picart, J. Mutterer, L. Richert, Y. Luo, G.D. Prestwich, P. Schaaf, J.C. Voegel, and P. Lavalle, *Molecular basis for the explanation of the exponential growth of polyelectrolyte multilayers.* Proceedings of the National Academy of Sciences of the United States of America, 2002. **99**(20): p. 12531-12535.

9.      C. Picart, P. Lavalle, P. Hubert, F.J.G. Cuisinier, G. Decher, P. Schaaf, and J.C. Voegel, *Buildup mechanism for poly(l-lysine)/hyaluronic acid films onto a solid surface.* Langmuir, 2001. **17**(23): p. 7414-7424.

10.     J. Hemmerle, V. Roucoules, G. Fleith, M. Nardin, V. Ball, P. Lavalle, P. Marie, J.C. Voegel, and P. Schaaf, *Mechanically responsive films of variable hydrophobicity made of polyelectrolyte multilayers.* Langmuir, 2005. **21**(23): p. 10328-10331.

11.     E. Ruoslahti, *Rgd and other recognition sequences for integrins.* Annual Review of Cell and Developmental Biology, 1996. **12**: p. 697-715.

12.     A. Reisch, J. Hemmerle, J.C. Voegel, E. Gonthier, G. Decher, N. Benkirane-Jessel, A. Chassepot, D. Mertz, P. Lavalle, P. Mesini, and P. Schaaf, *Polyelectrolyte multilayer coatings*

*that resist protein adsorption at rest and under stretching.* Journal of Materials Chemistry, 2008. **18**(36): p. 4242-4245.

13.    A. Reisch, J. Hemmerle, A. Chassepot, M. Lefort, N. Benkirane-Jessel, E. Candolfi, P. Mesini, V. Letscher-Bru, J.C. Voegel, and P. Schaaf, *Anti-fouling phosphorylcholine bearing polyelectrolyte multilayers: Cell adhesion resistance at rest and under stretching.* Soft Matter, 2010. **6**(7): p. 1503-1512.

14.    Y.K. Gong, L.P. Liu, and P.B. Messersmith, *Doubly biomimetic catecholic phosphorylcholine copolymer: A platform strategy for fabricating antifouling surfaces.* Macromolecular Bioscience, 2012. **12**(7): p. 979-985.

15.    J. Davila, A. Chassepot, J. Longo, F. Boulmedais, A. Reisch, B. Frisch, F. Meyer, J.C. Voegel, P.J. Mesini, B. Senger, M.H. Metz-Boutigue, J. Hemmerle, P. Lavalle, P. Schaaf, and L. Jierry, *Cyto-mechanoresponsive polyelectrolyte multilayer films.* Journal of the American Chemical Society, 2012. **134**(1): p. 83-86.

16.    J.M. Garza, P. Schaaf, S. Muller, V. Ball, J.F. Stoltz, J.C. Voegel, and P. Lavalle, *Multicompartment films made of alternate polyelectrolyte multilayers of exponential and linear growth.* Langmuir, 2004. **20**(17): p. 7298-7302.

17.    D. Mertz, J. Hemmerle, F. Boulmedais, J.C. Voegel, P. Lavalle, and P. Schaaf, *Polyelectrolyte multilayer films under mechanical stretch.* Soft Matter, 2007. **3**(11): p. 1413-1420.

18.    D. Mertz, J. Hemmerle, J. Mutterer, S. Ollivier, J.C. Voegel, P. Schaaf, and P. Lavalle, *Mechanically responding nanovalves based on polyelectrolyte multilayers.* Nano Letters, 2007. **7**(3): p. 657-662.

19.    D. Mertz, C. Vogt, J. Hemmerle, J. Mutterer, V. Ball, J.C. Voegel, P. Schaaf, and P. Lavalle, *Mechanotransductive surfaces for reversible biocatalysis activation.* Nature Materials, 2009. **8**(9): p. 731-735.

20.    C. Vogt, D. Mertz, K. Benmlih, J. Hemmerle, J.C. Voegel, P. Schaaf, and P. Lavalle, *Layer-by-layer enzymatic platform for stretched-induced reactive release.* Acs Macro Letters, 2012. **1**(7): p. 797-801.

21.    J. Barthes, D. Mertz, C. Bach, M.H. Metz-Boutigue, B. Senger, J.C. Voegel, P. Schaaf, and P. Lavalle, *Stretch-induced biodegradation of polyelectrolyte multilayer films for drug release.* Langmuir, 2012. **28**(38): p. 13550-13554.

22.    J. Bacharouche, F. Badique, A. Fahs, M.V. Spanedda, A. Geissler, J.P. Malval, M.F. Vallat, K. Anselme, G. Francius, B. Frisch, J. Hemmerle, P. Schaaf, and V. Roucoules, *Biomimetic cryptic site surfaces for reversible chemo- and cyto-mechanoresponsive substrates.* Acs Nano, 2013. **7**(4): p. 3457-3465.

23.    A.J. Engler, S. Sen, H.L. Sweeney, and D.E. Discher, *Matrix elasticity directs stem cell lineage specification.* Cell, 2006. **126**(4): p. 677-689.

24. K.E. Kubow, E. Klotzsch, M.L. Smith, D. Gourdon, W.C. Little, and V. Vogel, *Crosslinking of cell-derived 3d scaffolds up-regulates the stretching and unfolding of new extracellular matrix assembled by reseeded cells.* Integrative Biology, 2009. **1**(11-12): p. 635-648.

25. C.L. Zhong, M. Chrzanowska-Wodnicka, J. Brown, A. Shaub, A.M. Belkin, and K. Burridge, *Rho-mediated contractility exposes a cryptic site in fibronectin and induces fibronectin matrix assembly.* Journal of Cell Biology, 1998. **141**(2): p. 539-551.

26. R.M. Daniel, D.R. V, J.L. Finney, and S.J. C, *The role of dynamics in enzyme activity.* Annual Review of Biophysics and Biomolecular Structure, 2003. **32**: p. 69–92.

27. B. Choi and G. Zocchi, *Guanylate kinase, induced fit, and the allosteric spring probe.* Biophysical Journal, 2007. **92**(5): p. 1651-1658.

28. R.Y. Tsien, *The green fluorescent protein.* Annual Review of Biochemistry, 1998. **67**: p. 509-544.

29. J. Saeger, V.P. Hytonen, E. Klotzsch, and V. Vogel, *Gfp's mechanical intermediate states.* PLoS ONE, 2012. **7**(10): p. 11.

30. A.M. Klibanov, G.P. Samokhin, K. Martinek, and I.V. Berezin, *Enzymatic mechanochemistry - new approach to studying mechanism of enzyme action.* Biochimica Et Biophysica Acta, 1976. **438**(1): p. 1-12.

31. B.F. Poglazov, G.P. Samokhin, A.M. Klibanov, D.I. Levitsky, K. Martinek, and I.V. Berezin, *Effect of mechanical stretching of myosin rod component (fragment lmm+hmm s-2) on atpase activity of myosin.* Biochimica Et Biophysica Acta, 1978. **524**(2): p. 245-253.

32. Y. Ishimori, I. Karube, and S. Suzuki, *Mechanical control of the activity of glucose-oxidase immobilized on porous polyvinylchloride membrane.* Biotechnology and Bioengineering, 1981. **23**(11): p. 2601-2608.

33. Y. Ishimori, I. Karube, and S. Suzuki, *Stress sensitive glucose-oxidase nylon membrane.* European Journal of Applied Microbiology and Biotechnology, 1981. **13**(1): p. 19-23.

34. P.K. Agarwal and S.K. Bhattacharya, *Construction of a multi re module: Exploitation of mechanochemistry of restriction endonucleases.* Biotechnology and Bioengineering, 1999. **65**(2): p. 233-239.

35. N. Bruns, K. Pustelny, L.M. Bergeron, T.A. Whitehead, and D.S. Clark, *Mechanical nanosensor based on fret within a thermosome: Damage-reporting polymeric materials.* Angewandte Chemie-International Edition, 2009. **48**(31): p. 5666-5669.

36. K. Makyla, C. Muller, S. Lorcher, T. Winkler, M.G. Nussbaumer, M. Eder, and N. Bruns, *Fluorescent protein senses and reports mechanical damage in glass-fiber-reinforced polymer composites.* Advanced Materials, 2013. **25**(19): p. 2701-2706.

37.     J.N. Brantley, C.B. Bailey, J.R. Cannon, K.A. Clark, D.A. Vanden Bout, J.S. Brodbelt, A.T. Keatinge-Clayth, and C.W. Bielawski, *Mechanically modulating the photophysical properties of fluorescent protein biocomposites for ratio- and intensiometric sensor.* Angewandte Chemie-International Edition, 2014. **53**: p. 5088-5092.

<table>
<tr><td>Chapter</td><td>2</td></tr>
</table>

# Materials and Methods

## Contents

## 2.1. Materialsand samples build-up:

### 2.1.1.Chapter 3: Modulation of Green Fluorescent Protein spectral response under stretching constraints

**Materials**

*Polydimethylsiloxane substrate*

According to its viscoelastic properties and its easy way to put in shape, PDMS Sylgard-184 was chosen as a substrate for this study.

*Di-isocyanate/Di-isothiocyanate components*

In order to modify our PDMS substrate, different bi-functional linkers were used. PDIT and MDI were dissolved at 2mg.ml$^{-1}$ in anhydrous acetone solution while DIDS is dissolved at 1mg.mL$^{-1}$ in milli-Q water.
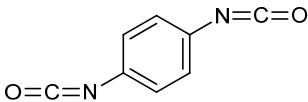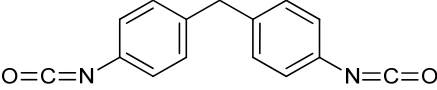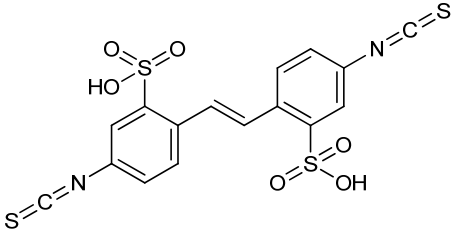
| Component | Structure | Supplier |
|---|---|---|
| 1,4-phenylene diisocyanate **PDIT** |  | Sigma-Aldrich |
| 4,4'methylenebis(phenyl )isocyanate **MDI** |  | Sigma-Aldrich |
| 4,4'-diisothiocyano 2,2'stilbenedisulfonic acid **DIDS** |  | Sigma-Aldrich |

*Table 2.1 :bi-functional linkers used for the surface modification*

*Poly(ethylene) glycol (PEG) solutions*

In order to prevent non-specific adsorption of protein on the PDMS substrate, antifouling PEG chains were grafted on it.PEG chains used during this project were solubilized in milli-Q water at a concentration of 1mg.mL$^{-1}$.
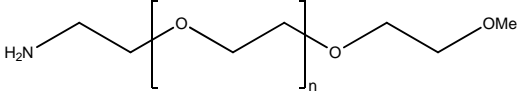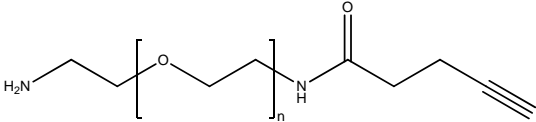
| Component | Structure | Mw (g.mol-$^1$) | Supplier |
|---|---|---|---|
| Poly(ethylene) glycol amine/MeO terminated | | 2000 | Iris-Biotech |
| Poly(ethylene) glycol amine/alkyne terminated | | 3000 | Iris-Biotech |

***Table 2.2 :****Poly(ethylene) glycol chains grafted on the PDMS surface.*

*Green Fluorescent Protein (GFP) solution*

The functionalization of the PDMS surface was performed using a solution at0.0275 mg.mL$^{-1}$of GFP in phosphate buffered saline (PBS, Sigma-Aldrich). More details about the specifically modified proteins are given in chapter 3.

*Click reaction reagents*

In order to covalently link the GFP to the surface, an alcyne/azide click reaction was performed. Copper sulfate, sodium ascorbate, aminoguanidine hydrochloride and phosphate buffered reagents were purchased from Sigma-Aldrich. Tris(3-hydroxypropyltriazolylmethyl)amine (THPTA) ligand (figure 2.1) was prepared in our laboratory by Dr. Jierry according to protocol elaborated by Fokin et al[1, 2].
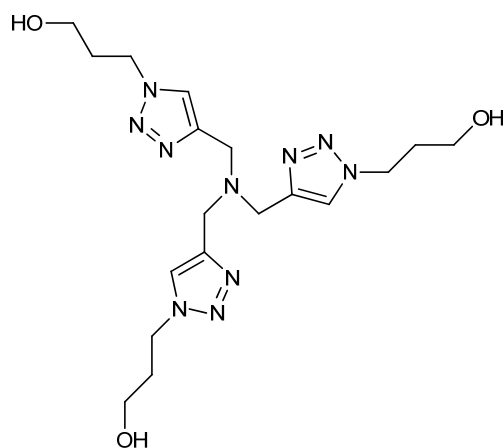
*Figure 2.1 (3-hydroxypropyltriazolylmethyl)amine (THPTA) ligand.*

## Methods

### PDMS Sylgard-184 substrates preparation

Poly(dimethylsiloxane) PDMS Sylgard-184 from Dow Corning was prepared using a mixture composed of a base and a curing agent in a rate of 10:1. After mixing the two components the mixture was degased for 1h in an under reduced pressure. The solution was melt into PMMA molds and cured overnight at 90°C at 254 mmHg. PDMS substrateswere then unmold and washed by immersion, first in500mL of a n-heptane and dodecanethiol (0.01 %) solution for 1 h and then two times in500mL of a n-heptane solution for 1h each time. These washing steps are performed in order remove the remaining unreacted chains and the Pt catalyst from the material. The silicone sheetswere then dried in two steps, first, under pressure at room temperature during 1h, and finally in the oven at 60°C overnight. The poly(dimethylsiloxane) PDMS obtained is a transparent and elastic material. Prior to the manipulations, PDMS substrates with a defined size of 2x1cm were prepared by cutting the silicone sheets and cleaned with ethanol (10mL)and rinsed with milli-Q water (3x10mL) to remove possible dust adsorption.

### Functionalization of the surface

In order to maximize the functionalization rate of the surfaces, the different steps of modification of the silicones were performed in a stretched state of 30%.

- *Di-isocyante/di-isothiocyanate functionalization of the surface*

PDMS substrates were first activated under UV-Ozone for 60mn. Immediately after, the substrates were immersed in a 20mL di-isocyanate solution at 1mg.mL$^{-1}$in acetonefor 1h at room temperature under slow agitation. After this reaction the surfaces wererinsed with acetone (10mL)andthen with milli-Q water (3x10mL).

- *PEG chains grafting on the surface*

Once the reaction with the isocyanates occurred, the samples were immersed in 10mL of asolutionof amino-PEG (Mw = 3000) terminated with an alkyne groups at 1mg.mL$^{-1}$ in milli-Q water at room temperature overnight in order to react the amine groups with the isocyanates from the silicone surface. After rinsing with milli-Q water (3x10mL)the samples were kept in 20mL of PBSbuffer (0.1M, pH 7.4) until use.

*Click reaction conditions and coupling procedure*

Once the PDMS surfaceswerefunctionalized with PEG/alkyne chains, the silicone substrate were relaxed to their initial state and the reaction between the modified GFP and the alkyne-terminated PEG was performed following an optimized Copper(I)-catalyzed Azide-Alkyne Cycloaddition (CuAAC) protocol for bioconjugation developed by Finn and coworkers[3]. For this reaction, all the reagents were mixedin a specific order to prevent degradation of the proteins. It must be noted that all the compounds except the GFP were solubilized in milli-Q water.

The reagents were added in a 2mL Eppendorf tube according to the following order:

- 432µL of a 3.35 µg.mL$^{-1}$ GFP solution in phosphate buffer(PBS, 0.1M, pH 7.4)
- 7.5µL of a premixed solution of CuSO$_4$/ THPTA. 2.5µL of a 20mM CuSO$_4$solution was mixed to 5µL of a 50mM THPTA solution.
- 25µL of 100mM aminoguanidinesolution.
- 25µL of 100mM sodium ascorbatesolution.

The solution was then quickly homogenized and put in contact with functionalized PDMS for one hour. Once the reaction occurred, the surfaces were washed (3x10mL), then stored in a phosphate buffer solution (PBS, 0.1M, pH 7.4) until beinganalyzed.

## 2.1.2. Project 2: Catalytic mechano-responsive polyelectrolyte multilayers based on conformational changes of enzymes

### Materials

*Substrate nature*

Silicone sheets with a thickness of 254µm(Specialty Manufacturing Inc. SMI, Michigan, USA) were used as an elastomeric substrate in order to perform stretching experiments.

*Polyelectrolyte solutions*

Polyelectrolyte compounds used to build multilayer films were dissolved in a solution of sodium chloride (NaCl) 150mM in ultra-pure water (resistivity of 18MΩ.cm, Milli-Q-plus water system, Millipore). Polyelectrolyte solutions were prepared at a concentration of 1mg.mL$^{-1}$ with adjusted pH of 7.4 (physiological conditions).
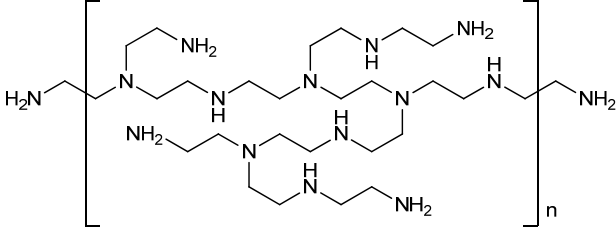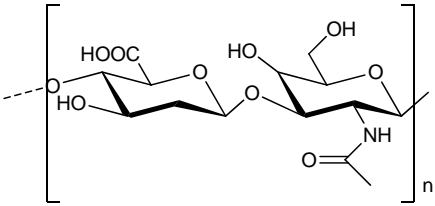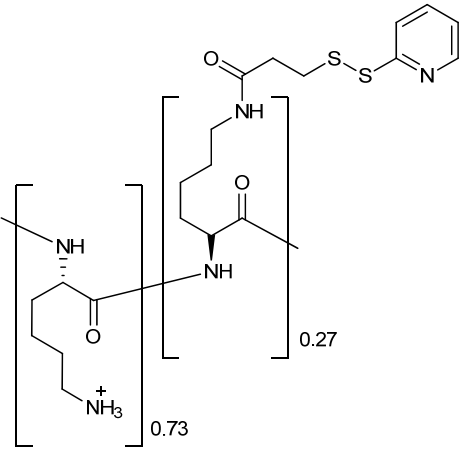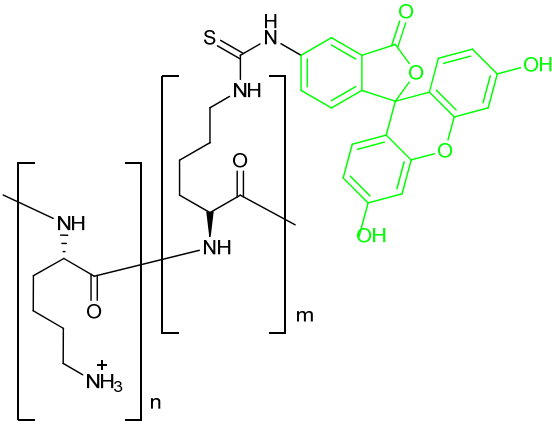
| Polyelectrolyte | Structure | Mw (g.mol$^{-1}$) | Supplier |
|---|---|---|---|
| Poly(Ethylene-Imine) **PEI** |  | 60 000 | Sigma-Aldrich |
| HyaluroniqueAcid **HA** |  | 132 000 | Lifecore-Biomedical |
| Poly(L-Lysine) labelled with thiopyridone **PLL-S-TP** |  | 26 000 | Made in laboratory |
| Poly(L-Lysine) labelledwith fluorescein **PLL** $^{FITC}$ |  | 70 000 | Made in laboratory |

**Table 2.3**: *Polyanions and polycations used for the build-up f the multilayer films.*

<u>*Fluorescent polyelectrolyte*</u>

In order to achieve confocal microscopy experiments, fluorescent polyelectrolytes were used. These commercial polymers were marked with a fluorescent dye, the fluorescein isothiocyanate(FITC, Sigma-Aldrich, $\lambda_{excitation}$ = 488 nm / $\lambda_{emission}$ =520nm)(figure 2.2).
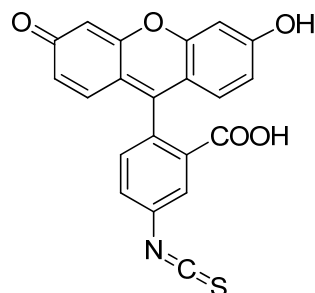


**Figure 2.2:** *Molecular structure fluorescent dye covalently grafted on polymers: fluorescein isothiocyanate ($\lambda_{excitation}$ = 488 nm / $\lambda_{emission}$ =520nm.*

The binding of this dye on polyelectrolytes such as poly(L-Lysine) was obtained by the nucleophile attack of the amine functions on the electrophile carbon from the isothiocyanategroup resulting in a covalent coupling between the fluorescent dye and the polymer. Characteristics of the PLL-FITC are given in table 2.3.

*Enzymes solutions*

For the enzymatic multilayer films build-up, the β-galactosidase (Escherichia coli Grade VI, lyophilized powder, 250-600 units/mg protein, Sigma-Aldrich) was used. It was dissolved at a concentration of 0.4mg.mL$^{-1}$ in a10mM HEPES buffer solutionatpH 6. For this study, a specific modified enzyme with maleimide groups was produced by C. Rios (see supporting information chapter 4 for protocol).

*Enzymatic substrate solutions*

The enzymatic activity of β-galactosidasewas monitored by dipping of multilayer films in solutions of fluorescein di-*β*-galactopyranoside (FDG)at a concentration of0.1mg.mL$^{-1}$ in a buffer solution of 0.1M TRIS/ 0.15M NaClat pH 7.4. Under the action of β-galactosidase, the FDG is hydrolyzed in fluorescein. The produced fluorescein ($\lambda_{excitation}$ = 490 nm / $\lambda_{emission}$ = 515nm)during the enzymatic reaction was detected by fluorescence measurement using a UV/Visible spectrophotometer.
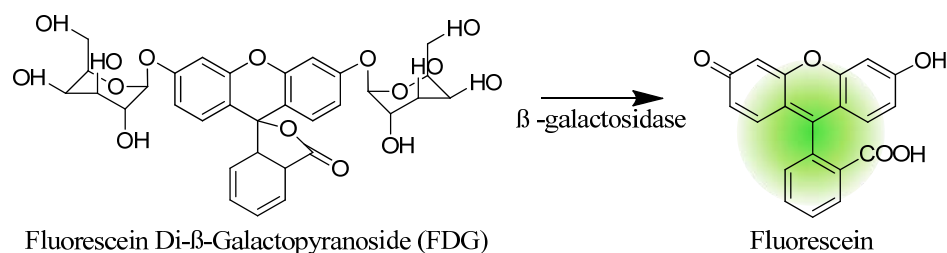
*Figure 2.3*: *Hydrolizis of FDG in fluorescein in presence of β-galactosidase.*

## Other compounds

EDC (1-Ethyl-3-(dimethylaminopropyl)carbodiimide hydrochloride), NHS (N-hydroxysuccinimide), ethanolamine solution, TCEP (tris(2-carboxyethyl)phosphine), HEPES (4-(2-hydroxyethyl)-1-piperazineethanesulfonic acid ) and TRIS (tris(hydroxymethyl)aminomethane))reagents were purchased from Sigma-Aldrich.

## Methods

### PDMS substrates preparation

Square surfaces of SMI silicone sheets were cut at defined dimensions of 18mm x18mm and deposited on glass slides permitting easier manipulations during the functionalization steps and the use of a dipping robot for the multilayer construction. Prior to the film elaboration, substrates were cleaned with ethanol (10mL) and then rinsed with milli-Q water (3x10mL).

### Polyelectrolyte multilayer film construction

In order to elaborate films owning high number of layers, a dipping robot was used (Dipping Robot, Riegler and Kirstein, GmbH, Berlin, GERMANY). During the construction, the substrates were alternatively immerged inpolyelectrolyte and rinsing solutions. The build-up process begun with a dipping step of the PDMS surfaces in a PEI solution for 10mn followed with a rinsing step in buffer solution of 4mn. This first step was performed in order to form an anchoring layer on the top of the silicone substrates. The PLL-S-TP/HA architecture was then obtained by dipping the silicone substrates in a hyaluronic acid (HA, polyanion) solution for 4mn followed by two rinsing steps of 5mn in NaCl 0.15M buffer solutions. The PLL-S-TP (polycation) was then deposited in the same manner. The build-up process was pursued by the alternated deposition of PLL-S-TP and HA. After deposition of n bilayers, the film is denoted (PLL-S-TP/HA)$_n$. We used films constituted of 24 PLL-S-TP/HA "bilayers".

*Crosslinking steps*

- Film reticulation

Once the PLL-S-TP/HA film wasbuilt, it was cross-linked by immersion of the PDMS substrates in 3mL of a 20 mM EDC / 50 mMSulfo-NHS in NaCl (0.15M in milli-Q water) solution for 24h at 4°C. This step was performed tohavecarboxylic acid groups from HA reacting with amine groups present on PLL. The films were then washed during 5 times with a10mL NaCl (0.15M in milli-Q water) solution and immersed in 3mL of 1M ethanolamine solution in NaCl (0.15M in milli-Q water) for 40mn to react with eventual remaining activated carboxylic groups. Once this step wasperformed the films were washed5 times with 10mL NaCl (0.15M in milli-Q water) solution.

- Enzyme crosslinking

100µL of enzyme solution (0.4mg/mL in a 10mM HEPES buffer solutionatpH 6) was deposited at the top of the multilayer film for 1h to permit its penetration inside the polymeric matrix. After removing the excess of enzyme solution on the top of the film, 200µL of a TCEP solution (1.14mM in TRIS10mM/NaCl150mM in milli-Q water) was brought in contact for 30mn without rinsing step. Once the reaction finished, the sample was rinsed with 10mL of TRIS10mM/NaCl 150mM in milli-Q water and enzymatic tests were performed.

*Enzymatic reaction tests*

The enzymatic activity of the polyelectrolyte multilayer films were monitored by placing them in a home-made stretching device (see part II.A.4) in a specifically manufactured support and adding 3.8mL of a FDG solution at $0.1mg.mL^{-1}$. The reaction was monitored by measuring the emission intensity at 515nm.

## 2.1.3.Project 3: Design of mechano-responsive materials based on multilayer films made from alginate-catechol and alkaline phosphatase

### Materials

All the reagents were purchased from Sigma-Aldrich: branched polyethyleneimine (PEI, Mw =750000), alkaline phosphatase (ALP, P-4002), 4-nitrophenylphosphate (PNP, disodium salt solution), sodium alginate (Mw = 350000) and $NaIO_4$, $CaCl_2$, $CH_3COONa$ salts buffersolutions.A rinsing buffer of sodium acetate ($NaCO_3$, 10mM, pH a 4.5) used during the build-up process was prepared. An additional buffer solution (TRIS. 50mM. pH 8.5) used for the storage and the washing of the film was prepared. All the solutions were prepared using ultra-pure water (resistivity of 18MΩ.cm, Milli-Q-plus water system, Millipore).

*Polyelectrolyte solutions*

Polyelectrolyte compounds used to build multilayer films were dissolved in a buffer solution of sodium acetate ($NaCO_3$) 10mM in ultra-pure water (resistivity of 18MΩ.cm, Milli-Q-plus water system, Millipore). Polyelectrolyte solutions were prepared at a concentration of 1mg/mL with adjusted pH of 4.5. As previously,the branched PEI was used as a first anchoring layer for the build-up of the polyelectrolyte multilayers.

In order to covalently bind our polymeric structure, a modified alginate-catechol polymer was synthesized in our laboratory. This polymer was elaborated by Dr. Tony Garnier according to the protocol from Kastrup et al. [4]and was denoted alginate-catechol (AC, Mw = 350000, grafting ratio 10%).



***Figure 2.4****: Alginate polysaccharide modified with catechol moieties (in red.*

*Enzyme solutions*

For this project, the polyanionneeded for the elaboration of multilayer films was replaced by a positively charged enzyme under specific experimental conditions: alkaline phosphatase (ALP, Sigma-Aldrich, P-4002). It wasdissolved at a concentration of 1mg/mL in a solution of sodium acetate ($NaCO_3$) 10mM in ultra-pure water (resistivity of 18MΩ.cm, Milli-Q-plus water system, Millipore) with adjusted pH of 4.5inferior to the isoelectric point of the ALP[5].

*Enzymatic substrates*

- *p* −nitrophenylphosphate (4-nitrophenyl phosphate, PNP)

The enzymatic activity of phosphatase alkaline was monitored by dipping of multilayer films in a solution of PNP (figure 2.5) at a concentration of 10%in a buffer solution of TRIS 50mM at pH 8.5. Under the action of alkaline phosphatase, the *p*-nitrophenyl phosphate (PNP) is hydrolized in *p*-nitrophenolate (PN) and in a phosphate ion. The produced PN during the enzymatic reaction can be detected by absorbance measurement at $\lambda_{absorbance}$ = 405nm witha UV/Visible spectrophotometer.



*Figure 2.5:Hydrolizis of PNP in presence of alkaline phopsphatase.*

- Fluorescein Di-Phosphate (FDP)

The enzymatic activity of alkalinephosphatase can also be monitoring by dipping multilayer films in a solution of fluoresceindi-phosphateat 0.1mg.mL$^{-1}$(FDP, Invitrogen) in a TRIS 50mM buffer at pH 7.4. The fluoresceindi-phosphate is a colourless and non-fluorescent substrate from alkaline phosphatase(figure 2.6) leading, after enzymatic transformation in fluorescein, to a better resolution in detection than PNP. The enzymatic hydrolysis of FDP takes place in two steps, leading first to the formation of fluorescein mono-phosphate and then to fluorescein ($\lambda_{excitation}$ = 490nm / $\lambda_{emission}$ = 515nm). It must be noted that FDP solutions used can own a low fluorescent background due to mono-phosphate fluorescein or initially present

fluorescein in the commercial reagent. As previously, the enzymatic activity occurring during the experiments was monitored by using a UV/Visible spectrophotometer.



Fluorescein Di-Phosphate (FDP)                    Fluorescein

*Figure 2.6: Hydrolysis of FDP in fluorescein in presence of alkaline phosphatase.*

## Methods

Multilayer films were prepared on silica slides (12mm diameter, VWR International, Strasbourg, France) or on silicone sheets (Specialty Manufacturing Inc. SMI, Michigan, USA)of 254μm thick and12mm diameter. Surfaces were cleaned with ethanol then pure water before use. The films were elaborated according to the layer-by-layer technique consisting in the successive adsorption of negatively and positively charged polyelectrolytes. In order to homogeneously coat the surfaces during the elaboration of the films, a PEI layer was deposited on the substrates by dipping them for 4mn in a solution of PEI. The PEI solution wasthen rinsed with asolution of sodium acetate 10mM pH 4.5for 2mn. Once this step wasperformed, the multilayer build-up was performed. The substrates were first dipped in a catechol functionalized alginate (AC, polyanion) solution for 4mn. Then a rinsing step was performed by dipping them 2mn in sodium acetate buffer (10mM, pH 4.5). The alkaline phosphatases (ALP) were then deposited according to the same conditions. The build-up process was pursued by the alternate depositions of alginate and enzymes leading to the multilayer films elaboration. After deposition of n bilayers, the film is noted PEI(AC/ALP)$_n$.

The surfaces were then put in contact with a solution of CaCl$_2$ 3,3 mM in sodium acetate buffer pH 4.5 for 10mn to complex the alginate, and then dipped in a solution of sodium periodate (NaIO$_4$) for various time. Under oxidative conditions, catechol groups become reactive and crosslink the multilayer film, leading to the formation of a covalently bound matrix. Once the crosslinking stepwas accomplished, the films were stocked in 30mL of TRIS 50mM pH 8.5 buffer until use in order to keep the integrity of the enzyme. The

buffer was replaced every 24 hours to wash the film from non-covalently linked species. After 3 days of washing, first enzymatic activity tests were performed.

*Enzymatic reaction monitoring:*

The enzymatic activity of the films was monitored measuring the absorbance of the produced PN during the reaction using a UV/Visible multidetectorspectrofluorimeter (Xenius XC, SAFAS, Monaco) equipped with a microplate reader. The films were put in a 24-well cell culture plate with 2mL of premixed PNP solution and absorbance measurements at 405nmwere performed each 30sec for 2h.

## 2.1.4. Stretching devices

In order to study our surfaces under constraint, a homemade stretching device was designed and elaborated in our group (figure 2.7). It permits to stretch our silicone substrate in a longitudinal way up to 100% elongation.



***Figure 2.7:*** *Stretching devices: The silicone sheets are placed between the two clamps and stretched manually.*

The stretching degree is defined as:

$$\alpha = \frac{(l - l_0)}{l_0} \cdot 100$$

With $l_0$ and $l$ corresponding respectively to the initial and the stretched length of the silicone substrate. All the stretching experiments were performed at room temperature under liquid conditions.

In order to detect the enzymatic activity of films during stretching experiments with a high sensitivity, an homemade support made of poly(methyl methacrylate) designed to permit fluorescence measurementswas used (figure 2.8).The monitoring of the reaction was

performed by adding 3.8 mL of the enzymatic substrate in the support, and analyzing the fluorescence response each 30sec for various times.



**Figure 2.8:** *Homemade support elaborate to monitor the enzymatic activity using a spectrofluorimeter SAFAS (Xenius XC, SAFAS, Monaco).*

## 2.2. Physico-chemical characterization

### 2.2.1. UV-Ozone oxidation process

**Principle:**

UV-Ozone treatment is a photo-sensitized oxidation technique based on the high reactivity of oxygen radical (O*). As shown in figure 2.9, two distinct UV wavelengths are involved in this process.
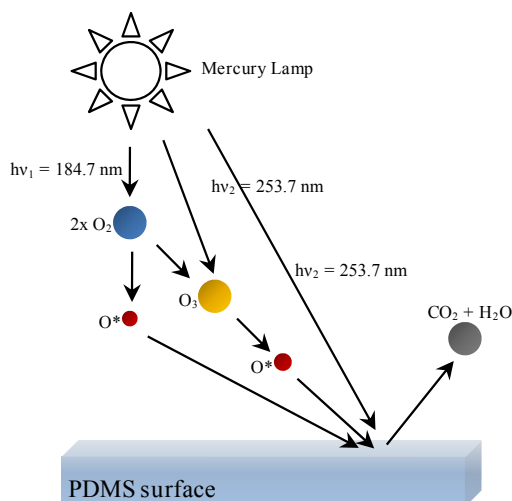


**Figure 2.9**: *UV-Ozone process: creation and reaction of atomized oxygen. A first wavelength hv1=184.7 nm is involved in the fission of diatomized oxygen leading to the creation of radical oxygen species and ozone molecules. The second wavelength hv2=253.7nm can directly react with the PDMS surface leading to the formation of carbon dioxide or water, or with ozone molecules to regenerate dioxygen molecules and radical oxygen species.*

The first radiation at λ=185nm is used to dissociate the $O_2$ molecule coming from the air to formradical oxygen reactive species. As a strong oxidant agent, atomic oxygen can generate $O_3$ by reacting with $O_2$ or by directly interacting with the surface of our substrate. The second wavelength at λ=254 nm corresponds to the energy needed for the ozone dissociation. If both are present a continuous creation and destruction of ozone occurs, increasing the quantity of O* formed. The second wavelength is also involved in the creation of radicals on the surface of our substrate by reacting with organic matter. All these reactions lead to the creation of functions at the surface of our material such as carboxylic acid or silanol groups [6] by reacting with methyl groups from PDMS. A reaction between carboxylic groups and ozone molecules can also occur and lead to the creation of volatile molecules such as carbon dioxide. It must be noted that a too long exposure time also leads to the formation of a breakable silica layer at the top of our PDMS substrate [7].

### Procedure:

UV-Ozone oxidation processes were performedusing a UV-ozone Pro Cleaner Bio Force Nanosciences machine that has a mercury vapor lamp, wavelengths of 254 nm and 185 nm with an UV intensity of 14.76 mW/cm$^2$. It was placed at 1 cm of distance from the sample for the PDMS surface activation.

### 2.2.2 Contact angle measurement:

Contact angle measurement is an easy and quick technique to control the surface properties of a material. The method consists in measuring the contact angle of a droplet deposited on a surface.

### Principle:

The shape of a droplet deposited on a material is the result of a combination of different interfacial energies occurring: liquid/vapor $\gamma_{LV}$, solid/liquid $\gamma_{SL}$ and solid/vapor $\gamma_{SV}$. The static contact angle θ between the outline tangent of the drop and the surface at the triple interface solid-liquid-vapor point is given by Young-Dupré's equation:

$$\gamma_{SV} - \gamma_{SL} = \gamma_{LV} \cos \theta$$
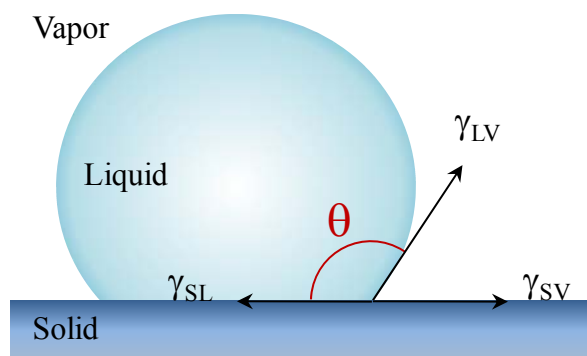
***Figure 2.10****: Schematic illustration of Young-Dupré's relation linking the shape of a liquid droplet (contact angle θ) with the different interfacial tensions in presence; liquid/vapor $\gamma_{LV}$, solid/liquid $\gamma_{SL}$ and solid/vapor $\gamma_{SV}$.*

It can be noted that if water is used as the liquid, the hydrophilic (small contact angle θ, high surface energy) or hydrophobic (high contact angle θ, low surface energy) properties of the surface can be deduced.

**Procedure:**

Contact angle measurements were performed with a DIGIDROP-GBX® coupled with a cameraby using 6μL pure water droplets. Series of three measures were performed and averaged for each treatment.

**2.2.3. UV-Visible spectroscopy**
**Principle:**

The UV-Visible spectroscopy is based on the properties of molecules owing chromophore groups to absorb specific wavelengths of the UV-Visible spectra. By measuring of the absorbance, this method permits the determination of the chromophore's concentration according to Beer-Lambert law. The absorption of a sample is measured by a spectrophotometer for a specific incident wavelength of the UV-Visible spectra (from 200nm to 900nm).

The Beer-Lambert law linksthe intensity of transmitted radiation *I* (that passed through the material) with the incident radiation $I_0$(initial intensity) and the length *l* of the sample study.

$$I = I_0 e^{(-\varepsilon l c)}$$

With $c$ and $\varepsilon$correspondingrespectively the concentration (mol·L$^{-1}$) and the molar extinction coefficient (L·mol$^{-1}$·cm$^{-1}$) of the chromophore group for a defined wavelength. It must be noted that this relation makes sense only for diluted middle with $c<$ 100mmol·L$^{-1}$.

In UV-Visible spectrophotometry, the absorbance A is the parameter used to draw spectra. It is unit less and expressed as a logarithmic ratio between the radiation falling up a material$I_0$ and the radiation transmitted through a material $I$.

$$A = -\log\left(\frac{I}{I_0}\right) = \varepsilon \cdot l \cdot c$$

**Procedure:**

During this thesis, spectrophotometry was used to monitor enzymatic activity of different enzymes such as $\beta$-galactosidase or alkaline phosphatase in presence of their respective substrates. Measurements were performed using an UV/Visiblemultidetectorspectrofluorimeter (Xenius XC, SAFAS, Monaco) equipped with a microplate reader.

**2.2.4.Fluorescence based microscopy**

**Principle of fluorescence:**

Fluorescence is the property of some molecules to adsorb a photon at a specific wavelength (h$\nu_{ex}$) and to re-emit it at a higher wavelength (h$\nu_{em}$)(figure 2.11;Jablonskidiagram). Under a specific wavelength, the molecule is first excited from its initial state $S_0$ to a superior energy level state $S_1$'. At room temperature, non-radiative loss of energy occurs. The molecule loses some of its energy due to vibrational relaxation and collisions with surrounding molecules, leading it to a lower energy state $S_1$. The return of the molecule to its initial state $S_0$ is linked to the emission of a photon. This photon is characterized by a lower energy than the initially absorbed one leading to a higher wavelength of emission than excitation. This difference of energy is called Stokes shift.
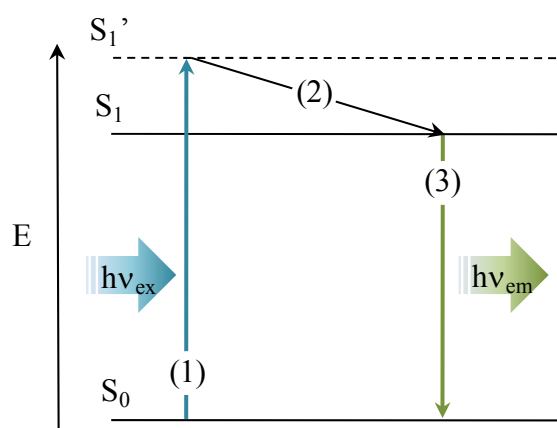
*Figure 2.11*: *Jablonski diagram. (1) The fluorescent molecule at its fundamental state $S_0$ adsorbs a photon and is promoted to the excited state $S_1$'. During its deexcitation process, a first non-radiative loss of energy due to intern conversion occurs (2) leading the molecule to a lower excited state $S_1$. Finally the molecule undergoes an electronic transition from its excited state $S_1$ to its initial state $S_0$ (3) leading to the emission of a photon characterized by $h\nu_{em} < h\nu_{ex}$.*

It must be noted that fluorescence intensity and emission/excitation wavelengths are specific for each molecules also called fluorophores. Generally, fluorophores are small molecules, which can be covalently linked to molecules of interest such as polymers or biological macromolecules. According to their important quantum yield of fluorescence they allow precise detections of labeled species by various techniques of fluorescence microscopy.

**Principle of the fluorescence microscopy:**

The fluorescence microscopy is a technique using a traditional optical microscope coupled with filters and lights sources to observe fluorescent species. According to the Stokes shift principle, it is possible to observe fluorescentmolecules by specifically excite them and filtering the returning light (figure 2.12). The light emitted by a mercury lamp or a laser is first filtered in order to define a specific wavelength of excitation. It is then directed by a dichroic mirror on the sample. The emission light of the sample is then filtered in order to only keep its fluorescent contribution. It must be noted that owning a low detection threshold, this technique permitsa better contrast observation than absorbance measurements, thus is used when low quantity of matter has to be characterized with precision.
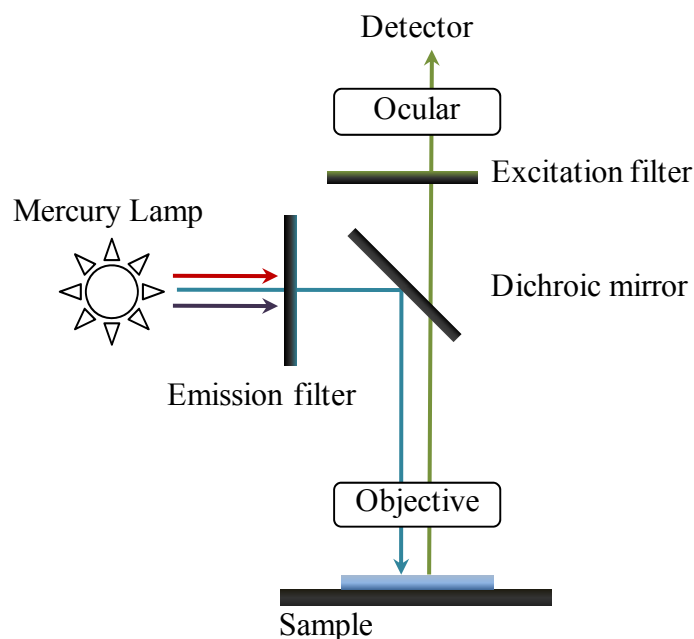
***Figure 2.12***: *Schematic representation of a fluorescence microscope.*

## Procedure:

The fluorescence measurements described in this work were performed using an inverted light microscope (Nikon Microphot-FXA, Japan) equipped with a mercury lamp and operating between 470nm and 490nm for excitation and above 500nm for detection. The image analyses were performed using ImageJ software (Raspband, W. S, ImageJ, U.S. National institutes of Health, Bethesda, USA).

## Principle ofConfocal Laser Scanning Microscopy (CLSM):

In standard fluorescence microscopy, the sample is illuminated in its integrality leading to a high amount of out-of-focus light perturbing the observation. In order to prevent this phenomenum and to increase the resolution of the fluorescence analysis, confocal laser scanning microscopy was developed. This technique consists in using a point illumination produced by a laser with a defined wavelength at a precise point of the sample (focal point). Parasite fluorescence coming from plans other than the focal one is removed using a pinhole leading to an increase of the signal-to-noise ratio. Thesample is scanned point per point along a defined line creating a two dimensional slice image. Three dimensional representation of the sample is obtained by stacking individual XY slices.
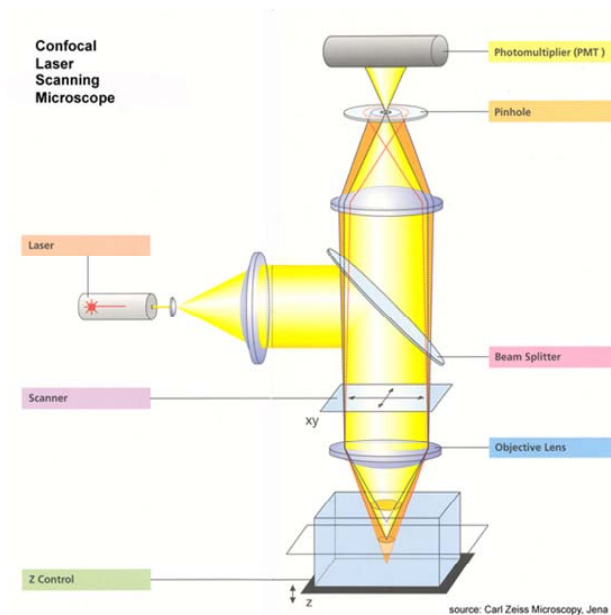
*Figure 2.13*: *Schematic representation of the confocal laser scanning microscopy principle. The laser beam is directed and focused on a specific point of the sample. Emitting light is filtered using a pinhole, leading to the elimination of out of focuse light. Final fluorescence is collected using a photomultiplier.*

## Procedure:

Confocal laser scanning microscopy observations were used in order to visualize build-up of polyelectrolyte multilayer films labeled with fluorescent polymers. Experiments were performed using a confocal microscope LSM 510 META (Carl Zeiss S. A. S., Le Pecq, France) equipped with Helium-Neon(543nm) and Argon (459,488 and 514nm) lasers. Images were obtained using 40x wet objective, scanning the samples with argon laser at 488nm for excitation, emission light taking back at 520nm. Images were treated using ImageJ software (Raspband, W. S, ImageJ, U.S. National institutes of Health, Bethesda, USA).

### 2.2.5.Atomic Force Microscopy (AFM):

The Atomic Force Microscopy (AFM) is a near-field microscopy developed in the middle of the 1980's by Binnig, Quate and Gerber. The AFM is a Scanning Tunneling Microscope variant used for the topography analyze of non-conductive surfaces. The AFM imaging consists in the detection of interactions occurring between a tip and the surface of a sample during a scanning process. This technique allows a resolution of a few nanometers in the (x,y) plan and Angström in the z direction. Development of this technique permits

moreoverthe studies of more characteristics of the surface such as mechanic, electrostatic and magnetic properties.

**Principle:**

The AFM imaging is based on the measurements of the interatomic forces (van der Waals, electrostatic forces, ionic forces…) occurring between a mono-atomic tip and a surface. This tip is attached at the end of a cantilever characterized by its spring constant *k*. During the scanning process, interactions between the tip and the surface generate a deflection $\Delta z$ of the cantilever. This deflection is monitored by analyzing the reflection of a laser beam on the cantilever using a photodiodes system.
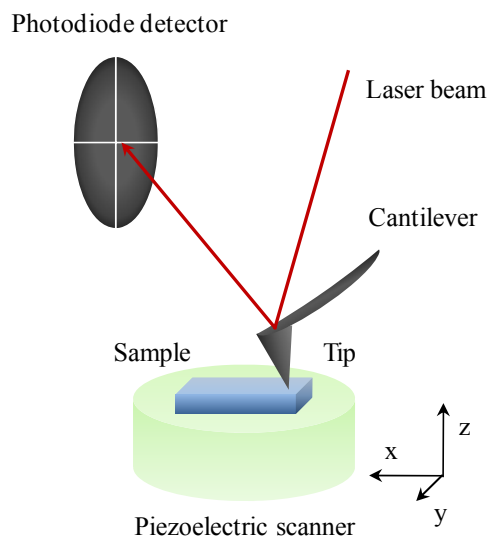


*Figure 2.14: Schematic representation of Atomic Force Microscopy (AFM).The sample is fixed on a piezoelectric scanner. The cantilever is approached to the surface. During the scanning process, interactions between the tip and the surface generate a deflection Δz of the cantilever. This deflection is monitored by analyzing the reflection of a laser beam on the cantilever using a photodiodes system.*

The variation of intensity detected on the different photodiodes allows determining with precision the cantilever deflection and, according to the Hook law, to the forces (F) occurring on the tip.

$$F = k\Delta z$$

**Imaging of the surface:**

The topography of the substrate is obtained by the determination of the cantilever deflection in each point (x,y) of the surface. Different modes of measurement were developed

in order to characterize the surface topography and physicochemical properties, the most used onesare: contact, no-contact and tapping modes (figure 2.15).
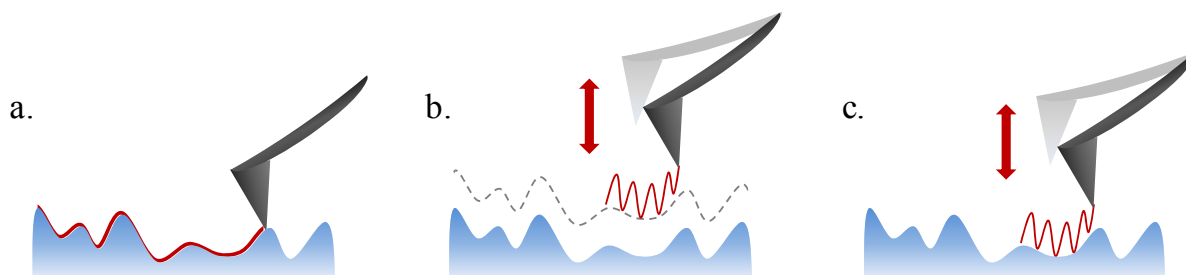


**Figure 2.15**: *Schematic representation of the main modes for AFM imaging: (a) contact mode, (b) no-contact mode and (c) tapping mode (intermittent contact).*

During this thesis, only the contact one was used. In this mode, the tip is kept in contact with the sample surface using a constant force (about 10nN). A retroactive process adjusts permanently the z position of the substrate.Analysis of this shifting leads to the creation of a topography imaging of the surface.

**Procedure:**

Atomic Force Microscopy (AFM) was performed using a Multimode/NanoscopeIV microscope (Veeco/Brucker, Santa Barbara, USA). All the pictures were imaged in contact mode using silicon nitride cantilevers with a spring constant k = 0.03N*m$^{-1}$ (MSCT model, Veeco/Brucker, Santa Barbara, USA) at scanning rate of 2Hz under liquid conditions.AFM imaging was performed on multilayer films and polymer matrices built on QCM quartz crystals, quartz slides and silicone substrates. The thickness of the samples was determined by analysing a profilometric section of the filmsmade with the end of a tweezer. Roughness was evaluated on 10 x 10 μm$^2$ area by calculating the root mean squared roughness. The image analyses were performed using Nanoscope software version 8.15 (Digital Instrument, Veeco).

### 2.2.6. Quartz Crystal Microbalance (QCM)

The Quartz Crystal Microbalance with Dissipation (QCM-D) is a high-resolution mass sensing technique based on the piezoelectric effect of a quartz crystal. This technique consists in measuring the changes in resonance frequency ($\Delta f$) and in dissipation ($\Delta D$) of a quartz crystal induced by material adsorption on its surface in order to estimate the quantity of matter deposited. It allows the measurement of mass deposition with a sensitivity in the ng·cm$^-$

[2]range. During our works, the QCM-D permitted us the monitoring *in-situ* of the multilayer films construction and by applying mathematical models to our results, to determine their hydrodynamic thickness.

**Principle:**

The principle of Quartz Crystal Microbalance (QCM) was developed in the 1960's by G. Sauerbrey based on the piezoelectric properties of quartz. Indeed, quartz is a material that deforms when it is submitted to an electrical potential difference, and inversely, under mechanical stress, a polarization appears at its terminals. The QCM substrates are composed of a quartz disc of 0.3mm thick, surrounded on both sides with conductive gold electrodes. One of the electrodes is coated with a silicon layer.By applying a potential difference between the two electrodes, a shear movement of the quartz crystal is induced. By fixing the lower side of the crystal on a stationary support, the upper side undergoes a horizontal translation movement resulting in mechanic oscillations (figure 2.16).
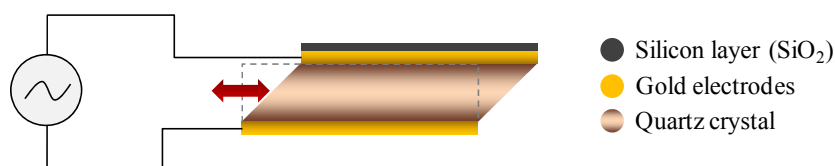


*Figure 2.16*: *Schematic representation of a quartz crystal coated with gold electrodes. Potential differency applied on it leads a shear constraint (represented by the red arrow) in a perpendicular way of the electric field application.*

Owing a fundamental frequency and overtones, the system can be compared to a harmonic oscillator characterized by its resonance frequency$f_r$.

$$f_r = \frac{1}{2\pi}\sqrt{\frac{k}{M}}$$

With *M* and *k* representing respectively the oscillator mass and spring constant. When a mass *m* (*m* <<*M*) is deposited on the surface of the quartz crystal, the total mass of the oscillator becomes m + M and a new resonance frequency *f* is associated to the system:

$$f = \frac{1}{2\pi}\sqrt{\frac{k}{M+m}} \approx f_r\left(1 - \frac{m}{2M}\right)$$

The deposition of a mass $m$ at the surface of the crystal quartz leads to a shift in resonance frequency $\Delta f$ corresponding to:

$$\Delta f = f - f_r = \frac{-mf_r}{2M} = -\frac{m}{C}$$

With $C$ a characteristic constant of the quartz crystal used, called Sauerbrey constant:

$$C = \frac{2M}{f_r}$$

The principle of the QCM consists in measuring the changes in resonance frequency ($\Delta f$) of the quartz crystal induced by materials deposited on its surface and so to determine the quantity of matter deposited. It must be noted that this mass deposition can not only be monitored at the quartz crystal fundamental frequency but also at all its overtones $v$ leading to an extension of Sauerbrey's law:

$$m = -C\frac{\Delta f_v}{v}$$

It must be noted that the Sauerbrey law can be used as a good first approximation in liquid condition when the values of $\frac{\Delta f_v}{v}$ corresponding to all the harmonics are superposed. It is only valid in ideal cases of thin rigid and uniform film depositions and in the absence of friction and viscoelastic effects. In the case highly hydrated films that behave like viscous liquids or gels, Sauerbrey's law is replaced by the Voigt-Voinova model taking in account the viscoelastic properties of the deposited material.

Recent technique evolutions and development of QCM-D, allow taking in account a new experimental parameter, the dissipation factor D (figure 2.17). This parameter is linked to the viscoelastic properties of the deposited film on the crystal surface and is defined as the proportion of energy lost at each crystal oscillation compared to the energy stored in the oscillator. It is experimentally obtained by measuring the relaxing time after mass deposition of a quartz crystal initially excited at its resonance frequency for a few μs. This relaxation time

is inversely proportional to the damping constant of the system and allows the determination of the factor D, characteristic of the viscoelastic properties of the films.
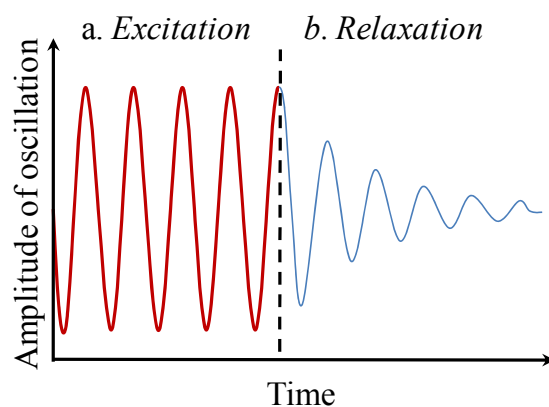


***Figure 2.17****: Oscillation amplitudes of the quartz crystal as a function of time during a QCM-D experiment. (a) Excitation of the quartz crystal at its resonance frequency. (b) Relaxation phase of the quartz crystal leading to the determination of the factor D.*

## Procedure:

The construction of the multilayer films was monitored *in situ* by Quartz Crystal Microbalance (QCM-D, Q-Sense E4, Götenborg, Sweden) at a stabilized temperature of 22°C. The quartz crystal is excited at its fundamental frequency (5MHz) and the measurements are performed at its overtone v1, v3, v5 and v7 (respectively 5, 15, 25 and 35 MHz). According to Sauerbrey's law, in first approximation, a shift in $\Delta f$ can be associated to a variation of mass adsorbed on the crystal. It must be noted that only the frequencies and dissipations at the end of the rinsing step following the layer adsorption are taken into consideration for the characterization of the film.

Before each experiment the QCM quartz crystal is cleaned under UV-Ozone during 10mn and put in contact with the buffer solution until stabilization. Once the crystal isstable, the build-up of the film is performed following the layer-by-layer deposition method. 600µL of corresponding solutions are alternatively injected with an automatic pump in the QCM cell. This volume is chosen in order to completely replace the previous solution injected in the system. The solution is then let in contact with the surface for 5mn. After each polymer deposition, the measurement cell is rinsed using a buffer solution for 5mn.

At the end of the experiment, the system is cleaned withfour successive rinsing solutions for 10mn: Hellmanex 2% solution, hydrochloric acid 0.1Msolution, sodium hydroxide 0.1M solution and finally milli-Q water. Compressed air is then used to dry the different QCM components.

### 2.2.7.Fourier TransformInfraRedspectroscopy (FTIR)

Infra-Redspectroscopy (IR) is a vibrational spectroscopy technique dealing with the mid-infrared region of the electromagnetic spectrum (4000-400cm$^{-1}$). It is used for the chemical characterization of gaseous, liquid and solid samples.The Fourier Transform Infrared Spectroscopy (FTIR) used during this work is a particular IR method based on the use of an interferometer in order to increase the sensitivity and the speed of the measurements.

### Principle:

Infrared spectroscopy is based on the fact that molecules absorb specific frequenciescharacteristic of their structure.Matching with the transition energy of the bond or group that vibrates, these absorptions are called resonance frequencies. The energies are determined by the shape of the molecular potential energy surfaces, the masses of the atoms and the associated vibronic coupling.

All the chemical bounds don't absorb in the same way in the infrared domain, depending in particular on the molecule symmetry. It exists different symmetric or asymmetric modes of vibration called elongation or deformation (figure 2.18). The masses of the atoms as well as their electronegativity also have an influence on the adsorption bands positions.
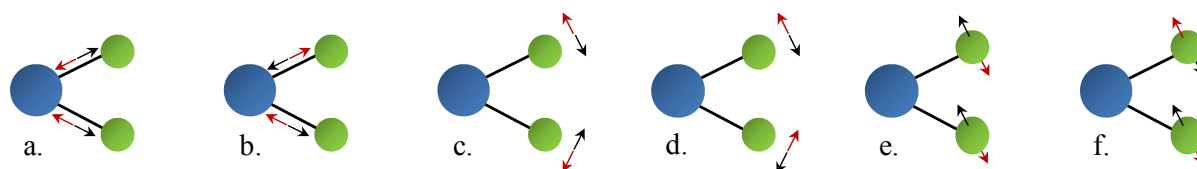


*Figure 2.18: Modes of vibrations: symmetric (a) and asymmetric (b) elongation; symmetric (c) and asymmetric (d) deformation in the plan; symmetric (e) and asymmetric (f) deformation out of the plan.*

Thus, the frequency of the vibrations is associated with a particular mode of motion and a particular bond type giving information about the chemical nature of the molecule.

During the experiment, an infrared incident beam (2.5-25µm)is going through a sample and an analysis of the transmitted beam in function of the wavelength is performed. The infrared spectrum is established by monitoring the energy absorbed at each wavelength.This acquisition can be performed with a monochromatic beam and modifying its wavelength with time or by using a Fourier transforms apparatus. In the FITR method, the sample is simultaneously lightened at all the wavelengths and the infrared spectrum is obtained in integrality by processing the transmitted signal. This technique allows short acquisition times improving both acquisition number and signal-to-noise ratio leading to high sensitivity detection.

**Attenuated Total Reflectance Fourier Transform Infra-Red spectroscopy (ATR-FTIR):**

Attenuated total reflectance mode uses a property of total internalreflection resulting in an evanescentwave.The infrared incident beam is directed through a ZnSe crystal characterized by its high refractive index ($n_1$). At the interface between the crystal and the less refractive index ($n_2$) middle, at least one reflection occurs. This reflectionforms the evanescentwaves which extendinto the sample. The penetrationdepthinto the sampleistypicallybetween 0.5 and 2µm.
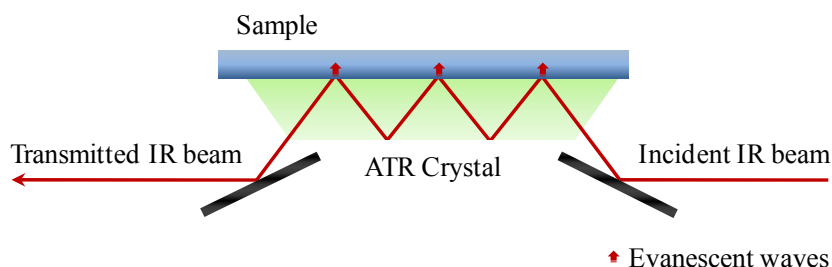


*Figure 2.19: ATR crystal multireflection principle.*

The advantage of using ATR-FITR over transmission-IR is the limitedpathlengthinto the sample, avoidingproblem of strongattenuationof the IR signal in absorbingsamplessuch as highlyhydratedmaterials. Moreover developments of specificexperimentscellspermit*in-situ*build-up of multilayer films in aqueous conditions on the crystal surface, leading to an infrared monitoring of the multilayer film elaboration.

**Procedure:**

Duringtheseworks, the ATR-FTIR spectroscopywas used for the characterization of both PDMS substrates and layer-by-layer films.

(a) Surface characterization

This method wasperformed by putting the surface of interest in contact with the ATR crystal. It must benotedthat if the characterizationneeded to occur in liquid conditions, the sampleswere prior to the analysisimmersed in a $D_2O$ solution for one night. Thisstepisperformed in order to replace $H_2O$ with $D_2O$ in the samplesand thuslimitinfraredbeamabsorption.

(b) In-situ multilayer films elaboration

Beforeeachexperiment the ATR germanium crystal iscleanedwithethanol solution, placed in the FTIR liquidcelland put in contact with the buffer solution untilstabilization. Once the crystal is stable, the build-up of the film isperformedfollowing the layer-by-layer depositionmethod. 1mL of corresponding solutions are alternativelyinjectedwith a syringe in the specific ATR-FTIR liquidcell. This volume ischosen in order to completely replace the previous solution injected in the system. The solution isthen let in contact with the surface for 10mn. Aftereachpolymerdeposition, the measurementcellisrinsedusing a buffer solution for 10mn and an infraredspectrum isacquired. It must benotedthatpolymer and buffer solutions are preparedshortlybefore the manipulation using $D_2O$. If necessary, pH adjustments are performedusingDCl and OD solutions.

At the end of the experiment, the system iswashedwith four successive rinsing solutions for 10mn: Hellmanex 2% solution, hydrochloricacid 0.1M solution, sodium hydroxide 0.1M solution and then milli-Q water. Compressed air is finally used to dry the different ATR-FTIR components.

All the experimentswereperformedusing an FTIR spectrometer (Vertex 70, Bruker, Billerca, MA, USA) equippedwith a deuteratedtriglycine sulfate (DTGS) detector. Total

reflectance ATR ZnSe crystalaccessorywasused for IR measurements. All spectra acquisitions wereperformedat 2cm$^{-1}$resolution over 20 scans within the range 4000-800cm$^{-1}$.

## 2.3. References

1.      V. Hong, S.I. Presolski, C. Ma, and M.G. Finn, *Analysis and optimization of copper-catalyzed azide-alkyne cycloaddition for bioconjugation.* Angewandte Chemie-International Edition, 2009. **48**(52): p. 9879-9883.

2.      J.E. Hein, Krasnova, L. B., Iwasaki, M., Fokin, *Cu-catalyzed azide-alkyne cycloaddition: Preparation of tris((1-benzyl-1h-1,2,3-triazolyl)methyl)amine.* Organic Syntheses, 2012: p. 238–246.

3.      Q. Wang, T.R. Chan, R. Hilgraf, V.V. Fokin, K.B. Sharpless, and M.G. Finn, *Bioconjugation by copper(i)-catalyzed azide-alkyne 3+2 cycloaddition.* Journal of the American Chemical Society, 2003. **125**(11): p. 3192-3193.

4.      C.J. Kastrup, M. Nahrendorf, J.L. Figueiredo, H. Lee, S. Kambhampati, T. Lee, S.W. Cho, R. Gorbatov, Y. Iwamoto, T.T. Dang, P. Dutta, J.H. Yeon, H. Cheng, C.D. Pritchard, A.J. Vegas, C.D. Siegel, S. MacDougall, M. Okonkwo, A. Thai, J.R. Stone, A.J. Coury, R. Weissleder, R. Langer, and D.G. Anderson, *Painting blood vessels and atherosclerotic plaques with an adhesive drug depot.* Proceedings of the National Academy of Sciences of the United States of America, 2012. **109**(52): p. 21444-21449.

5.      A. Garen and C. Levinthal, *A fine-structure genetic and chemical study of the enzyme alkaline phosphatase of e. Coli. I. Purification and characterization of alkaline phosphatase.* Biochimica et biophysica acta, 1960. **38**: p. 470-83.

6.      K. Efimenko, W.E. Wallace, and J. Genzer, *Surface modification of sylgard-184 poly(dimethyl siloxane) networks by ultraviolet and ultraviolet/ozone treatment.* Journal of Colloid and Interface Science, 2002. **254**(2): p. 306-315.

7.      Y. Berdichevsky, J. Khandurina, A. Guttman, and Y.H. Lo, *Uv/ozone modification of poly(dimethylsiloxane) microfluidic channels.* Sensors and Actuators B-Chemical, 2004. **97**(2-3): p. 402-408.

# Modification of the Green Fluorescent Protein spectral response under mechanical constraints

## Contents

## 3.1. Introduction

The goal of mythesis was to designmechano-responsive materials that transform a mechanical stress into a chemical signal by mimicking physico-chemical processes taking place during cell adhesion, namely based onstretched induced protein conformational changes. We planned to achieve this goal by covalently grafting enzymes onto stretchable substrates. Stretching suchsubstratesshould induce changes in the conformation of grafted enzymes and lead tochanges in their enzymatic activity[1-3]. In order to make a proof of concept we first intended to "visualize" conformational changes in proteins that respond physically to such stretching. For this purpose green fluorescent proteins (GFP) seemed to be examples of choice since it is known[4]that GFP conformational changes are accompanied by changes in their absorption or fluorescence spectra. We thus first intended to covalently linkspecifically GFP moleculesonto silicone substrates (see figure 3.1) and verify iffluorescence changes are detectableby stretching.



Specific modification of the GFP with azide groups

Unstretched state « fluorescence on »

Stretched state « loss of fluorescence »
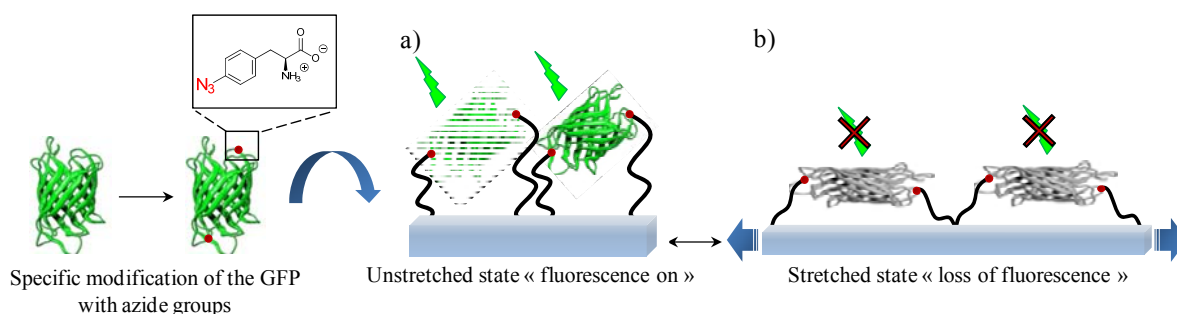
*Figure 3.1* : *Schematic representation of the mechano-responsive surface. At rest (a), modified GFP are grafted onto a stretchable substrate, fluorescence is detected. Under stretching (b) the GFPthree dimensionalstructures is put out of shape leading to a loss of its fluorescence response.*

This study was performed within the framework of the International Research Training Group (IRTG). The IRTG « Soft Matter Science (SoMaS) : Concepts for the Design of FunctionalMaterials »  is a European collaboration between the universities of Freiburg (Germany), Strasbourg, Mulhouse (France) and Basel (Switzerland), promotinggraduateeducation and scientific exchange in this modern field of research on soft mattermaterials. This study corresponds to a joint project withChunyan Yao from the University of Freiburg and took place at the interface between soft matter and biologicalsystems. It wasdivided in two distinct and successive parts:

The first part was devoted to the design and the production of GFPmolecules modified by introducing specific non-natural aminoacids at two defined positions along the protein structure. These modificationswere performedusing a methoddeveloped by P.G Schultz and collaborators[5]consisting in site specific incorporation of unnatural amino acids with expanded genetic code.P-azido-phenylalaninwere chosen so as to allow the introduction of reactive chemical groups for further grafting through click chemistry processes between azide and alkyne groups. This reaction was selected because it takes place rapidly under mild conditions and is orthogonal to reactions taking place between amines, carboxylic and thiol groups, all present in proteins[6-9].This part of the project was entrusted to our IRTG partner from Freiburg: Pr. Schiller (Freiburg Universität) and Chunyan Yao (PhD student), experts in this field.

I was responsible for the second part of this work, namely to elaboratestretchable substrates, host for the covalent coupling of the proteins and in particular for the coupling of modified GFPs, and to develop thestretching experiments. More precisely, I first had to develop a substrate that is stretchable, transparent, homogeneousand allows covalent grafting of proteins all over the surface. Moreoverthe surface must prevent protein adsorption in order to avoid the presence of non-grafted proteins on the surface.Then I had to graft covalentlythe GFPs onto the substrate. Different constraints inherent to these proteins such as low temperature, adjusted pH, and soft chemical reactions to preserve the protein functions had to be taken in account. Finally, I had to investigate the influence of mechanical stressapplied on the material on itsfluorescence response. The different steps of the project are summarized in figure 3.2.

It must be noticed that a paper about the results of this study has been written(annexe2)and sent for publication.
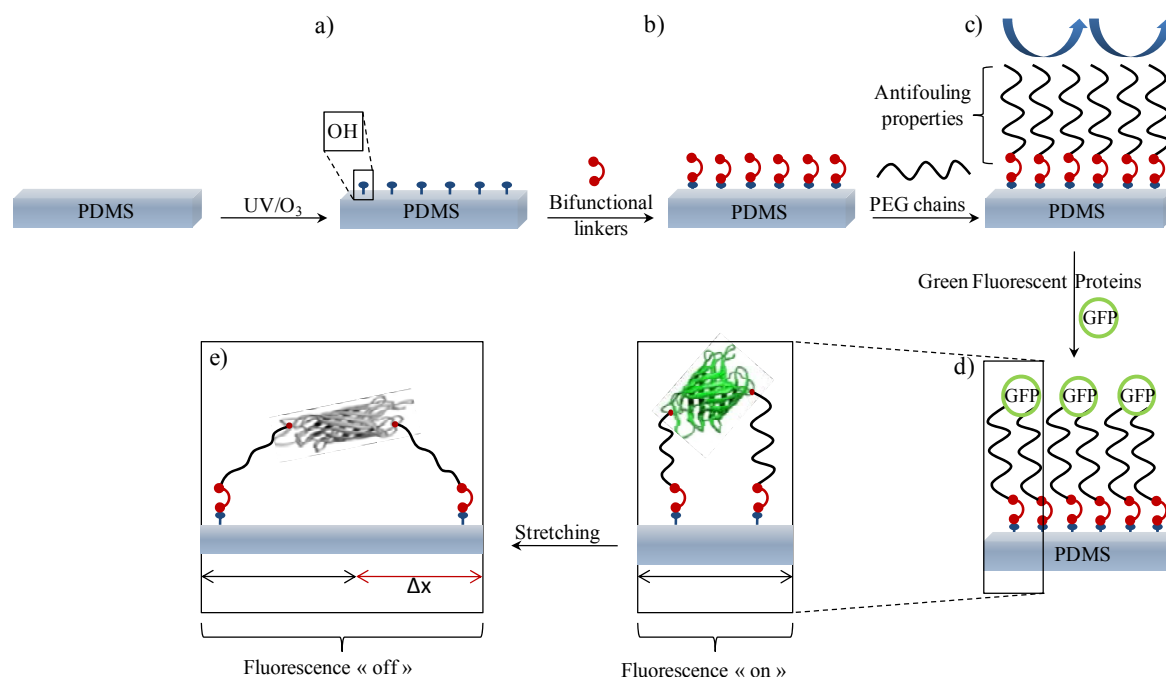
***Figure 3.2****: Schematic representation of the different parts of the project corresponding to (a) oxidation of the surface; (b) surface functionalization; (c) Grafting of alkyne terminated poly(ethylene glycol) chains to allow further protein grafting through click-chemistry and to avoid non-specific protein adsorption; (d) GFP coupling and (e) stretching experiments.*

## 3.2. Materials and chemicals for this project

### 3.2.1. Green Fluorescent Protein (GFP)

#### Introduction to Green Fluorescent Protein

In the 1960's Osamu Shimomura first isolated a bioluminescent protein from the *AequoraVictorya* jellyfish, the *aequorin*[10]. Shimomura and collaborators observed that in the animals, green light was producedwhereas *aequorin* normally generated blue light. Such observations were explained by the discovery of interactions between the *aequorin* and specific proteins named "Green Fluorescent Proteins" (GFP). A bioluminescence resonance energy transfer (BRET) occurred from the *aequorin* to the GFP chromophore producing a bright green fluorescence [11]. Despite the establishment of the GFP chromophore structure in 1979 by Shimomura and its full sequence determination and cloning by Ward and Prasher in 1992[12], its recognition as an essential tool in biology had to wait until 1994 with the works of Martin ChalfieandRogerTsien. With the expression of GFP in *Escherichia coli*and in neurons of *Caenorhabditiselegans*, Chalfie et al. established the possibility of GFP to be used as *in vivo* fluorescent markers [13]. In the same time, Tsien et al. worked on the changes of spectral

properties from GFP and produced a Blue Fluorescent Protein [14]. Their works permitted the elaboration of a vast array of fluorescent proteins from the blue to the near red region[15], increasing the interest for GFP as a biological marker for gene expression, protein localization or biosensors for non-invasive *in-vivo* measurements [11, 16]. It must be noted that Martin Chalfie, Osamu Shimomura, and Roger Y. Tsien were awarded the 2008 Nobel Prize in Chemistry on for their discovery and development of the green fluorescent protein.

More recently with the development of a new generation of materials called « smart materials » which aredefined by their capacity to adapt to their environment, a new field of research has emerged: the field of mechano-biochemistry. Due to the important implication of its structural conformation on its fluorescence properties[17], GFP was naturally anticipated to be an ideal candidate for mechanosensing. Indeed, a deformation of the chromophore of the β-barrel of GFP molecule results in a reduction of the fluorescence intensity and a blue-shift of the fluorescence spectrum[15, 18].Due to this property, GFP was anticipated to be a good candidate for our project.

One can notice that very recently, Bielawski et al. [19]used this property to create a mechanically sensitive biocomposite containing GFP characterized by its change of fluorescence under pressure by modification of the GFP tridimensional structure.

## Characteristicsof the Green Fluorescent Protein

The green fluorescent protein (GFP) from *Aequorea Victoria*is a protein composed of 238aminoacids residues (26.9 kDA) forming aneleven-stranded beta barrel structure with an alpha helix running through the center of the barrel. Along it central helix, inside the hydrophobic core, a p-hydroxybenzylidene-imidazolidonechromophore(HBI) takes place (see figure 3.3). This chromophore, responsible of the GFP fluorescence is formed from an internal cyclisation of Ser65, Tyr66 and Gly67 into a conjugated structure[20].
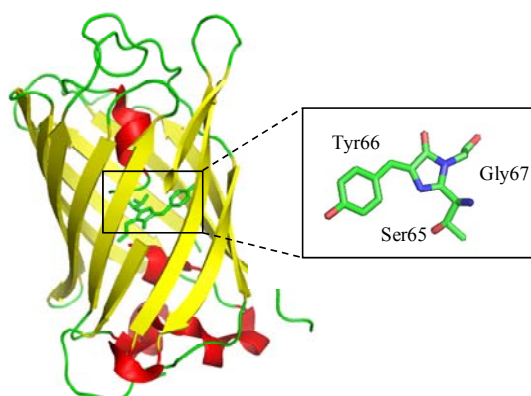
***Figure 3.3****:Cartoon representation of an Aequorea Victoria Green Fluorescent Protein (GFP) including its beta barrel (yellow), its alpha helix (red) and its detailed HBIchromophore (4KW4 RCSB Protein Data Bank).*

Wild type GFP (wGFP) has one specific excitation peak at a wavelength of486 nm. Its mean emission peak appears at 514 nm corresponding to the green part of the visible spectrum[21] (figure 3.4).
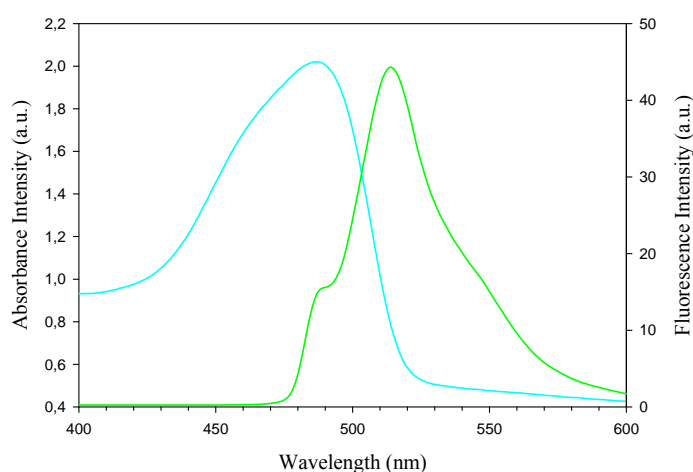


***Figure 3.4****:Excitation and emission spectra of the Green Fluorescent Protein. The maximum of excitation (in blue) is observed at λ=486 and thefluorescence peak (in green) appearsatλ=514nm.*

## GFP modification: choice of the unnatural amino-acid insertion

A crucial part of the IRTG project was to develop a way of linking the Green Fluorescent Proteins onto the surface in order to modify its structure under a mechanical stress. In this context, specific modifications of the proteins were needed. They were performed by Chunyan Yao from Pr. Schiller team. Her work was dedicated to the

determination and the introduction of unnatural amino acids containing azide functions in the GFP sequence. Due to a chemical structure close to the natural amino acids tyrosin or phenylalanine, P-azido-phenylalanin (pAzF) amino acid was used for the modification (see figure 3.5). This similarity prevents changes in the protein structure and keeps its integrity. The insertion sites were then defined by following some constraints. The azide groups had to be accessible for the linking step. The unnatural amino acids pAzF hadthusto be on the external part of the protein and exhibit their side chains to the outside of the core protein. Furthermore they had to take place at opposite positions in order to optimize the GFP deformation when stretched. The *Aequorea Victoria*crystal structure was used as reference structure for the determination of the modification sites. Responding to all these constraints, positions Y39 and Y182 were finally chosen in the GFP sequence for the amino-acids insertions.It must be noted that wild type GFP and mono-modified GFP were also produced to conduct the control tests needed during the different parts of the project.
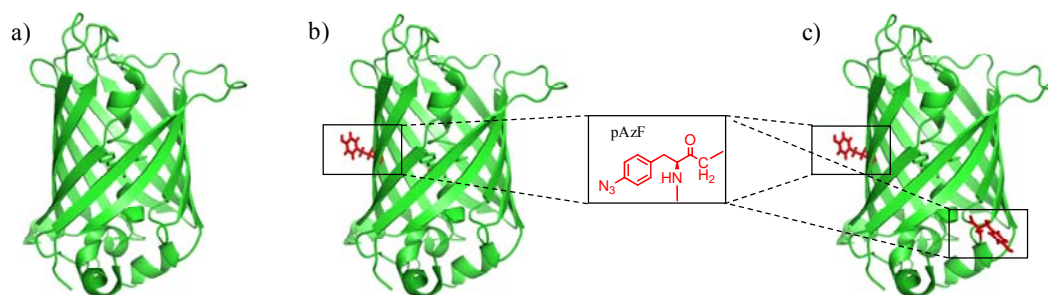


*Figure 3.5: Specifically modified GFP by insertion of unnatural amino-acids containing azidegroups in the protein sequence (RCSB Protein Data Bank). (a) Wild type GFP, (b) mono-azide modified GFP and (c) bis-azide modified GFP.*

### 3.2.2.Choice of the substrate: polydimethylsiloxane (PDMS)

As mentioned previously, the choice of the substrate was dictated bydifferent constraints:

- Be transparent in order to allow for fluorescentmeasurements with an inverted fluorescence microscope
- Be highly stretchable (high elongation at rupture)
- Be homogeneous and highly functionalizable all over its surface

Despite its chemical inertness, we selected polydimethylsiloxane (PDMS), also called silicone, because it is transparent and highly stretchable. In order to have a precise control over the PDMS sheet thickness and to reduce the risk of adsorbed contamination during their

preparation, we decided to prepare our own PDMS by using the commercial PDMS sylgard-184 reagents (see material and methods) for our study.

## 3.3. Modification of the PDMS surface

As just mentioned, PDMSpresents one drawback: its chemical inertness. Thereforemodifications ofits surface characteristics were needed before different proteins and macromolecules could be anchored onto the substrate. It was reported in the literature that in order to modify PDMS surface properties, different physical or chemical treatments [22, 23] or a combination of both [24, 25]can be used.Use of oxygen plasma was for exampledescribed[26, 27]. Howeverstudies reported that plasma oxidation treatment propagate deep into the polymer surface causing irreversible changes of the silicone properties [28, 29]. Moreover the creation of a thin brittle silica layer leading to the formation of cracks on the PDMS surface is usually observed[28].To avoid such changes of the PDMS material, another method of functionalization based on the formation of oxidative species by irradiationwas reported: the UV-Ozone (UVO) treatment [30]. Milder than an oxygen plasma treatment, this method should allow for a better regulation of the oxidative process by controlling the exposure time. Due to its availability in our laboratory and its ease of use, we selected this method for the remainder of the project. It must be noticed that all the oxidation treatments by UVO on silicone substrates were done under atmospheric pressure at room temperature.

### 3.3.1.Creation of chemical species on the PDMS substrate under UV-Ozone treatment

As mentioned previously, the oxidation of the PDMS substrate by the UV-ozone process leads to chemical modifications of the PDMS surface, mainly to the formation of carboxylic acid and silanol groups. It results in changes of the silicone surface properties with exposure time (figure 3.6).
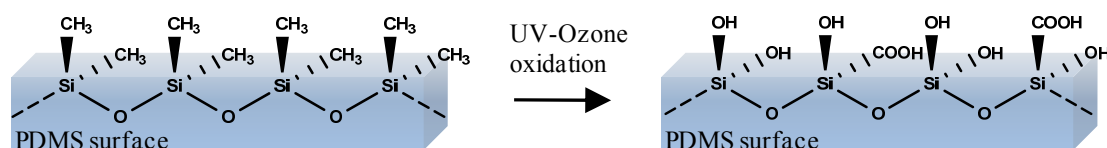


*Figure 3.6:Formation of various reactive species on the top of the silicone substrate by UV-Ozone treatment.*

Indeed, theformedsilanol groups are responsible for rendering the initial hydrophobic PDMS substrate increasingly hydrophilic. This evolution can be monitored by water contact

angle measurements as a function of the UV-Ozone exposure time.The experiments were performed by increasing the UV-Ozone exposure time of a PDMS Sylgard-184 substrate. Silicone properties were monitored from 0mn to 120mn by 30mn steps. Starting from a hydrophobic surface, we observe a linear decrease of contact angle with time, from about 110° for an unexposed surface to 20° after 120mn of UV-Ozone exposure (Figure 3.7). It must be noted that this change of behavior from hydrophobic to hydrophilic is temporary. Indeed, after an oxidation treatment, the surface recovers its initial features within a few hours. This is explained by the migration of free PDMS chains from the bulk of the material to the surface[31]. Therefore all the following experiments and analysis were done immediately after the UV-Ozone oxidation.
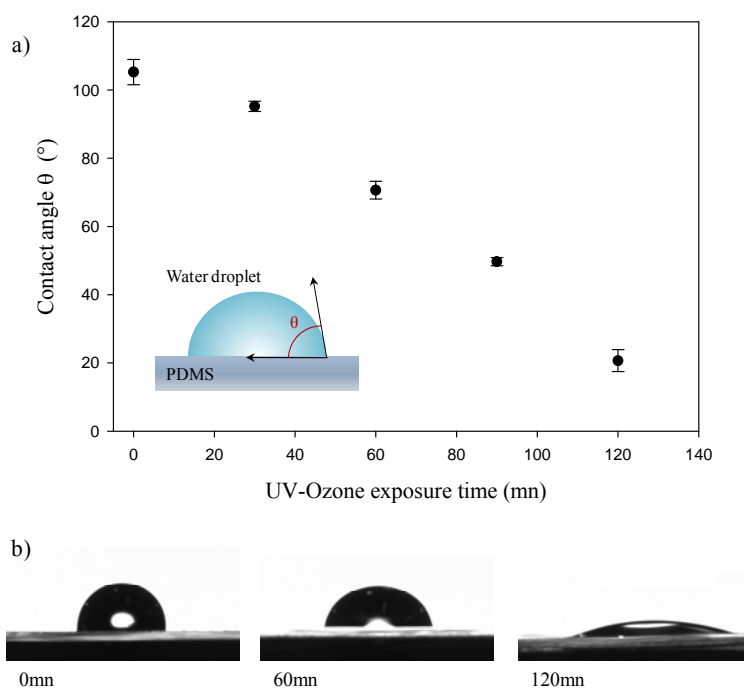


*Figure 3.7*: *(a) Evolution of water droplet contact angle mean value as a function of the UV-Ozone exposure time of the PDMS substrate; (b) Images of water droplets on silicone surfaces treated by UV-Ozone for 0mn, 60mn and 120mn.*

According to previous works from Genzer and collaborators [30], the increase of hydrophilic properties of PDMS Sylgard-184 with the exposure time to UV-Ozone can be explained by analyzing the FTIR spectra in attenuated total reflectance (ATR) configuration of the corresponding surfaces. In this mode one is only sensitive to the outer part of the substrate and thus to the surface.These authors found the formation of polar groups such as

hydroxyl and carbonyl derivatives responsible of the hydrophilic behavior of the silicone when oxidized. In order to characterize our process we thus also performed an infrared monitoring of the PDMS surface as a function of the UV-Ozone exposure time (figure3.8).
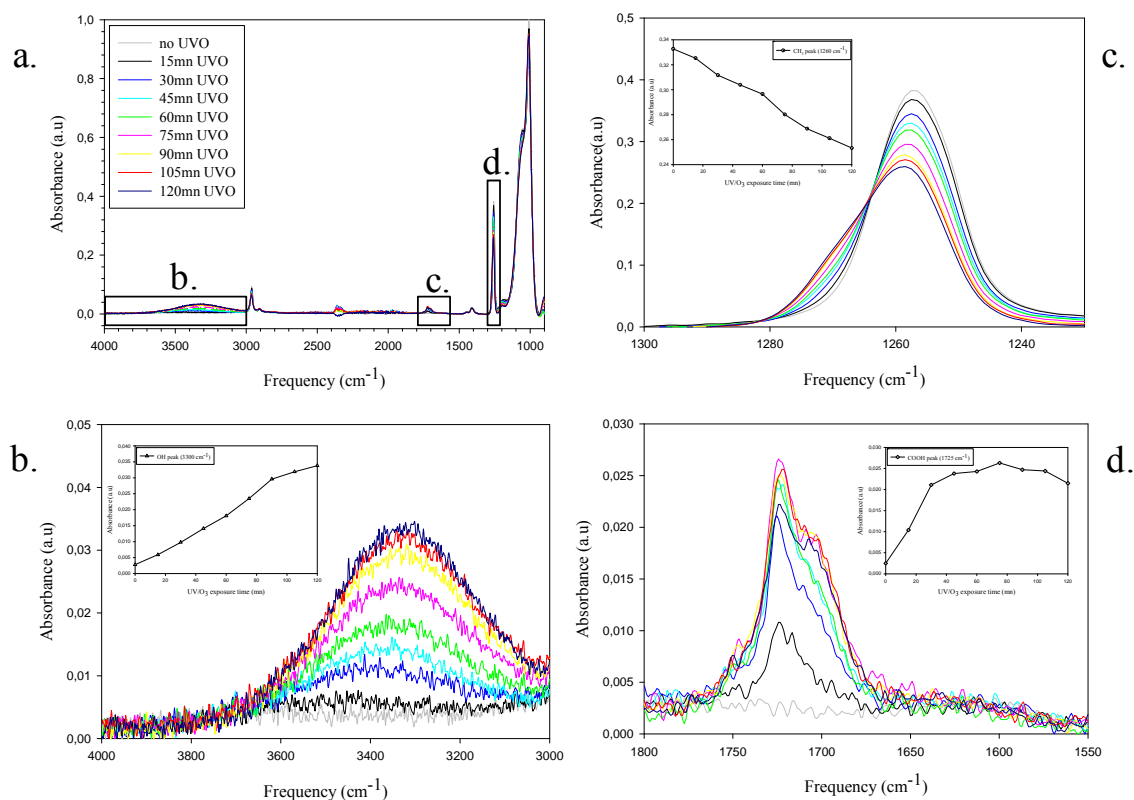


***Figure 3.8****: (a) Overlapping of the infrared spectra of native PDMS surface at different times of exposure to UV-Ozone; (b) increasing of the OH band intensity with UV-Ozone exposure time from 0mn to 120mn;(c) decreasing of the $CH_3$ band intensity with UV-Ozone exposure time from 0mn to 120mn; (d) evolution of the COOH band intensity with UV-Ozone exposure time from 0mn to 120mn.*

In this study we were particularly interested in three specific wavelengths, $3300cm^{-1}$, $1725cm^{-1}$ and $1260cm^{-1}$ corresponding respectively to the hydroxyl, carbonyl and methyl groups. As expected, a large band at $3300cm^{-1}$ is growing with the exposure time(figure3.8.b). Corresponding to the OH stretching band, it is probably due to the formation of silanolgroups. In the same time at $1725cm^{-1}$, we observe the increase of the band corresponding to the carbonyl groups between 0mn to 60mn followed by a slightdecreaseof the intensity of this band (figure3.8.d). This evolution can be explained by the appearanceat the beginning of the process of COOH groups at the top of the surface followed by their oxidation leading to the formation and desorption of CO or $CO_2$ compounds. On the contrary, the intensity of thelast band at $1200cm^{-1}$ is decreasing throughout the UV-Ozone exposure time (figure3.8.c). It is

explained by the oxidation of the methyl groups from the PDMS leading to the formation of other species.

According to the results obtained by contact angle measurements and FTIR analyses, we can conclude that the hydrophilic behavior of the silicone when oxidized corresponds to the continuous formation of hydroxyl groups with exposure time. The appearance of a breakable silica layer on our substrate is observed for a too long exposure time to UV-Ozone. This can be explained by an over oxidation of the silanol groups leading to the formation of Si-O-Si bonds. Such modification leads to the formation of cracks on the silicone when stretched. Responsible of inhomogeneous surface deformations under stretch and of a decrease of the substrate visco-elastic properties, cracks have to be avoided for the next steps of our project. **Experiments showed that 60mn of UV-Ozone oxidation permits the substrate to be stretched at a ratio near to 50% without crack formation. This parameter was kept for all the future experiments.**

### 3.3.2.Functionalization of the PDMS surface

Once the UV-Ozone exposure conditions were defined, the next step of our study was dedicated to functionalization of the oxidized surface. As seen previously, two main reactive groups were formed during the oxidation step: carboxylic acids and silanol functions. Different methods using oxidized silicone surfaces were reported in the literature such as the use of siloxane compounds to attach different chemical groups on this surface[32]. However previous works based on surface silanization performed in our team showed that the surfaces became inhomogeneous after modification[33]. We thus focused on two differentways of coupling using these specific species: the peptidic coupling reaction and the use of isocyanatereactants.

**Use of peptidic coupling**

We first concentrated on the COOH groups formed through UV-Ozone treatment. We chose to make a peptidic coupling reaction between the surface carboxylate groups on the PDMS sheet and primary amine containing reactives utilizing EDC-NHS chemistry(see figure 3.9). EDC-NHS is well established in organic and bioconjugatechemistry, efficient in solution this coupling method is also used on surfaces[34]. EDC (1-Ethyl-3-(dimethylaminopropyl) carbodiimide hydrochloride) is a crosslinking agent used to bind carboxyl-acid groups to

primary amines by the formation of an amine-reactive intermediate (O-acyl urea). Unstable, this intermediate can react directly with an amine or be hydrolyzed. The addition of NHS (N-hydroxysuccinimide) stabilizes this intermediate by converting it to amine-reactive sulfo-NHS ester, increasing the efficiency of the coupling reaction.
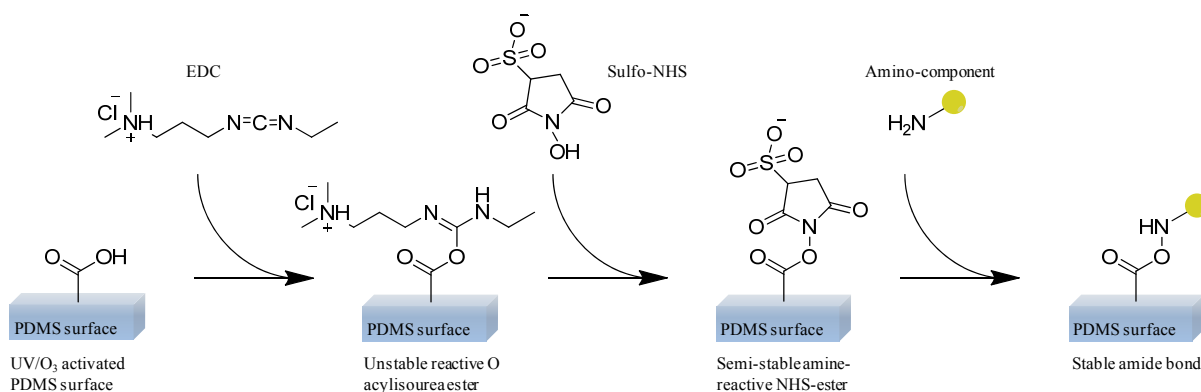


***Figure 3.9****: EDC-NHS chemistry: EDC reacts with a carboxylic group on the surface forming an amine-reactive intermediate. Unstable, this intermediate may directly react with an amine or be stabilized by the addition of sulfo-NHS, leading to the formation of an amine-reactive NHS-ester increasing the efficiency of the coupling.*

As described in figure 3.9, the coupling reaction takes place in two main steps. First the carboxylic acid groups are "activated" with EDC/NHS and then the reaction with the amine occurs. The first part of my study was dedicated to the optimization of the activation step.To validate this way of functionalization, different experimental conditions were tested. In order to achieve this, experiments were performed by varying the time of activation by EDC/NHS. The surface was then put in contact with a fluorescent amino-component. The results of the coupling reaction were monitored by fluorescence microscopy as follows:

Immediately after UV-Ozone oxidation (60mn) the silicone samples were brought in contact with anaqueous solution containing both EDC/NHS at concentrationsrespectively of 20mg.mL$^{-1}$ and 2mg.mL$^{-1}$ for various time.Afterdifferent contact times (30mn, 60mn 120mn and 240mn) the surfaces were washed with MQ water and put in contact with a solution of fluorescein-amine (figure 3.10.a.) at 0.1mg.mL$^{-1}$in water for 60mn. After a rinsing step, they were analyzed by fluorescence microscopy using an inverted light microscope (Nikon Microphot-FXA, Japan) equipped with a mercury lamp and operating between 470 and 490nm wavelength for excitation and above a wavelength of 500nm for detection. The measurements were done using a 10x objective in different areas of the samples. The quantification of the fluorescence intensity was done using the software ImageJ$^{®}$. Results

aresummarized in figure 3.10. It must be noted that low fluorescence intensity is detected for the native silicone due to its auto-fluorescence. This contribution was so considered as a fluorescence background and was represented as a red line in figure 3.10.b.
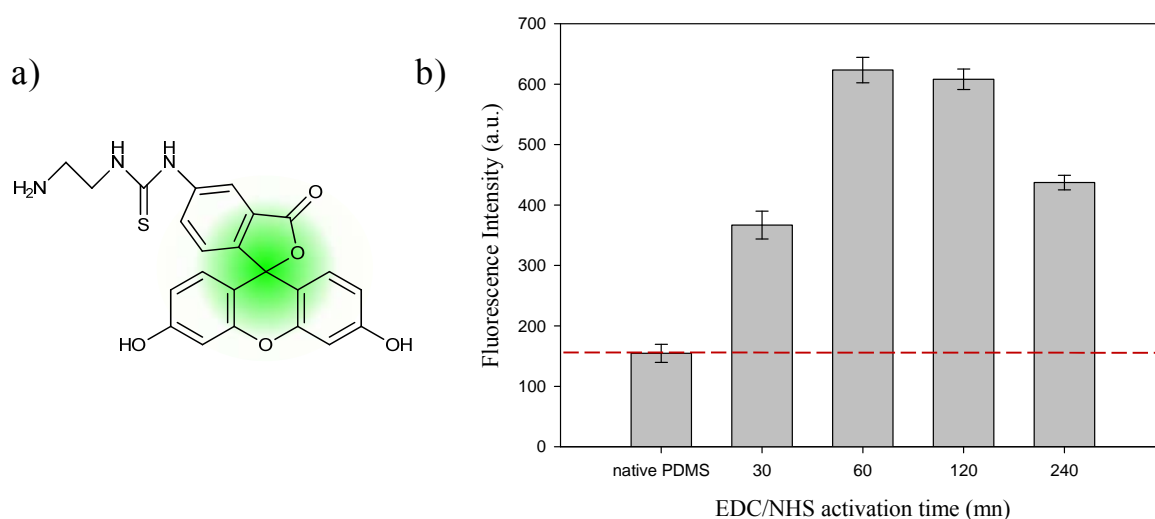


***Figure 3.10****: (a) Fluorescein-amine dye (b) Fluorescence microscopy intensity analyses obtained for various times of EDC-NHS surface activation from 0mn to 240mn after coupling with fluorescein dye.*

The highest fluorescence intensity was observed for an activation step by EDC-NHS of 60mn. We noticed a decrease of the coupling yield after 60mn. This result could be explained by the de-activationof the amine-reactive intermediateby water.

**Functionalization by bis-iso(thio)cyanate linkers**

Due to the high reactivityof iso(thio)cyanatestowards a variety of nucleophiles such as amines, alcohols or carboxylic acids, a new approach based on di-iso(thio)cyanates functionalization was performed. The aim of this strategy was to react a di-functional compound only by one side on the PDMS surface and use the second one to link molecules of interest (figure 3.11).
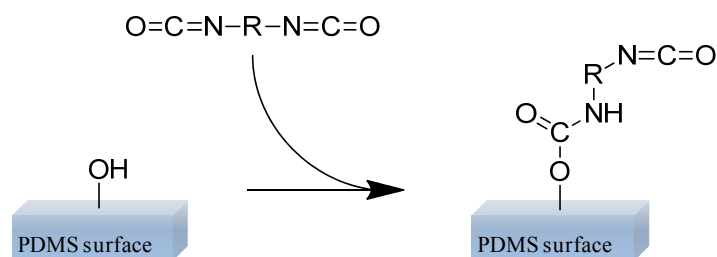


***Figure 3.11****: Coupling reaction between isocyanate compound and oxidized surface.*

In order to maximize the number of reactive sites for the next steps of the project, different commercial iso(thio)cyanatecompounds were tested.

Characterized by its short size and the steric effect of its phenol group 1,4-phenylène diisocyanate was first chosen. Indeed due to its structure weexpected it to be able to bindonly by one side to the surface. Another isocyanatewidely used in industry4,4'Methylenebis(phenylisocyanate) (MDI) was also chosen.It must be noted that these isocyanates were solubilized in acetone for the experiments. However, acetone inflates PDMS whichbecomes fragile and hard to manipulate. To avoid breaking the substrate during functionalization and manipulations, anotherbis-isocyanate, 4,4'-Diisothiocyano-2,2'-stilbenedisulfonic acid soluble in water was tested. All the isocyanate structures are given in table 3.1.
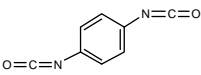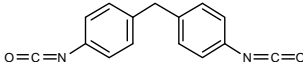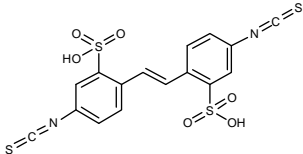
| 1,4-Phenylène diisocyanate (PDIT) | 4,4'Methylenebis(phenyl)isocyanate (MDI) | 4,4'-Diisothiocyano 2,2'stilbenedisulfonic acid (DIDS) |
| --- | --- | --- |



***Table 3.1****: Chemical representation of the different bis-isocyanates tested.*

As previously explained, the PDMS surfaces were first oxidized by UV-Ozone for 60mn to create silanol and carboxylic acid functions on their surface. They were then immersed into an iso(thio)cyanate solution MDI and PDIT at 1mg.mL-1 in acetone for one hour. After this treatment the silicones were rinsed with acetone,then with MQ water and brought in contact with an aqueous solution of fluorescein-amine dye at 0.1mg.mL$^{-1}$ for one hour. The surfaces were then washed three times with MQ water. For the 4,4'-Diisothiocyano-2,2'-stilbenedisulfonic acid all the experimental conditions were similar to the previous ones except that the isocyanate solution was diluted at 1mg.mL$^{-1}$ in MQ water. Comparison between the different isocyanatecoupling experiments are given in figure 3.12. It should be noticed that the MDI compound owned auto-fluorescence. Its intensity was evaluated and subtracted in each fluorescence measurements.
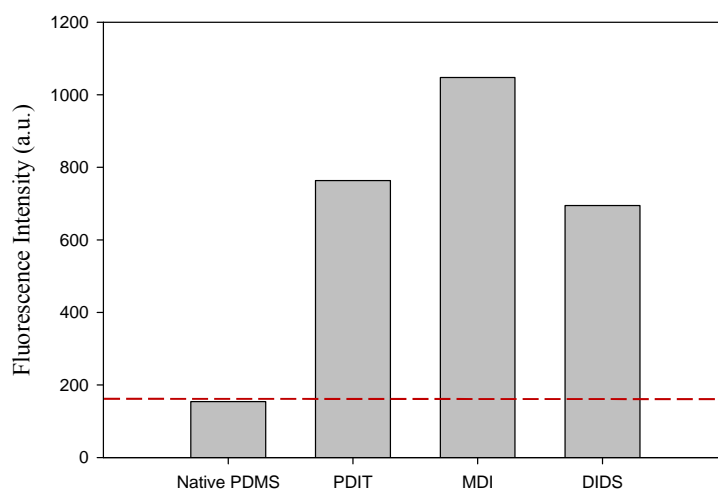
***Figure 3.12****: Fluorescence microscopy intensity analyses obtained for various bi-functionnal molecules after coupling with fluorescein dye.*

As observed in figure 3.12, the highest fluorescence intensity wasdetected for the reaction involvingthe MDI coupling. Moreover the fluorescence intensity obtained with the MDI coupling is much higher than that obtained with the peptidic coupling. This indicates a higher efficiency of the MDI coupling compared to all the other coupling methods explored.

**Thus, despite the fact that acetone brought additional experimental constraints, the functionalization with MDI was chosen for the project.**

### 3.3.3.Use of polyethylene glycol chains as spacers for specific GFP binding
**Reaction of wild type GFP with free isocyanate groups**

Once the PDMS functionalization method was chosen, first tests of direct grafting of wild type Green Fluorescent Protein were performed. In this part we forecasted that the amines present all around the protein were able to react with the free isocyanate groups on the modified surface. To realize this coupling, an aqueous solution of wild type protein at $0.025mg.mL^{-1}$ was brought in contact with an isocyanate modified surface for one hour at room temperature. Three rinsing steps with TRIS 50mM/NaCl 150mM buffer at pH 7.4were performed to clean the surface at the end of the binding step. A negative test on unmodified silicone was performed at the same time. Results monitored by fluorescence microscopy are shown in figure 3.13.
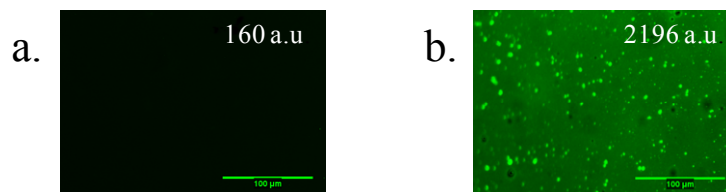
***Figure 3.13****: Fluorescence microscopy images after contact with wild type GFP of (a) a native silicone surface and (b) an isocyanate modified silicone surface.*

We observe that no fluorescence is detected on the native silicone.This can be explained by the fact that the silicone is non-adsorbent to protein or that GFP molecules are denatured when adsorbed on this surface, losing their fluorescence property. On the contrary, high fluorescence intensity is observed on the modified silicone surface. However, its distribution is inhomogeneous due to the presence small bright green spots over the entire surface.This may be due to small aggregates present in solution. These experiments were used as reference for the further functionalization of the surface by poly(ethylene glycol) chains.

**Antifouling PolyEthylene Glycol (PEG) chain grafting**

Prevention of non-specific adsorption of proteins on the surface is an essential condition for the success of our strategy.Indeed,non-specific adsorbed GFP are expected not to be sensitive to mechanical constraints applied to the surface.A common method to reduce protein adsorption at a solid-water interface is the immobilization of antifouling polymers such as polyethylene glycol on the surface[35, 36]. The non-fouling character of PEG is not an absolute property but depends on complex interactionsof several factors such as steric repulsion, van der Waals attraction and hydrophobic interaction free energies [37].Others parameters such as polymer molecular weight and grafting density are also involved in this behavior. It should be noted that a too high molecular weight (<3400kDa) [38]maylimit grafting density onto the surface due to steric repulsive effect. Previous workby Bacharouche et al. [39], described that an optimum antifouling effect is observed by using 2 kDapolyethylene glycol chains grafted on a silicone surface. Moreover, polyethylene glycol is widely used as an inert and biocompatible linker in surface engineering [38, 40] and in the modification of proteins [41-43].According to these results, experiments were performed by using PEG chains with a molecular weight of Mw = 3000 g/mol.

## Optimization ofthe antifouling behavior of the PEGylated PDMS surface

As mentioned previously,the non-adsorbent properties of PEGylated surfaces are dependentonthe PEG grafting density whichshould bedirectly linked to the quantity of available reactive sites on top of our PDMS surface after oxidation and MDI functionalization.In order to maximize the antifouling properties of the surfaces different parameters of functionalization were tested.

First, directly after 60mn of UV-Ozone oxidation followed by the reaction with MDI, the PDMS samples were put in contact with an aqueous solution of commercial PEG3000-amine terminated at $1mg.mL^{-1}$ overnight. Once the reaction between the amines and isocyanate groups occurred(figure3.14), the substrates were kept in TRIS 50mM/NaCl 150mM buffer at pH 7.4 until use.
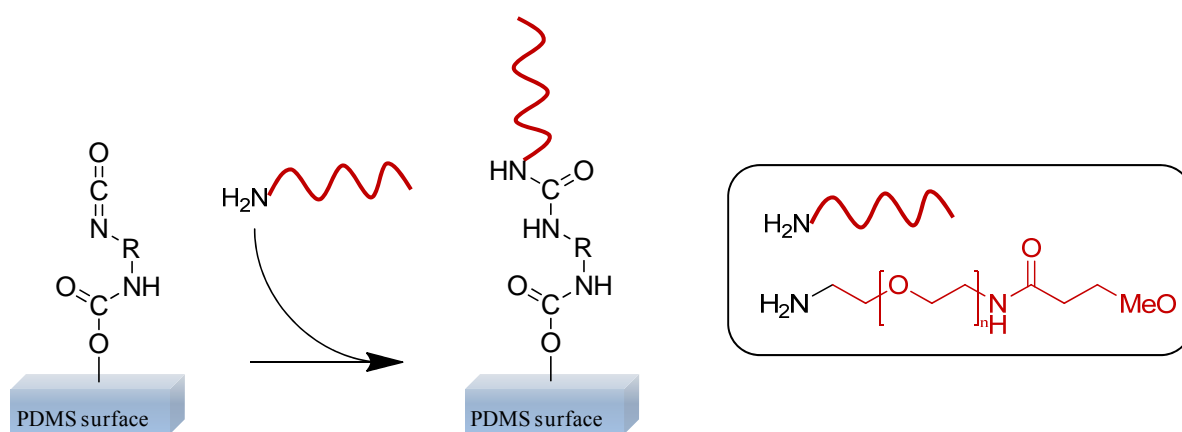


***Figure 3.14***: *Coupling reaction between isocyanate compound and amine functionalized polyethylene glycol chain.*

Non-adsorbent properties of the coating were evaluated by putting the surfacesin contact with an aqueous solution of wild type GFP at $25\mu g.mL^{-1}$ for one hour. The samples were then washed three times with the buffer solution and analyzed by fluorescence microscopy (figure 3.15 (b)).A high fluorescence was measured. In order to increase the antifouling property of the substrate, a second test (c) was performed by increasing the UV-Ozone exposure from 60mn to 90mn leading to the creation of more reactive groups on the surface and so more sites of functionalization, all the others parameters of the experiments were kept constant. Results of antifouling tests are given in figure 3.16. One observes indeed a decrease of the fluorescence compared to the case of 60mn UV-Ozone exposuretime.

To even further increase the anti-fouling character of the substrate, a third method described in literature by Genzer and Efimenko[30] consisting of stretching the substrate during the oxidation step toincrease the final density of reactive groups was tested. Using this way of functionalizationthey showed that it was possible to increase the surface density of grafted polymer chains on an elastomeric PDMS substrate when it was returned to the non-stretched state. Indeed, when the PDMS surface is stretched, its area is increased and the density of hydroxyl groups created under UV-Ozone oxidation is expected to be the same as on a non-stretched substrate. At the end of the process, the surface is relaxed to its initial state, the decrease of its area then leads to an increase of the surface density of hydroxyl groups. (Figure 3.15).
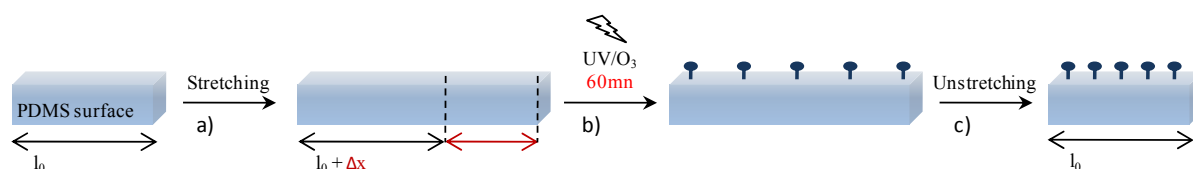


*Figure 3.15*: *Schematic representation of the different steps allowing an increase of the surface reactive group density under UV-Ozone treatment. The PDMS surface is first stretched (a), oxidized (b) and finally relaxed to its initial state to concentrate its new oxidized functions (c).*

According to these observations, new experiments were performed by stretching the silicone substrates during all the modification steps (UV-Ozone treatment, MDI treatment, PAG grafting). A ratio of 30% of stretching was chosen in order to avoid silicone breaking during the different functionalization steps. The UV-Ozone oxidation time was chose to be 60mn. All other parameters were kept equal to those used on the non-stretched substrates. It should be noted that the surfaces were relaxed at the end of the PEG functionalization before antifouling tests. Results of the different antifouling tests are shown in figure 3.16.
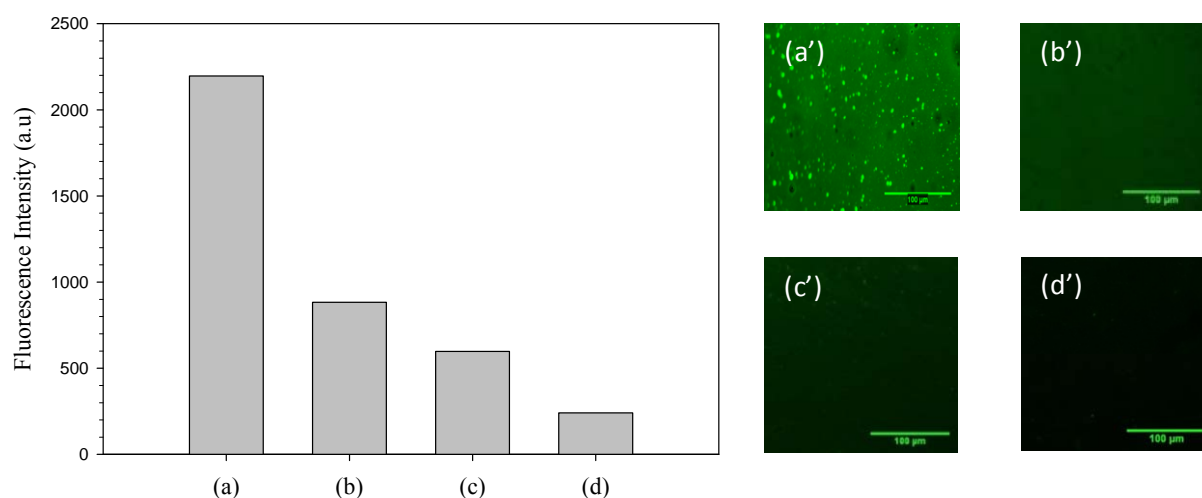
***Figure 3.16****: Antifouling tests of different modified surfaces monitored by fluorescence microscopy; (a) UV-Ozone 60mn/MDI 60mn, (b) UV-Ozone 60mn /MDI 60mn/ PEG overnight, (c)UV-Ozone 90mn /MDI 60mn/ PEG overnight and (d)(UV-Ozone 60mn /MDI 60mn/ PEG overnight)under stretch and (a')(b')(c') and (d') respective surface pictures.*

As shown in figure 3.16, the three methods used to avoid the GFP adsorption observed in contactwith MDI functionalization permit a decrease of non-specific protein adsorption.Despite the fact that no protein aggregations were observed on the PEG functionalized surfacesafter contact with native GFP (b,c,d), a low fluorescence intensity was detected for (b) and (c). A too low PEG grafting density on our PDMS substratecan explain this result.

**Best antifouling properties were obtained for the PDMS surface modified under stretch (d). A homogenous modification of the surface was observed. This way of functionalization was kept for the rest of the study.**

**3.3.4.Specific binding of Green Fluorescent Proteins through click chemistry**

**Introduction to click chemistry**

Click chemistry was initially developed by K. B. Sharpless in 1998 and fully described by Sharpless, Hartmuth Kolb, and M.G. Finn in 2001[6]. It refers to chemical reactions which bind in a quick and reliable way small units.

One of the most popular reaction in click chemistry is the azide-alkyne Huisgencycloaddition using a copper (Cu) catalyst at room temperature[44] (figure 3.17). This

reaction was first reported in 2002 in independent publications by the groups of K. B. Sharpless[45]and M. Meldal[46] and consists in a variant of Huisgen 1,3-dipolar cycloaddition developed by Huisgen et al. reported in 1963[47]. Also called Copper(I)-catalyzed Azide-Alkyne Cycloaddition (CuAAC), this addition is known for its high rate of reaction, its efficiency, its high yield and to proceed to completion at low temperature in aqueous solvent. These arenecessary conditions to keep the integrity of proteins [48].Moreover alkyne and azide functions are independently stable and do not react with common organic reagents or functional groups in biomolecules. This reaction is thus widely used in protein bioconjugation.

$$R-N=\overset{+}{N}=\overset{-}{N} \ + \ R'\!\!\!-\!\!\!\equiv \quad \xrightarrow{\text{Cu(I), RT°}} \quad R-N\underset{N=N}{\overset{\displaystyle\diagup\diagdown R'}{\diagdown\diagup}}$$
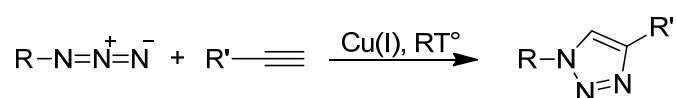
***Figure 3.17***:*Click chemistry reaction between an azide and an alkyne in presence of Cu(I) at room temperature.*

## Specific click chemistry conditions for GFP bioconjugation

Proteins are fragile and have to stay in specific environment to avoid degradation. Different constraints such as low temperature, adjusted pH, no toxic reactants and soft reactions are needed. The modified GFP containing two opposite azido groups synthesized by Chunyan Yao from our IRTG collaboration was an ideal candidate to react on surfaces through "click reaction" such as the HuisgenAzide-Alkynecycloaddition. However, as shown in figure 3.18, the reaction occurs in the presence ofCu(I) which is known to be responsible of the denaturation of biocomponents[49]. Such results were corroborated by previous works performed by Chunyan Yao aboutthe denaturationofGFP in solution in the presence of click reactants.

To prevent these degradations, specifics conditions of reaction in the presence of a tris(triazolyl)amine ligand developed by Finn et al.[49]wereused. The ligand plays a crucial role in stabilizing the Cu(I) oxidation state and protecting the protein from denaturation due to the oxidative agents produced in the presence of ascorbate[50]. It was also used to accelerate the CuAAC reaction leading to a decrease of the copper concentration needed for our experiments. ATris(3-hydroxypropyltriazolylmethyl)amine (THPTA) ligand(figure 3.18) prepared in our laboratory by Dr. Jierry according to protocol elaborated by Fokin et al. was used[51, 52].
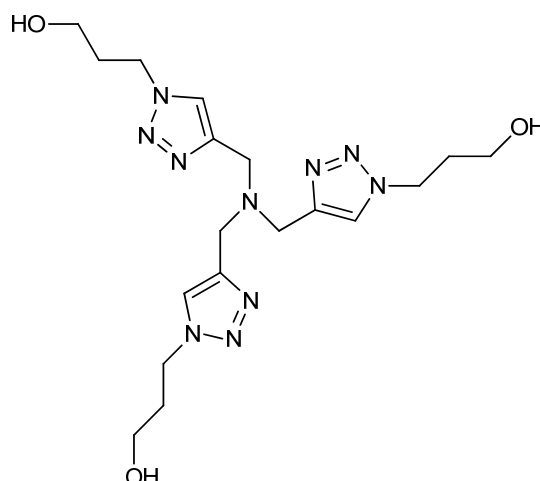
***Figure 3.18****: Tris(3-hydroxypropyltriazolylmethyl)amine (THPTA) ligand.*

In order to immobilize the proteins on the top of our PEGylated surfaces, functionalizations of our PDMS were performed by using an alkyne-terminated PEG3000-amine compound (figure 3.19). We performedseveral tests to show that the antifouling properties of the surface were kept (figure 3.21a).
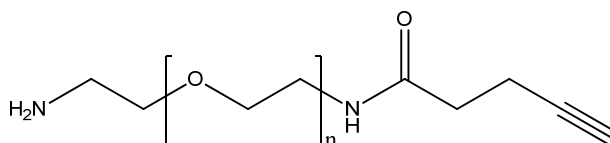


***Figure 3.19****:Alkyne-terminated PEG3000-amine compound.*

Once the PDMS surface wasfunctionalized with alkine groups, the reaction between the modified GFP and the alkyne-terminated PEG was performed following an optimized CuAAC protocol for bioconjugation developed by Finn and coworkers[51](figure 3.20). For this reaction, all the reagents were added in a specific order to prevent degradation of the proteins. First a premixed solution of $CuSO_4$ and THPTA (an excess ligand to copper ratio ofabout 5:1 was used due to its dual purpose of protecting the biomolecules and intercepting radicals and peroxide derivatives during the reaction)was added to a solution of GFP in phosphate buffer at pH 7.4. A solution of aminoguanidine used to prevent reaction between side chains of the proteins anddeshydroascorbate was then added to the mixture. The reducing agent, sodium ascorbatewas added in the last time and the solution was quickly homogenized and put in contact with our functionalized PDMS for one hour.Once the reaction occurred, the surfaces were washed and stored in a phosphate buffer solution until analysis.
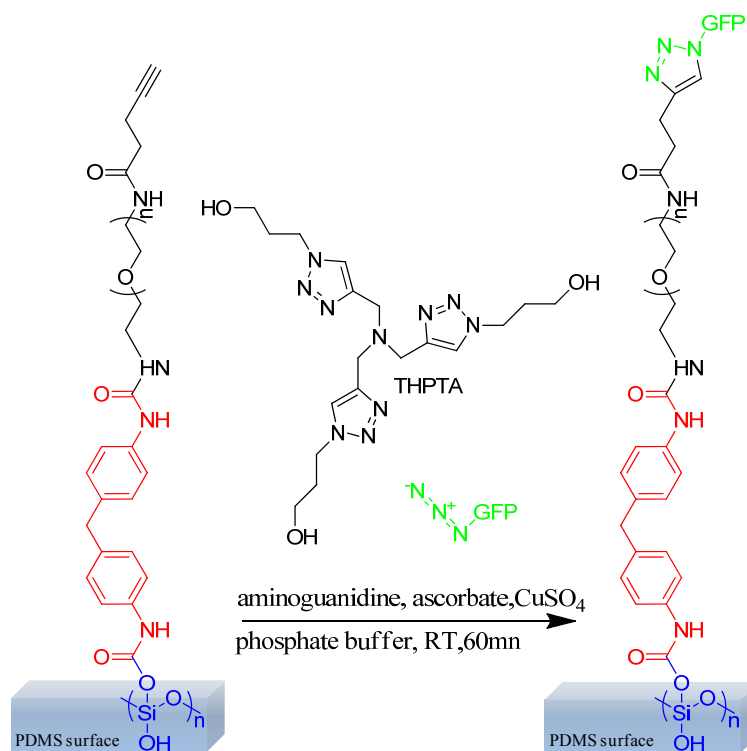
*Figure 3.20*:*CuAAbioconjugation between PEG-alkyne and azide-modified GFP.*

## Resultsof the GFP coupling

The covalent attachment of GFPon the surface was confirmed by measuring the fluorescence of the surface previously in contact with azide modified GFP (figure 3.21b). Wild type GFP, in the absence of azide groups on the surface, did not lead to fluorescence, indicating that the measured fluorescence with bis-azide-modified GFP was due to covalent attachment through click chemistry of the proteins onto the surface (figure 3.21a). Moreover after functionalization the surfaces observed were homogenous without any protein aggregation. Yet we could not directly prove that the proteins were attached on the surface simultaneously through the two azide groups.
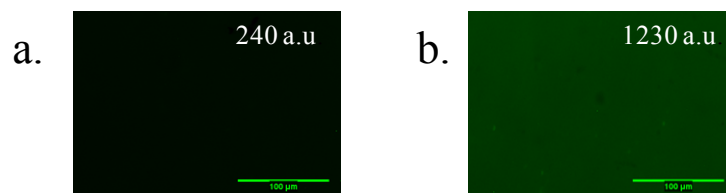


*Figure 3.21*: *Fluorescence microscopy images after contact of a PEG-alkyne functionalized surface in presence of Cu(I) for 60mn of (a) native GFP and (b) bis-azide-modified GFP.*

## 3.4. Stretching tests

Once the Green Fluorescent Proteins were bound on top of the silicone substrates, stretching tests were performed in order to investigate the influence of mechanical stress on the spectral response of our material. Experiments were performed on two different GFPs provided by our IRTG partner: abis-azide-modified GFP and aGFP bearing only one azide group. This second onewas used as a control because these proteins can be anchored onto the surface but cannot unfold by stretching.

### 3.4.1. Stretching devices

In order to study our surfaces under mechanicalconstraint, a homemade stretching devicewas designed and elaborated in our group (figure 3.22. It permits to stretch our silicone substratesin a longitudinal way up to 100% elongation.
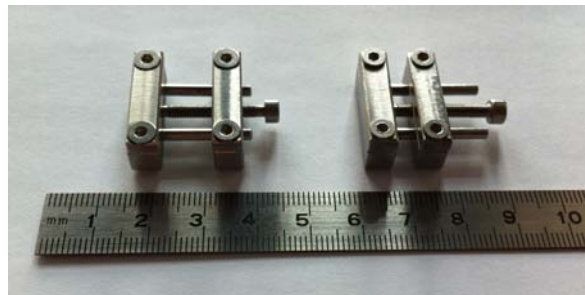


*Figure 3.22: Stretching devices.*

Thestretching degreeis defined as:

$$\alpha = \frac{(l - l_0)}{l_0} \cdot 100$$

With $l_0$ and l corresponding respectively to the initial and the stretched length of the silicone substrate. All the stretching experiments where performed at room temperature under liquid conditions.

### 3.4.2.Evolution of the fluorescence of the substrate with the stretching degree due to a "dilution" effect": use of fluorescein

Under stretch, a decrease of the fluorophore density on the PDMS surface appears. This "dilution" is the result of the local constraints occurring on the surface when stretched. In order to determine the contribution of the decrease of fluorescence due to this dilution effect we determined the fluorescence of surface functionalized by MDI-fluorescein at various stretching degrees. A regular stretch was applied to the PDMS substrate and fluorescence intensity was measured in the center of the silicone surface (figure 3.23).
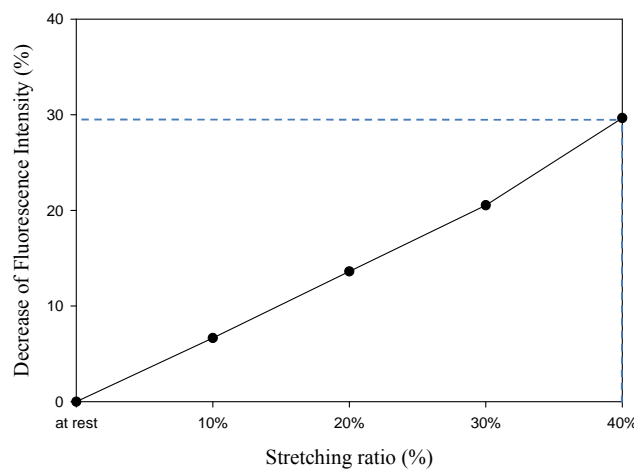


*Figure 3.23: Decrease of fluorescence density with stretching degree.*

A linear decrease of fluorescence with the surface elongation is observed. However for a stretching degree of 40% a loss of only about 30% of the fluorescence intensity is observed. This difference in the decrease of fluorescence can be explained by the manner in which stretching is performed.
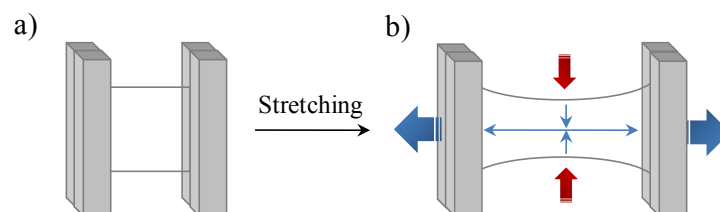


*Figure 3.24: Schematic representation of the PDMS substrate between the clamps of the stretching device: (a) at rest (b) Under constraints, longitudinal and perpendicular deformations occurring on the surface are shown in blue.*

Indeed, as shown in figure 3.24, when the silicone is stretched, a lateral contraction of the film takes place. The final decrease of fluorescence intensity is thus the combination of longitudinal elongation and lateral contraction, resulting in an overall increase of the area with the stretching degree. This effect has to be taken into account when analyzing the effect of stretching GFP covered surfaces.

### 3.4.3.Stretching experiments of substrates covered with GFP

As mentioned previously, experiments were performed with mono and bis-functionalized GFP. Both proteins were grafted on the silicone substrate functionalized as described previously. The substrates were then stretched up to 30% in stages. Thus stretching degrees0%, 10%, 20% and 30% were performed and surface fluorescence was measured for each ones.A return to the PDMS initial non-stretched state was also performed in order to check the reversibility of the system. It must be noted that all the experiments had to be performed in liquid conditions consisting in a drop of buffer on the top of the surface to prevent proteins degradations by drying. The results of these experiments are summarized in figure 3.25 where the fluorescence of the surface is represented as a function of the stretching degree of the substrate.These data were obtained from 4 independent experiments.
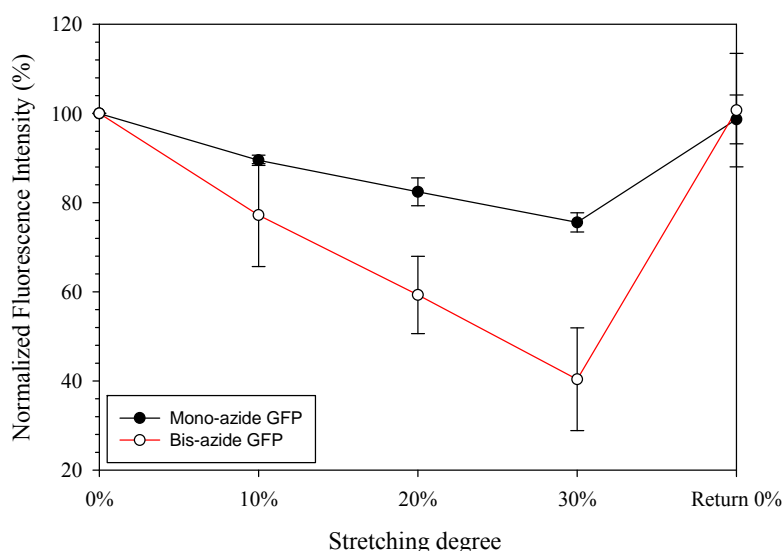


***Figure 3.25****: Normalized fluorescence intensity in function of stretching degree of the substrate for mono-azide modified GFP (in black) and bis-azidemodified GFP (in red).*

One observes a decrease of the fluorescence for both the bis and mono modified GFP. Yet, for the bis-functionalized GFP the fluorescence decrease is about 60% of the initial fluorescence whereas it is only 20% for the mono-functionalized GFP. The decrease for the mono-functionalized GFP can be attributed to a decrease of the overall GFP surface density by stretching as determined above. These results indicate that the fluorescence of the stretched bis-functionalized GFP decreases strongly by stretching the substrate. Thelarger decrease of fluorescence of the bis-modified GFP compared to the mono-modified GFP can be attributed to the deformation of the GFP itself leading to important modifications in its fluorescence.Reversibility of the systems was then studied by making cycles of stretching-unstretching of the PDMS substrate,fluorescence intensity was measured for each state (figure 3.26).

a)                                              b)
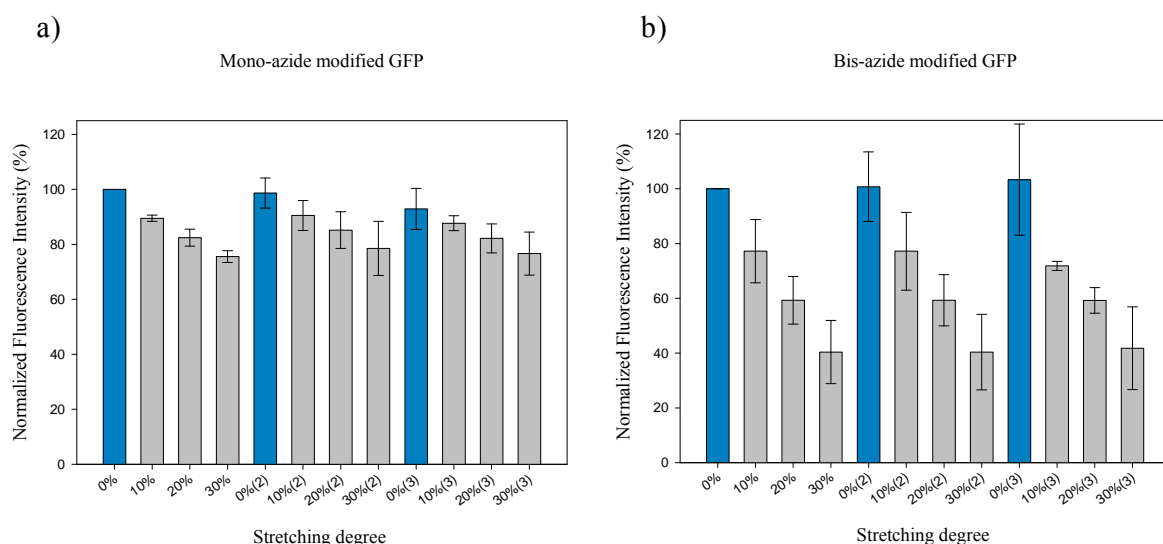


**Figure 3.26**: *Normalized fluorescence intensity as a function stretching-unstretching cycles of the substrate for mono-azide modified GFP (a) and bis-azide modified GFP (b).*

**Cycles of reversibility were observed for the substrates.**

## 3.5. Conclusion and perspectives

The aim of this chapter was dedicated to make a proof of principle ofmechano-responsive materials based on stretched induced protein conformational changes. To achieve this goalwe functionalizedsilicone sheets with modified Green Fluorescent Proteins. The project was split in two main parts, first the functionalization of the substrate and then the stretching experiments.

The beginning of our project was the determination of the UV-Ozone treatment conditions of our silicone substrate. These conditions were optimized to maximize further chemical grafting on the PDMS substrate whilst preventing the formation of a brittle silica layer. Once succeeded, we focused on the chemical functionalization of the PDMS surface with reactive groups which allowed grafting of polyethylene glycol chains in order to make it antifouling. This characteristic was a crucial constraint of our project and was reached by the combination of physical and chemical treatments. To finish the functionalization of our material, GFP bioconjugation, was performed through soft click chemistry conditions, in order to keep the integrity of the proteins. In summary, during this first step, we were able to specifically bind GFP on our surfacewhile avoiding its adsorption and denaturation.

In the second part of this project, stretching tests were performed in order to investigate the influence of mechanical stress on the spectral response of the material. We find differences of fluorescence responses under stretching between mono and bis modified GFP. Such differences were explained by changes in chromophore environment coming from structural deformation of bis modified GFP when stretched. Moreover reversibility tests were performed with success on our surfaces, showing that the proteins weren't irreversibly damaged during stretching.

It must be noted that new batches of modified GFP were synthesized by the group of Freiburg to make additional tests and reproducibility experiments. However we were unable to anchor these GFP proteins onto the surface. To understand wherethe difference in behavior of the two GFP batches come from, all the steps of the surface functionalization were performed again and analyzed separately. We came to the conclusion that the GFP coupling step that was no longer efficient with the new batches. These results were confirmed by ChunyanYao which could not further confirm the presence of accessible azide groups on the modified GFP.

## 3.6.References

1.    C.Y. Tseng, A. Wang, and G. Zocchi, *Mechano-chemistry of the enzyme guanylate kinase.* Epl, 2010. **91**(1): p. 6.

2.    G. Kalnitsky, J.P. Hummel, H. Resnick, J.R. Carter, L.B. Barnett, and C. Dierks, *The relation of structure to enzymatic activity in ribonuclease.* Annals of the New York Academy of Sciences, 1959. **81**: p. 542-69.

3.    H.S. Kim, S.H. Ha, L. Sethaphong, Y.M. Koo, and Y.G. Yingling, *The relationship between enhanced enzyme activity and structural dynamics in ionic liquids: A combined computational and experimental study.* Physical Chemistry Chemical Physics, 2014. **16**(7): p. 2944-2953.

4.    J. Saeger, V.P. Hytonen, E. Klotzsch, and V. Vogel, *Gfp's mechanical intermediate states.* PLoS ONE, 2012. **7**(10): p. 11.

5.    C.J. Noren, S.J. Anthonycahill, M.C. Griffith, and P.G. Schultz, *A general-method for site-specific incorporation of unnatural amino-acids into proteins.* Science, 1989. **244**(4901): p. 182-188.

6.    H.C. Kolb, M.G. Finn, and K.B. Sharpless, *Click chemistry: Diverse chemical function from a few good reactions.* Angewandte Chemie-International Edition, 2001. **40**(11): p. 2004-+.

7.    J.M. Baskin and C.R. Bertozzi, *Bioorthogonal click chemistry: Covalent labeling in living systems.* Qsar & Combinatorial Science, 2007. **26**(11-12): p. 1211-1219.

8.    E.M. Sletten and C.R. Bertozzi, *Bioorthogonal chemistry: Fishing for selectivity in a sea of functionality.* Angewandte Chemie-International Edition, 2009. **48**(38): p. 6974-6998.

9.    C. Besanceney-Webler, H. Jiang, T.Q. Zheng, L. Feng, D.S. del Amo, W. Wang, L.M. Klivansky, F.L. Marlow, Y. Liu, and P. Wu, *Increasing the efficacy of bioorthogonal click reactions for bioconjugation: A comparative study.* Angewandte Chemie-International Edition, 2011. **50**(35): p. 8051-8056.

10.   O. Shimomura, F.H. Johnson, and Y. Saiga, *Extraction, purification and properties of aequorin, a bioluminescent protein from the luminous hydromedusan, aequorea.* Journal of cellular and comparative physiology, 1962. **59**: p. 223-39.

11.   V. Baubet, H. Le Mouellic, A.K. Campbell, E. Lucas-Meunier, P. Fossier, and P. Brulet, *Chimeric green fluorescent protein-aequorin as bioluminescent ca2+ reporters at the single-cell level.* Proceedings of the National Academy of Sciences of the United States of America, 2000. **97**(13): p. 7260-7265.

12.   D.C. Prasher, V.K. Eckenrode, W.W. Ward, F.G. Prendergast, and M.J. Cormier, *Primary structure of the aequorea-victoria green-fluorescent protein.* Gene, 1992. **111**(2): p. 229-233.

13.   M. Chalfie, Y. Tu, G. Euskirchen, W.W. Ward, and D.C. Prasher, *Green fluorescent protein as a marker for gene-expression.* Science, 1994. **263**(5148): p. 802-805.

14.    R. Heim, A.B. Cubitt, and R.Y. Tsien, *Improved green fluorescence.* Nature, 1995. **373**(6516): p. 663-664.

15.    V. Sample, R.H. Newman, and J. Zhang, *The structure and function of fluorescent proteins.* Chemical Society Reviews, 2009. **38**(10): p. 2852-2864.

16.    N. Doi and H. Yanagawa, *Design of generic biosensors based on green fluorescent proteins with allosteric sites by directed evolution.* Febs Letters, 1999. **453**(3): p. 305-307.

17.    H. Mizuno, T.K. Mal, M. Walchli, A. Kikuchi, T. Fukano, R. Ando, J. Jeyakanthan, J. Taka, Y. Shiro, M. Ikura, and A. Miyawaki, *Light-dependent regulation of structural flexibility in a photochromic fluorescent protein.* Proceedings of the National Academy of Sciences of the United States of America, 2008. **105**(27): p. 9227-9232.

18.    B. Barstow, N. Ando, C.U. Kim, and S.M. Gruner, *Coupling of pressure-induced structural shifts to spectral changes in a yellow fluorescent protein.* Biophysical Journal, 2009. **97**(6): p. 1719-1727.

19.    C.B.B. Johnathan N. Brantley, Joe R. Cannon, Katie A. Clark,, J.S.B. David A. Vanden Bout, Adrian T. Keatinge-Clay,* and, and C.W. Bielawski, *Mechanically modulating the photophysical properties of fluorescent protein biocomposites for ratio- and intensiometric sensors.* Angewandte Chemie, 2014.

20.    J.J. van Thor, *Photoreactions and dynamics of the green fluorescent protein.* Chemical Society Reviews, 2009. **38**(10): p. 2935-2950.

21.    A. Warren and M. Zimmer, *Computational analysis of thr203 isomerization in green fluorescent protein.* Journal of Molecular Graphics & Modelling, 2001. **19**(3-4): p. 297-303.

22.    J.Y. Park, D. Ahn, Y.Y. Choi, C.M. Hwang, S. Takayama, S.H. Lee, and S.H. Lee, *Surface chemistry modification of pdms elastomers with boiling water improves cellular adhesion.* Sensors and Actuators B-Chemical, 2012. **173**: p. 765-771.

23.    S. Kuddannaya, Y.J. Chuah, M.H.A. Lee, N.V. Menon, Y.J. Kang, and Y.L. Zhang, *Surface chemical modification of poly(dimethylsiloxane) for the enhanced adhesion and proliferation of mesenchymal stem cells.* Acs Applied Materials & Interfaces, 2013. **5**(19): p. 9777-9784.

24.    M.K. Chaudhury, *Surface free-energies of alkylsiloxane monolayers supported on elastomeric polydimethylsiloxanes.* Journal of Adhesion Science and Technology, 1993. **7**(6): p. 669-675.

25.    S.K. Thanawala and M.K. Chaudhury, *Surface modification of silicone elastomer using perfluorinated ether.* Langmuir, 2000. **16**(3): p. 1256-1260.

26.    G.S. Ferguson, M.K. Chaudhury, H.A. Biebuyck, and G.M. Whitesides, *Monolayers on disordered substrates - self-assembly of alkyltrichlorosilanes on surface-modified polyethylene and poly(dimethylsiloxane).* Macromolecules, 1993. **26**(22): p. 5870-5875.

27.     S.H. Tan, N.T. Nguyen, Y.C. Chua, and T.G. Kang, *Oxygen plasma treatment for reducing hydrophobicity of a sealed polydimethylsiloxane microchannel.* Biomicrofluidics, 2010. **4**(3): p. 8.

28.     M.J. Owen and J.L. Stasser, *Plasma treatment of polydimethylsiloxane.* Abstracts of Papers of the American Chemical Society, 1997. **213**: p. 563-POLY.

29.     H. Hillborg, J.F. Ankner, U.W. Gedde, G.D. Smith, H.K. Yasuda, and K. Wikstrom, *Crosslinked polydimethylsiloxane exposed to oxygen plasma studied by neutron reflectometry and other surface specific techniques.* Polymer, 2000. **41**(18): p. 6851-6863.

30.     K. Efimenko, W.E. Wallace, and J. Genzer, *Surface modification of sylgard-184 poly(dimethyl siloxane) networks by ultraviolet and ultraviolet/ozone treatment.* Journal of Colloid and Interface Science, 2002. **254**(2): p. 306-315.

31.     H. Hillborg and U.W. Gedde, *Hydrophobicity recovery of polydimethylsiloxane after exposure to corona discharges.* Polymer, 1998. **39**(10): p. 1991-1998.

32.     V. Sunkara, D.K. Park, H. Hwang, R. Chantiwas, S.A. Soper, and Y.K. Cho, *Simple room temperature bonding of thermoplastics and poly(dimethylsiloxane).* Lab on a Chip, 2011. **11**(5): p. 962-965.

33.     R.N. César, *Design of mechanoresponsive surfaces and materials.* 2013.

34.     J. Bart, R. Tiggelaar, M.L. Yang, S. Schlautmann, H. Zuilhof, and H. Gardeniers, *Room-temperature intermediate layer bonding for microfluidic devices.* Lab on a Chip, 2009. **9**(24): p. 3481-3488.

35.     S.B. Heo, Y.S. Jeon, Y.J. Kim, S.H. Kim, and J.H. Kim, *Bioinspired self-adhesive polymer for surface modification to improve antifouling property.* Journal of Coatings Technology and Research, 2013. **10**(6): p. 811-819.

36.     F. Zhang, E.T. Kang, K.G. Neoh, P. Wang, and K.L. Tan, *Modification of si(100) surface by the grafting of poly(ethylene glycol) for reduction in protein adsorption and platelet adhesion.* Journal of Biomedical Materials Research, 2001. **56**(3): p. 324-332.

37.     S.I. Jeon, J.H. Lee, J.D. Andrade, and P.G. Degennes, *Protein surface interactions in the presence of polyethylene oxide .1. Simplified theory.* Journal of Colloid and Interface Science, 1991. **142**(1): p. 149-158.

38.     X.L. Sun, C.L. Stabler, C.S. Cazalis, and E.L. Chaikof, *Carbohydrate and protein immobilization onto solid surfaces by sequential diels-alder and azide-alkyne cycloadditions.* Bioconjugate Chemistry, 2006. **17**(1): p. 52-57.

39.     J. Bacharouche, F. Badique, A. Fahs, M.V. Spanedda, A. Geissler, J.P. Malval, M.F. Vallat, K. Anselme, G. Francius, B. Frisch, J. Hemmerle, P. Schaaf, and V. Roucoules, *Biomimetic cryptic site surfaces for reversible chemo- and cyto-mechanoresponsive substrates.* Acs Nano, 2013. **7**(4): p. 3457-3465.

40.     J.M. Harris and S. Zalipsky, Poly(Ethylene Glycol): Chemistry and Biological Applications. ACS Symposium Series, 1997: p. 489.

41.     S. Zalipsky, *Chemistry of polyethylene-glycol conjugates with biologically-active molecules.* Advanced Drug Delivery Reviews, 1995. **16**(2-3): p. 157-182.

42.     A. Abuchowski, J.R. McCoy, N.C. Palczuk, T. Vanes, and F.F. Davis, *Effect of covalent attachment of polyethylene-glycol on immunogenicity and circulating life of bovine liver catalase.* Journal of Biological Chemistry, 1977. **252**(11): p. 3582-3586.

43.     J.M. Harris, *Introduction to biomedical and biotechnical applications of polyethylene glycol.* Abstracts of Papers of the American Chemical Society, 1997. **213**: p. 21-POLY.

44.     H.C. Kolb and K.B. Sharpless, *The growing impact of click chemistry on drug discovery.* Drug Discovery Today, 2003. **8**(24): p. 1128-1137.

45.     V.V. Rostovtsev, L.G. Green, V.V. Fokin, and K.B. Sharpless, *A stepwise huisgen cycloaddition process: Copper(i)-catalyzed regioselective "ligation" of azides and terminal alkynes.* Angewandte Chemie-International Edition, 2002. **41**(14): p. 2596-+.

46.     C.W. Tornoe, C. Christensen, and M. Meldal, *Peptidotriazoles on solid phase: 1,2,3 -triazoles by regiospecific copper(i)-catalyzed 1,3-dipolar cycloadditions of terminal alkynes to azides.* Journal of Organic Chemistry, 2002. **67**(9): p. 3057-3064.

47.     *Proceedings of the chemical society. October 1961.* Proceedings of the Chemical Society, 1961(October): p. 357-396.

48.     E. Lallana, R. Riguera, and E. Fernandez-Megia, *Reliable and efficient procedures for the conjugation of biomolecules through huisgen azide-alkyne cycloadditions.* Angewandte Chemie-International Edition, 2011. **50**(38): p. 8794-8804.

49.     Q. Wang, T.R. Chan, R. Hilgraf, V.V. Fokin, K.B. Sharpless, and M.G. Finn, *Bioconjugation by copper(i)-catalyzed azide-alkyne 3+2 cycloaddition.* Journal of the American Chemical Society, 2003. **125**(11): p. 3192-3193.

50.     S.C. Fry, *Oxidative scission of plant cell wall polysaccharides by ascorbate-induced hydroxyl radicals.* Biochemical Journal, 1998. **332**: p. 507-515.

51.     V. Hong, S.I. Presolski, C. Ma, and M.G. Finn, *Analysis and optimization of copper-catalyzed azide-alkyne cycloaddition for bioconjugation.* Angewandte Chemie-International Edition, 2009. **48**(52): p. 9879-9883.

52.     J.E. Hein, Krasnova, L. B., Iwasaki, M., Fokin, *Cu-catalyzed azide-alkyne cycloaddition: Preparation of tris((1-benzyl-1h-1,2,3-triazolyl)methyl)amine.* Organic Syntheses, 2012: p. 238–246.

# Chapter 4

## Catalytic mechano-responsive polyelectrolyte multilayers based on conformational changes of enzymes

## 4.1. Introduction

In this 4th chapter, *beta-galactosidase enzyme* was used in order to elaborate a catalytic active material. To increase the number of immobilized enzymes inside the material, and thus increasing its response to the stretching, a strategy based on the elaboration of a polymeric matrix loaded with the enzymes was developed. Under stress a deformation on the enzymes leads to modification in the material catalytic activity (figure 4.1). This chapter was performed within the collaboration of César Rios and written as a publication in order to be submitted. Thus all the experimental details relative to this work are given in the "experimental section" (ES). It must be noted that additional experiments were performed after the paper writing and are so presented in a specific part at the end of this chapter.
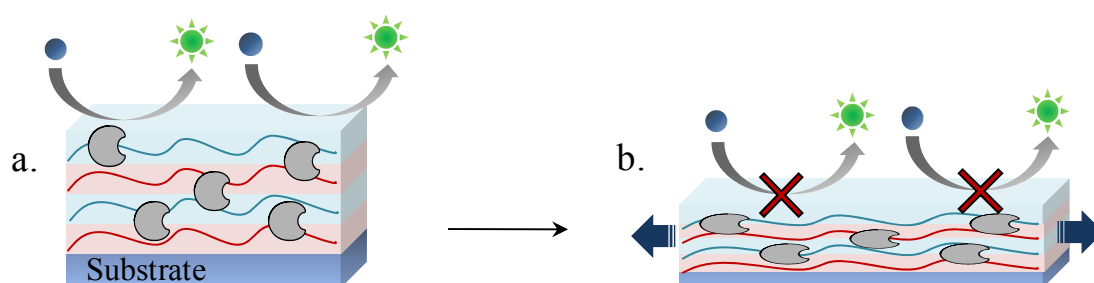


*Figure 4.1*: *Schematic representation of the mechano-responsive film. (a) At rest enzymatic activity occurs. (b) Under mechanical stress, enzyme structure is putting out of shape leading to a loss of activity.*

## 4.2. Article: Catalytic mechano-responsive polyelectrolyte multilayers based on conformational changes of enzymes

Chemo-mechano-responsive materials emerge as a new class of materials that respond chemically to a mechanical stress by triggering a chemical reaction. For example, new types of polymeric materials were designed that include mechanophores which change color under mechanical stress or release protons under compression [1]. Whereas in these materials, the chemical reaction results from stress-sensitive chemical groups incorporated in polymer chains which undergo a chemical transformation under high tension, nature uses rather less energy demanding processes based on protein conformational changes. For example, stretching domain-proteins such as fibronectin exposes cryptic sites that allow cell adhesion or trigger osteogenic differentiation [2]. Enzymes constitute a class of proteins that act through

a precise topology of the residues involved in their active site. Moreover, structural dynamics of enzymes play a major role in the enzymatic activity [3]. Thus, enzyme activity should also be able to be modulated by applying on them a mechanical stress. In 1974, Berezin *et al*. have degraded nylon fiber surfaces to create microcracks and embed or link enzymes inside [4, 5]. Variations of the catalytic activity of the enzymes were indeed observed by stretching the fibers, suggesting that the effect originates conformational changes of the enzymes induced by stretch. More recently, the influence of mechanical force on enzyme conformation and thus enzyme activity was clearly demonstrated by the groups of Gaub and Blank who manipulated an enzyme with a periodic stretch through single molecule force spectroscopy [6]. This was also confirmed by Tseng *et al.* who used DNA molecular springs that are coupled on two positions of an enzyme to create a protein-DNA chimeras, the DNA applying a mechanical stress on the enzymes [7]. Using nature's strategy, our goal is to develop a general method to produce mechano-responsive enzyme-containing films based conformational changes of the enzymes induced by stretch.

Polyelectrolyte Multilayer (PEM) films offer a unique opportunity to achieve this goal. Based on the alternate deposition of polyanions and polycations onto a solid substrate, PEM can be used whatever the chemical nature and shape of the substrate and for these reasons widespread applications are foreseen [8-10]. In particular, it allows to confer biologic and enzymatic activity to a film by incorporation of proteins or enzymes [11]. Several requirements have to be fulfilled to obtain potentially chemo-mechano-responsive films: *i)* they should be elastic and stretchable,[12, 13] *ii)* the enzymes should remain active in the film and *iii)* the enzymatic substrate should be able to diffuse in the film in order to react with the enzymes.

We used poly(L-lysine)/hyaluronic acid (PLL/HA) exponentially growing PEM films deposited on silicone substrates because these films reach micrometer thicknesses after less than 15 deposition steps and allow for the immobilization of large amount of enzymes, as required for our purpose. β-galactosidase (β-Gal), a hydrolase enzyme that catalyses the breakdown of lactose, has been chosen due to its tetramer structure comprised of four active sites and four polypeptide chains held together through non-covalent interactions (Figure 4.2) [14-16].
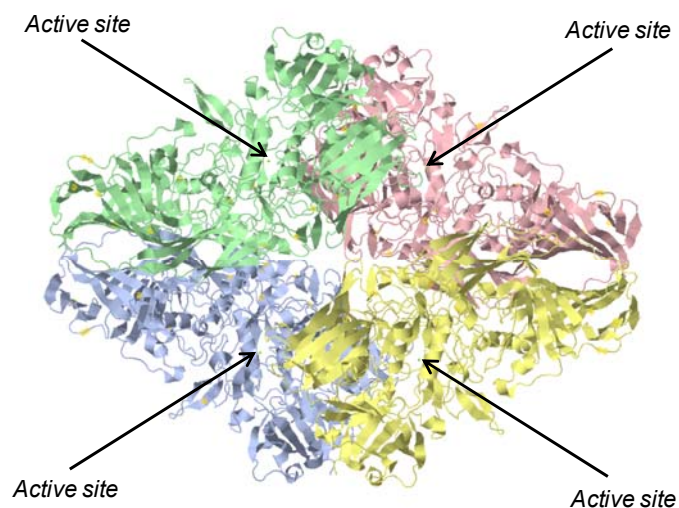
***Figure 4.2****: View of the β-Gal tetramers by coloring each subunit. Black arrows show the localization of the four active sites of the enzyme. Image taken from PDB (code: 1BGL).*

Each active site of the enzyme includes residues belongs to two different subunits. Because these subunits are non-covalently linked, the catalytic center is anticipated to be sensitive to external forces applying onto the enzyme. Fluorescein di(β-D-galactopyranoside) (FDG) is used as a substrate of β-Gal. This fluorogenic substrate is transformed into fluorescein and β-D-galactopyranoside under the action of β-Gal (see §1, Scheme S4 in Experimental Section). The reaction can thus be followed by monitoring the fluorescence of the solution in contact with the film. The enzyme had to be covalently linked to the multilayer network to respond to a mechanical stress and in consequence we used PLL chains chemically modified by thiopyridyl (S-TP), named PLL-S-TP (grafting ratio of 27%) and β-Gal enzyme modified by maleimide groups (mal, 70% of grafting ratio), named β-Gal-mal. The synthesis of these compound is given in §1 of the ES.

In a first set of experiments multilayers were grown on silicone substrates by alternating the deposition of PLL-S-TP and HA. After the deposition of 24 bilayers a thickness of 5 µm was reached (§3 in ES). These films were then cross-linked through carbodiimide chemistry by bringing it in contact with an ethyl(dimethylaminopropyl) carbodiimide and N-hydroxysuccinimide (EDC-NHS) solution [17]. They were then brought in contact with a 500 µg.mL⁻¹ β-Gal-mal solution without deprotection of PLL-S-TP, so that the enzymes are not cross-linked to the film through maleimide-thiol coupling reaction (see figure

4.3). We first verified that the enzyme has diffused into the reticulated film. Using β-Gal-mal$^{FITC}$, confocal microscopy images show that the whole cross-linked PLL-S-TP/HA film section is labeled in green (Fig. S5). When this film was brought in contact with the substrate, *i.e.* a FDG solution, fluorescence in solution increased linearly with time. This indicates that despite the cross-linking of polyelectrolyte chains, the enzyme embedded into the film remains enzymatically active. When this film was stretched at 50% and then at 100%, no significant change in the enzymatic activity was observed (Fig. 4.4a). This result suggests that enzymatic activity of the film is not affected by stretching if enzymes are uncoupled to the polyelectrolyte chains. We also checked that the absence of variation of fluorescence intensity with stretching cannot be attributed to a leaching of enzymes out of the film during the stretching cycles (see §3.5 in ES).
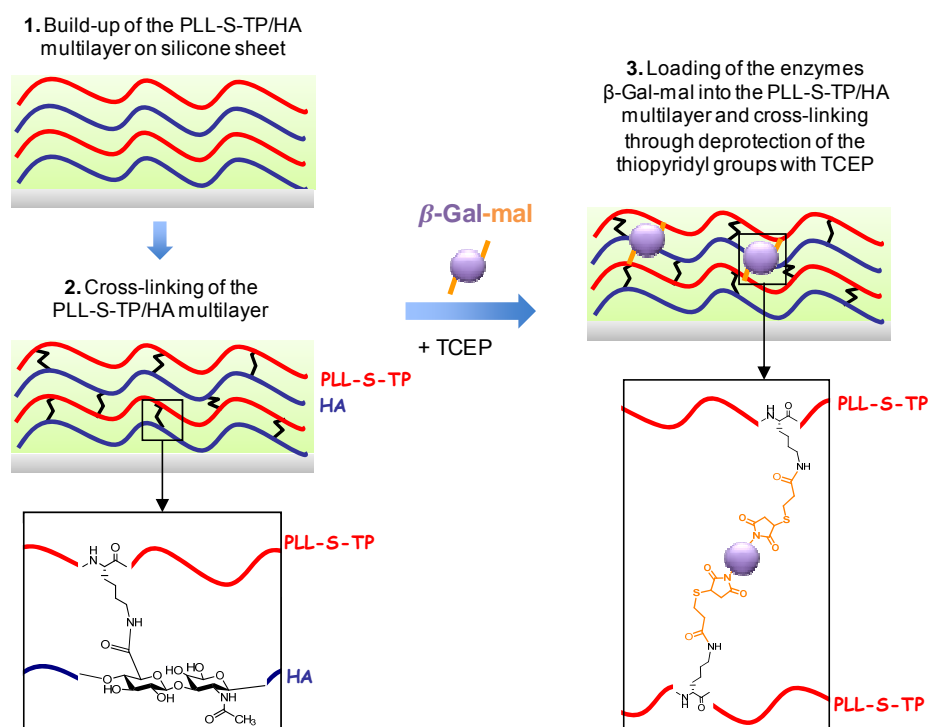


*Figure 4.3: Description of the different stages necessary to cross-link β-Gal in the stretchable multilayer.*

For the second set of experiments, the cross-linked PLL-S-TP/HA films were brought in contact with β-Gal-mal enzymes in the presence of TCEP ((Tris(2-carboxyethyl) phosphine hydrochloride) to deprotect the thiopyril moieties (S-TP) of PLL which then react with

maleimide groups of β-Gal. β-Gal-mal become thus covalently linked to the film (figure 4.3). The deprotection reaction was monitored by measuring the supernatant absorbance at 343nm (Fig. S5). The increase in absorbance corresponds to the release of the thiopyridone molecules in solution. The reaction takes place during approximately 30 minutes.
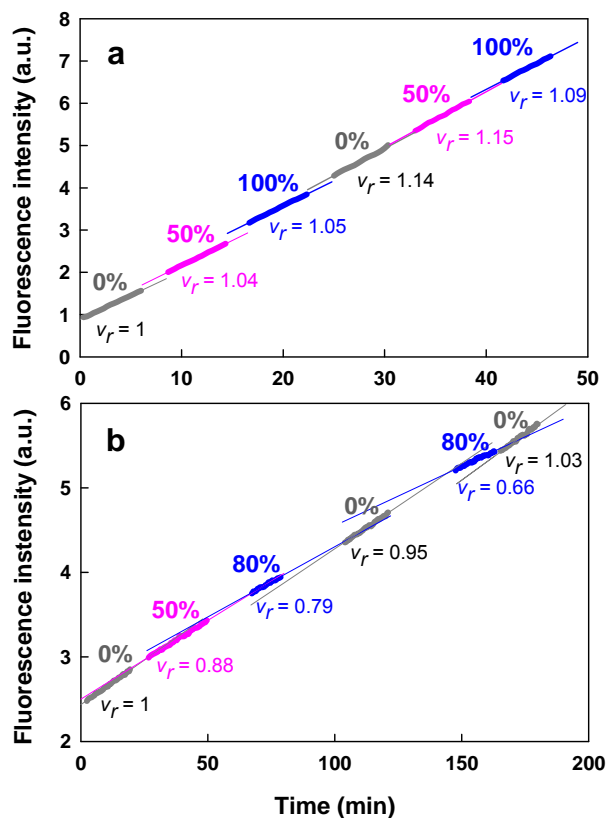


***Figure 4.4**: Evolution of the enzymatic activity monitored via production of fluorescence and measured in solution over time during stretching (50%, 80% or 100%) / unstretching (0%) cycles. The fluorescence intensities corresponding to a given strain have been fitted with a linear equation. The coefficients $v_r$ are the ratios of the slopes at each strain to the slope in the initial state (i.e. initial curve without stretching, first gray curve). Thin lines are linear regressions and bold lines are raw data. Modified enzymes, β-Gal-mal, were loaded in the EDC-NHS reticulated (PLL-S-TP/HA)$_{24}$ films and (a) no TCEP was yet introduced (no covalent coupling of the enzymes to the film), (b) after TCEP was added to the film, the enzymes were covalently fixed to the multilayer.*

By using a calibration curve (Fig. S4), the enzyme concentration in the film was estimated to be of the order of 850 µg.mL$^{-1}$ (see details in § 3 in ES). These cross-linked PLL/HA films containing covalently attached β-Gal-mal enzymes were then stretched in a stepwise manner up to 80-100%. Figure 4.4b shows a typical evolution of the fluorescence intensity monitored when a FDG solution is put in contact with the film during the stretching.

First in the non-stretched state, the films are enzymatically active indicating that the covalent immobilization of the enzymes within the cross-linked polyelectrolyte network does not affect their activity. Under stretching, the fluorescence production rate monitored in the solution decreased and this diminution was amplified when the strain was increased. This evolution of the enzymatic activity was different from that observed with non-cross-linked enzymes where the fluorescence production remained almost constant or even increased slightly under stretching. This experiment was repeated several times and results are summarized in Figure 4.5a and 4.5b where the fluorescence production rates, averaged over different experiments, are plotted as a function of the strain. The stretching of immobilized enzymes in the PEM film affected its enzymatic activity about 30% compared to the non-stretched state. It is expected that the decrease of the enzymatic activity is due to a stretching-induced change of the enzyme conformation. This hypothesis is in agreement with very recent work published by Bielawski *et al.* where Yellow and Green Fluorescent Proteins where both covalently incorporated in biocomposite materials [18]. Under compression a shift or a decrease of the fluorescence emission was observed, an effect attributed by these authors to conformational changes of the proteins.
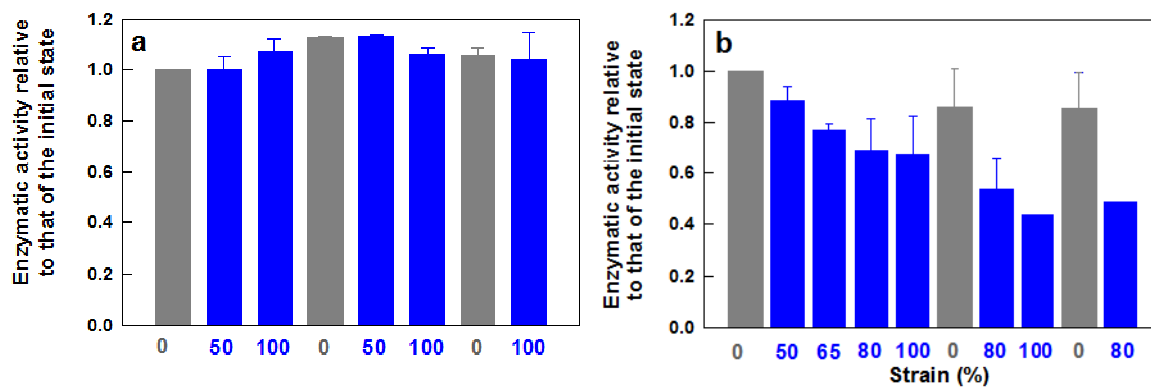


***Figure 4.5****: Evolution of the mean enzymatic activity monitored via production of fluorescence for different strains. (a) enzymes not covalently linked to PLL/HA network and (b) enzymes covalently linked toPLL/HA network. The activities have been normalized to the rates measured in the initial, non-stretched state. The rate values correspond to the mean value of 2 experiments in (a) and up to 7 experiments in (b) and error bars correspond to standard deviations. The Kruskal-Wallis test reveals non-significant influence of the strain in (a) (p = 0.166) whereas significant influence is suggested in (b) (p = 0.021) if one refers to risk level of 0.05.*

Next, we investigated the reversibility of the enzymatic activity change. The films were stretched at 80 or 100% and then brought back to the non-stretched state (Figure 4.5b). By release of the stretch, an increase of the enzymatic activity is obtained which is about $87 \pm$

15% of the initial production rate. When repeated a second time with the same films, the stretching/unstretching process induced again a decrease/increase of the enzymatic activity. The stretch-induced change of the enzymatic activity is thus partially reversible. These results highlight the enzymatic mechano-responsive properties of the designed PEM film.

Our PEM based system, demonstrates the proof of concept of the strategy developed and exhibits reasonable performances (30% reduction of enzymatic activity and partial reversibility). However, it could be optimized in the future and in particular a multidirectional stretching device will be designed to stretch enzymes in several directions. Indeed, as enzymes are oriented randomly to the material, some of them might not sense the unidirectionnal stretch and should not or slightly be affected by the stretch. This distribution of stresses might be at the origin of both limited range of the effect and incomplete reversibility.

This study is a proof of principle demonstrating the use of cross-linked enzyme containing PEM films to create chemo-mechano-responsive materials based on local modification of enzymatic conformation. Due to the versatility of the PEM tool, this work will help the community to design new functionalized materials where activity is controlled by a mechanical stretch.

## 4.3. Experimental section (SE)

It must be noticed that in order to stay in agreements with the publication shaping, the experimental section owns a specific numbering.

## 1. Chemicals and chemical modifications of polymers and enzymes

### 1.1. Chemicals

The polyelectrolytes poly(L-lysine) (PLL, Mw = 2.60 × 104 Da) and hyaluronic acid (HA, Mw = 1.32 × 105 Da) were purchased from Sigma Aldrich (Saint-Quentin Fallavier, France) and Lifecore Biomedical (Chaska, USA) respectively. Coupling agents as N,N′-Dicyclohexylcarbodiimide 99% (DCC), N-(3-Dimethylaminopropyl)-N′-ethylcarbodiimide hydrochloride ≥ 98% (EDC), N-Hydroxysuccinimide 98% (NHS), and N-Hydroxysulfosuccinimide sodium salt (sulfo-NHS) ≥ 98% were all purchased from Sigma Aldrich. The enzyme β-galactosidase (β-Gal) from Escherichia coli Grade VI, lyophilized powder, 250-600 units/mg protein and the enzyme substrate fluorescein di(β-D-galactopyranoside) (FDG) were purchased from Sigma Aldrich. 2,4,6-Trinitrobenzenesulfonic acid (TNBS), Tris(2-carboxyethyl)phosphine hydrochloride powder, ≥ 98% (TCEP), tris(hydroxymethyl)aminomethane (TRIS) and 4-(2-Hydroxyethyl)piperazine-1-ethanesulfonic acid (HEPES), sodium chloride (NaCl), sodium bicarbonate (NaHCO3) anhydrous solvents for synthesis dichloromethane (CH2Cl2), N,N-Dimethylformamide (DMF) were all purchased from Sigma Aldrich. Dialyzed cellulose ester membrane (MWCO 3500 Da) was purchased from Carl Roth (Lauterbourg, France) and bicinchoninic assay protein quantification kit was purchased from Uptima (Montluçon, France). Thiopyridone mercaptopropionic acid (TP-MPA) was synthesized by the procedure describe by Xie et al [19]. Maleimide succinimide ester was synthesized by the procedure describe by Thibaudeau et al [20]. Poly(dimethylsiloxane) (PDMS) sheets of 250 µm thickness (Specialty Manufacturing Inc., Saginaw, USA) and circular glass slides with 12-mm diameter and 150-µm thickness (Menzel-Gläser, Braunschweig, Germany) were chosen as substrates for the construction of polyelectrolyte multilayer (PEM) films.

## 1.2. Chemical modification of PLL with thiopyridone protecting groups (PLL-S-TP)

The modified poly(L-Lysine) with thiopyridone groups (PLL-S-TP) was obtained in a two-step reaction. The first step consists in the activation of the thiopyridone mercaptopropionic acid (TP-MPA) with the *N*-hydroxysuccinimide (NHS) followed by the second step where the amines of the PLL will make a nucleophilic attack on the activated acid cited before.

### 1.2.1. First step: activation of the TP-MPA acid with NHS
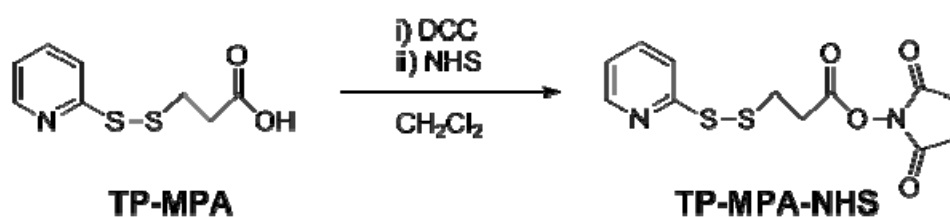


*Scheme S1*: *Synthesis of TP-MPA-NHS*

The TP-MPA (186mg, 0.864mmol) was dissolved in 8mL of $CH_2Cl_2$ followed by the addition of DCC (178mg, 0.864mmol, 1eq) and NHS (99mg, 0.864mmol, 1eq). The reaction was stirred at room temperature for 24h. The solution was filtered and the solvent was removed under pressure until dryness to obtain a yellow solid compound TP-MPA-NHS in a quantitative yield which will be used in the next step without further purification. The characterization of this compound is described by Xie *et al* [19].

### 1.2.2. Second step: coupling reaction between TP-MPA-NHS and the PLL
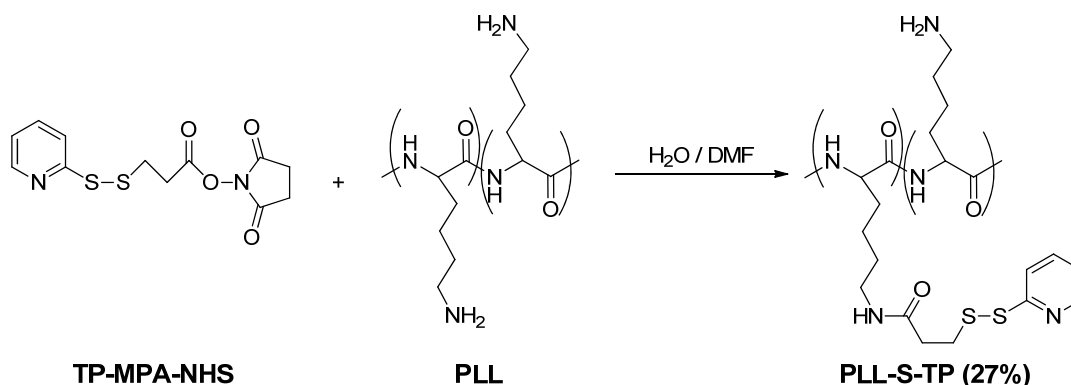


*Scheme S2*: *Synthesis of PLL-S-TP*

The PLL (300mg, 1.44mmol) was dissolved in 15mL of Milli-Q water followed by the addition of a solution of TP-MPA-NHS (269.9 mg, 0.864 mmol, 0.6eq) in 3mL of DMF. The reaction was stirred at room temperature for 24 h. The solution was filtered and dialyzed (cellulose ester membrane (MWCO 3500 Da)) against a 2L solution of NaCl 0.30 M for 1 day at 4°C and then changed two times against 2 L of Milli-Q water for another 2 days at 4°C. Lyophilisation of the solution afforded PLL-S-TP as a white like foam with a 75 % yield.

$^1$H NMR (D$_2$O, 400 MHz, δ ppm): 8.30 (br s, 0.27H, Ar), 7.75 (br s, 0.54H, Ar), 7.20 (br s, 0.27H, Ar) 4.35 (br s, 1H, C$\alpha$<u>H</u>), 3.05 (br s, 0.54H, CH$_2$ thiopyridyl), 2.99 (br s, 2H, CH$_2$ $\alpha$NH$_2$), 2.70 (br s, 0.54H, CH$_2$ thiopyridyl) 1.85 (br m, 4H CH$_2$CH$_2$), 1.40 (br s, 2H, CH$_2$).

By comparison of the integration of one aromatic signal and the integration of the broad singlet at 4.25 (H on the carbon α of the lysine amino acid), the percentage of modification on the PLL by thiopyridone groups is estimated to be 27%

### 1.3. Chemical modification of β-galactosidase with maleimide groups (β-Gal-mal)

### 1.3.1. Chemical modification
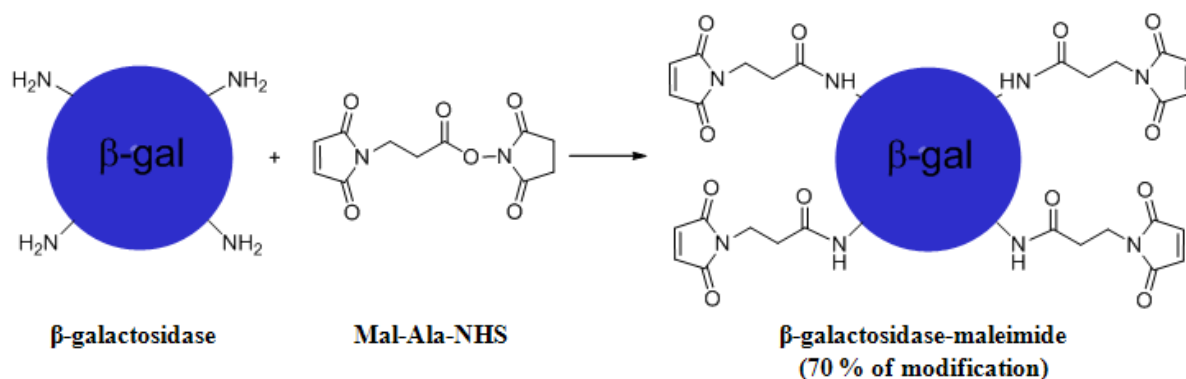


*Scheme S3*: *Synthesis of ß-Gal-mal.*

β-Gal from Escherichia coli (7mg, 1.61 × 10-5 mmol) was dissolved in 1mL of NaHCO3 0.1 M at pH 8.5 followed by 4mL of HEPES 50mM at pH 6. Then, 500μL of a 1mg.mL$^{-1}$ (0.5mg, 1.87 × 10$^{-3}$mmol) 3-(Maleimido)propionic acid N-succinimidyl ester (Mal-Ala-NHS) solution in DMF is added to the β-Gal solution and stirred at room temperature for 3h. The solution was dialyzed (cellulose ester membrane (MWCO 10000 Da)) against a 2L solution of 50mM

HEPES and two times against a 2L solution 10 mM HEPES pH 6 at 4°C for 3 days. Aliquots of 250µL were prepared and conserved at -20°C. The modified enzymes with maleimide groups (ß-Gal-mal) were not lyophilized after chemical modification to avoid the loss of enzymatic activity as observed in previous experiments where this lyophilization was performed.

### 1.3.2. Determination of the modified enzyme (ß-Gal-mal) concentration

We used the bicinchoninic acid (BCA) assay test to determine the concentration of the solutions of the modified enzyme [21]. A fresh set of protein standards, from $20\mu g.mL^{-1}$ to $1mg.mL^{-1}$, were prepared using the bovine serum albumin (BSA) at 2 mg.mL-1. β-Gal-mal and β-Gal (control) solutions at $1mg.mL^{-1}$ were prepared and then diluted to $0.25mg.mL^{-1}$ in NaHCO3 0.1M solutions at pH 8.5. Then 2mL of BC Assay reagent (mixture of 50 parts of bicinchoninic acid and 1 part of CuSO4) were added to the test tubes, mixed and incubated at 60°C for 20min. All the test tubes were mixed at room temperature and their optical absorbance read at 562nm against the blank NaHCO3 in a 96-well plate. Then the protein concentrations can be calculated with a reference curve obtained for a standard protein. Finally, we obtained a concentration of $0.4$ mg.mL$^{-1}$ for β-Gal-mal and $0.5mg.mL^{-1}$ for β-Gal.

### 1.3.3. Verification of the catalytic activity of the modified enzyme

The enzymatic activity of the β-Gal-mal was verified against the unmodified enzyme β-Gal in presence of the substrate fluorescein di(β-D-galactopyranoside) (FDG). The principle of this experiment is the hydrolysis in 2 steps of the FDG in the presence of the enzyme to obtain fluorescein (Scheme S4).



**Fluorescein di(*β*-D-galactopyranoside) (FDG)**

**Fluorescein**
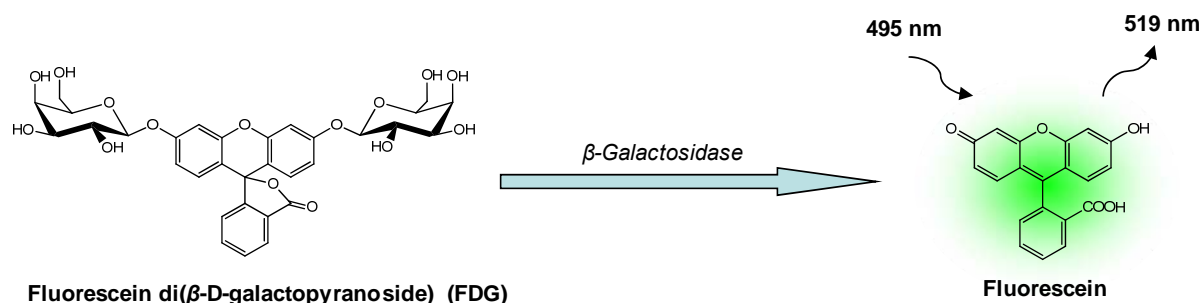
*Scheme S4*: *Hydrolysis reaction of the FDG by the β-Gal.*

In a 96-well plate, we added 200 µL of FDG at 0.071mg.mL$^{-1}$ and 50µL of the enzymes separately at 0.0048mg.mL$^{-1}$. Then, the catalytic activity was recorded with the spectrofluorimeter equipped with a microplate reader (λex/em: 495nm / 519nm; see 2.2 below). The modified enzymes appear 3.4 times less active than the non-modified β-Gal.
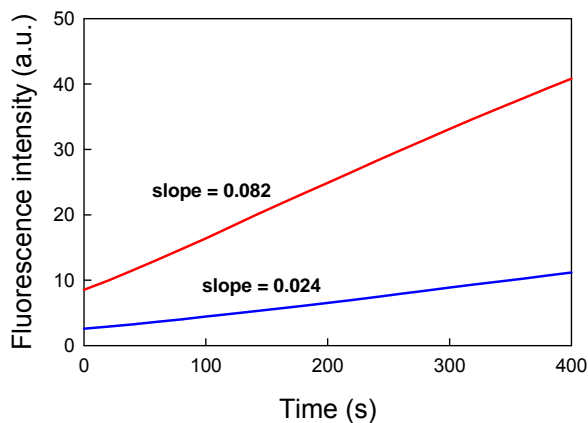


***Figure S1:*** *Comparison of the enzymatic activity of the modified (β-Gal-mal) (blue line) and unmodified (β-Gal) enzyme (red line).*

### 1.3.4. Free-amines TNBS test

The grafting rate on the modified β-Gal with maleimide groups was obtained using the 2,4,6-Trinitrobenzenesulfonic acid (TNBS) also known as picrylsulfonic acid. This test consists in the covalent coupling reaction between the picrylsulfonic acid and the primary amine groups that are present on the protein to form a highly chromogenic derivative (Scheme S5) [22].
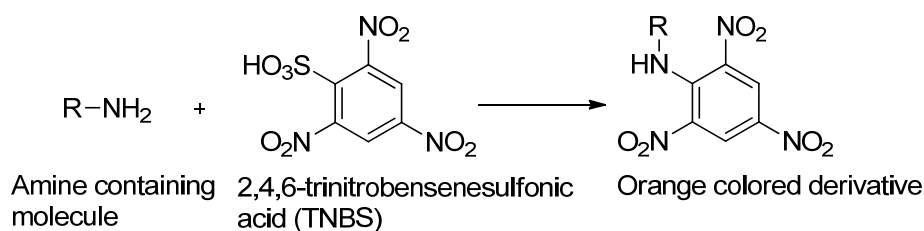


***Scheme S5:*** *TNBS may be used to detect or quantify amine groups through the production of a chromogenic derivative.*

Different concentrations of glycine (standard) were prepared ranging from $10^{-1}$mM to $10^{-3}$mM in 0.1M of NaHCO$_3$ at pH 8.5 from glycine 1mM. 1mL of the standard solutions was mixed with 25μL of a 30mM picrylsulfonic acid solution. In the same way, 300μL of the β-Gal (control) and β-Gal-mal solutions at 0.1mg.mL$^{-1}$ in 0.1M of NaHCO$_3$ pH 8.5 and 7.5μL of a picric sulfonic acid solution were added into the Eppendorf tubes. They were incubated for 40min at room temperature. After that 200μL of the glycine (standard), β-Gal (control) and β-Gal-mal solutions were transferred into a 96-well plate and the optical absorption was measured at 420nm with a spectrophotometer (see 2.2). In Figure S1, the lysine concentration can be calculated with a reference curve obtained for a glycine solution (standard). The grafting ratio was calculated from the relation:

$$GR = \frac{modified\ groups}{total\ groups} = \frac{total\ groups\ -\ non-modified\ groups}{total\ groups}$$

Where total and non-modified groups represent the UV absorbance of the β-Gal and β-Gal-mal, respectively. A grafting ratio of 70% was obtained after modification of the β-Gal with maleimide groups.

## 1.4. Chemical modification of enzymes with fluorophores

### 1.4.1. Chemical modification of β-Gal with fluorescein isothiocyanate (β-Gal$^{FITC}$)

3.1mg of β-Gal was dissolve in 3mL of 100mM NaHCO$_3$ buffer at pH 8.5 followed by the addition of 3.75μg of fluorescein isothiocyanate (FITC) in methanol solution (100μL). The reaction mixture was stirred for 3h at room temperature and dialyzed with a cellulose ester membrane (MWCO 3500) against a 2L solution of NaCl 0.3M for 8h and finally with 2L of Milli-Q water for another 24h. Lyophilization of the solution afforded 2.5mg of β-Gal$^{FITC}$ as a yellow powder.

### 1.4.2. Chemical modification of β-Gal-mal with FITC (β-Gal-mal$^{FITC}$)

2mg of β-Gal-mal was dissolved in 3mL of 100mM NaHCO$_3$ buffer at pH 8.5 followed by the addition of 3.75μg of FITC in methanol solution (100μL). The reaction mixture was stirred for 3h at room temperature and dialyzed with a cellulose ester membrane

(MWCO 3500) against a 2L solution of NaCl 0.3M for 8h and finally with 2L of Milli-Q water for another 24h. Lyophilization of the solution afforded 1.7mg of β-Gal-mal$^{FITC}$ as a yellow powder.

## 2. Experimental methods

### 2.1. Stretching device

Figure S2 represents the homemade stretching device used for the experiments. It is made on stainless steel and it allows stretching manually the sample in an unaxial direction. The silicone sheet covered with the enzymatic active film is inserted in two jaws. These jaws can be moved continuously one with respect to the other. This stretching device is inserted in a black support made of poly(methylmethacrylate). This support was design to use the minimum amount of enzyme substrate (FDG). The strain, α, is defined by the relation

$$\alpha = 100 \times \frac{\ell - \ell_0}{\ell_0} \ \text{(in \%)}$$

Where $\ell$ and $\ell_0$ represent respectively the length in the stretched and non-stretched states. All the experiments were performed at room temperature with the PEM-coated silicone side facing down.



***Figure S2:*** *Devices used for the stretching of modified silicone sheets. The silicone sheets are placed between the two clamps and stretched manually.*

### 2.2. Spectrofluorometer with microplate reader

A multidetector spectrofluorimeter (Xenius XC, SAFAS, Monaco) equipped with a microplate reader was used to monitor the fluorescein release in the supernatant which mirrors the catalytic activity of enzymes within the PEM films supported on silicone sheets in contact with its substrate, FDG ($\lambda_{ex/em}$: 495nm / 519nm). Thiopyridyl group deprotection of PLL-S-TP was also monitored by UV experiments at 343nm.

### 2.3. Confocal laser scanning microscope (CLSM)

Confocal laser scanning microscope (CLSM) observations of PEM films were carried out with a Zeiss LSM 510 microscope using a × 40/1.3 oil immersion Objective and with 0.43 μm z-section intervals. FITC fluorescence was detected after excitation at $\lambda = 488$nm with a cut-off dichroic mirror of 488nm and an emission band-pass filter of 505–530nm (green emission). An average of three images in the same location was acquired at $256 \times 256$ pixels. Virtual film section images were taken from the film in the presence of liquid (NaCl 0.15 / TRIS 10mM), hence allowing the determination of the thickness of the film. All the experiments are performed in the presence of liquid (0.15M NaCl/10mM Tris, pH = 7.4) and the multilayer films were never dried.

## 3. Mechano-responsive film construction

### 3.1. Polyelectrolyte multilayer film construction

PEM films were built with an automated dipping robot (Riegler & Kirstein GmbH, Berlin, Germany) on silicone sheets (Specialty Manufacturing Inc., Saginaw, MI, USA) of 254μm thickness or microscope slides. Silicone sheets of $18 \times 18$ mm$^2$ were previously cleaned with ethanol and then extensively rinsed with water. The polyelectrolytes used for the construction of the multilayers were dissolved in a 0.15M NaCl solution prepared with ultrapure water (18.2 MΩ.cm Milli-Q plus system, Millipore) and used at a concentration of 1mg.mL$^{-1}$. Silicon substrates were first dipped in a PLL-S-TP solution (polycation) for 4min. Then, two rinsing steps were performed by dipping the sheets two times for 5min in 0.15M NaCl solution. The polyanion (HA) was then deposited in the same manner. The buildup process was pursued by the alternated deposition of PLL-S-TP and HA. After deposition of *n*

bilayers, the film is denoted (PLL-S-TP/HA)$_n$. We used films constituted of 24 PLL-S-TP/HA "bilayers".

### 3.2. Loading β-Gal enzymes into PLL-S-TP/HA films

### 3.2.1 Characterization of the loading by confocal microscopy
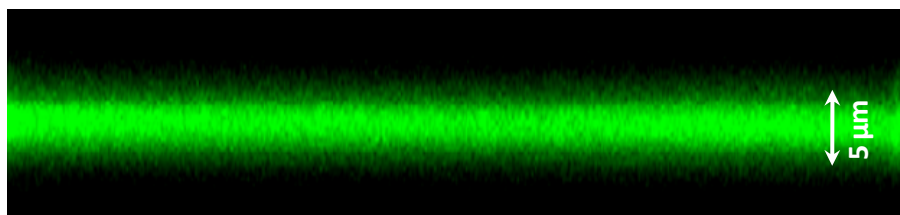


*Figure S3*: *Confocal microscope section (x,z) images of (PLL-S-TP/HA)$_{24}$ films deposited on silicone sheets and brought in contact with a β-Gal$^{-FITC}$ solution at 500μg.mL$^{-1}$. The image was taken after contact between the film and the β-Gal$^{FITC}$ solution before cross-linking following addition of TCEP. The thickness of the film is around 5μm.*

### 3.2.2. Determination of the amount of β-Gal-mal enzymes loaded in the cross-linked PLL-S-TP/HA film.

We adapted a method developed by Vodouhê *et al.*[5] to determine the amount of β-Gal-mal enzymes loaded in the cross-linked PLL-S-TP/HA film.

Once PLL-S-TP/HA film was built, the film was cross-linked through 20mM EDC / 50mM Sulfo-NHS solution as described above. Then, the film was brought in contact with an ethanolamine 1M solution prepared in 0.15M NaCl for 40 min. This treatment desactivates the activated carboxylic groups within the film. Later, a 400µL of β-Gal-mal$^{FITC}$ solution at 0.5mg.mL$^{-1}$ was added for 1 hour, after that the enzyme solution was removed and replaced by 500µL of 1mM TCEP solution for 30min. Finally, the PEM film was rinsed with the buffer solution 0.15M NaCl / 10mM TRIS at pH 7.4. Some (x,z) images were then taken by confocal microscopy at different locations in the film. From these images, the mean fluorescence was determined.

Then, we removed the film from the confocal microscope and replaced it with a glass slide onto which we deposited 100µL of β-Gal-mal$^{FITC}$ at 0.5mg.mL$^{-1}$ solution. Successively,

the concentration of the β-Gal-mal$^{FITC}$ was diluted with the addition of NaCl/TRIS solution. For each concentration, the fluorescence was determined from images taken in the solution with the same experimental parameter setups as for the measurements in the film. This allowed to determine a calibration curve (figure S6) from which we calculated the concentration of β-Gal-mal$^{FITC}$ inside the PEM film. Finally, the concentration of β-Gal-mal$^{FITC}$ in the PLL-S-TP/HA film was about 850µg.mL, when 400µL of β-Gal-mal$^{FITC}$ at 500µg.mL$^{-1}$ were deposited on it for 30min and an extensive rinsing step was performed.
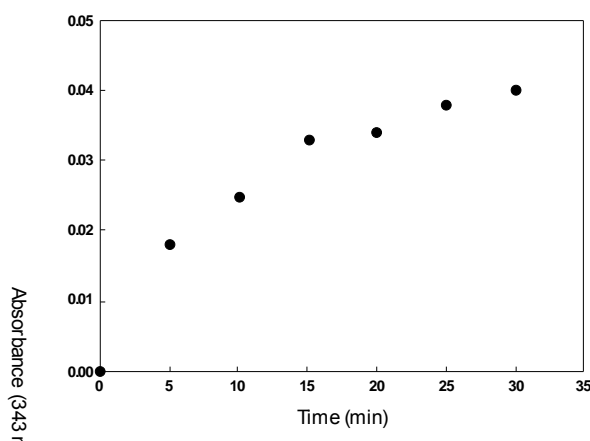


***Figure S4****: Calibration curve for the determination of the β-Gal-mal concentration in the PLL-S-TP/HA cross-linked film. The equation of the curve is I = 2.25 C – 648.92, where I is the fluorescence intensity in a.u. and C the concentration of β-Gal-mal$^{FITC}$ in µg.mL$^{-1}$. The solid line represents the linear regression and the dashed lines represent the 95%-confidence interval.*

## 3.3. Deprotection of thiopyridyl groups on PLL-S-TP

The sample was put in the home made stretching device that was previously coated with parafilm to prevent leaking of the aqueous solution after its addition. A 100µL β-Gal-mal (0.4mg.mL$^{-1}$) in NaCl/TRIS solution was added on the sample containing the cross-linked PEM film (PLL-S-TP/HA) supported on PDMS for 1h. Later, the enzyme solution was replaced by 150µL of TCEP 1mM solution prepared in NaCl/TRIS. Sampling 150µL of TCEP solution was done every 5min and replaced by other 150µL of TCEP solution. UV measurements at 343nm wavelength were performed with the spectrofluorimeter equipped with microplates reader in a 96-well plate with 100 µL of the sampling solution for each

period of time and total time of 30min. Full deprotection of thyopiridone groups are completed after 30min of treatment with TCEP solution (figure S5).
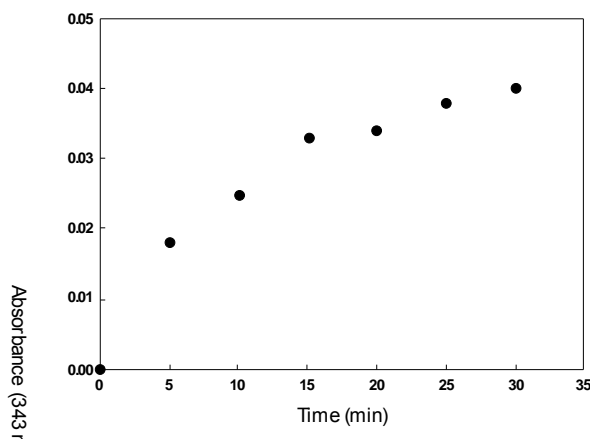


***Figure S5****: Deprotection of the thiopyridyl groups in contact with the TCEP followed by UV spectroscopy at 343 nm wavelength. Most of the reaction takes place over 30 min.*

### 3.4. Cross-linking of the enzyme β-galactosidase-maleimide within the PEM film

The reticulated PEM film on silicone sheets was placed in a homemade stretching device. The homemade device was held together tightly with clips that were previously coated with parafilm to prevent leaking of the aqueous solution after its addition. 100μL of β-Gal-mal at 0.4mg.mL$^{-1}$ prepared in NaCl/TRIS buffer solution was then added for 1h. The modified enzyme was later pippeted and replaced by 200μL of 1mM TCEP prepared in 0.15M NaCl/10mM TRIS buffer solution for 30min. Finally, the PEM film was rinsed with the buffer solution 0.15M NaCl / 10mM TRIS at pH 7.4.

### 3.5. Control experiments to verify the non-leaching out of non-covalently linked enzymes in cross-linked PLL-S-TP/HA films during stretching

To confirm the absence of leaching, we performed an experiment with β-Gal-mal enzymes loaded in the PLL-S-TP/HA film but without cross-linking these enzymes to the film (*i.e.* without TCEP, conditions similar to experiments in Fig. 3a). Then, two stretching/unstretching steps have been performed in pure buffer with return to the non-stretched state. Next, FDG, the enzyme substrate, was added to the supernatant. Enzymatic kinetics was monitored and an enzymatic activity was measured (Fig. S6a below). When the

film was withdrawn from the cuvette, no more evolution in the fluorescence intensity was observed as depicted in Fig. S6b.
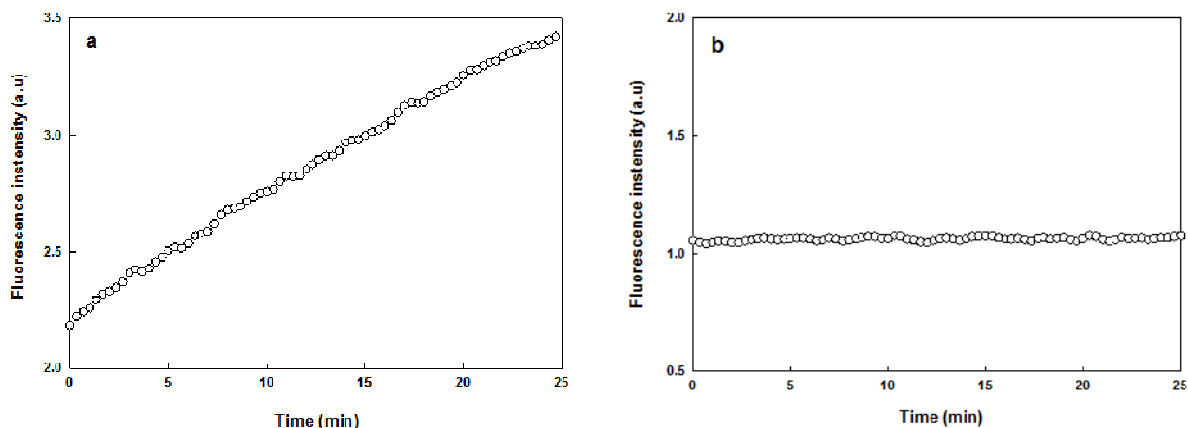


***Figure S6***: *Evolution of the enzymatic activity monitored via production of fluorescence and measured in solution over time. a) Activity of a cross-linked (PLL-S-TP/HA)$_{24}$ film loaded with β-Gal-mal. The β-Gal-mal molecules were not linked to the film because the deprotecting agent TCEP was not introduced. The enzymatic activity was measured using FDG as the substrate. b) Following the experiment depicted in a), the supernatant was maintained in place but the enzymatic film was removed from the measurement's cuvette and the enzymatic activity was monitored again.*

## 4. Localization of lysine residues on β-galactosidase

Chemical modification of β-Gal with maleimide groups as described in scheme S3 was performed on part of the lysine residues. A mapping of these lysine residues and in particular those appearing on the external face of the enzyme can be obtained from Protein Databank.
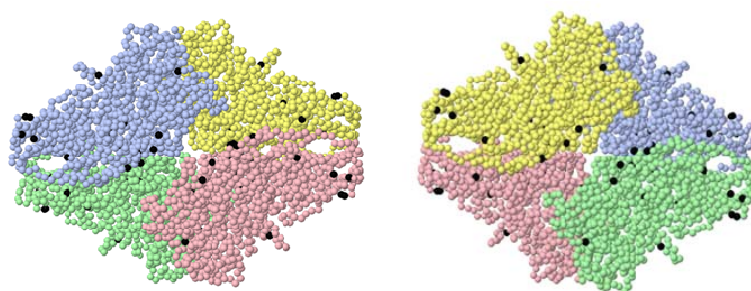


***Figure S7***: *3D representation of β-Gal residues with a labeling in dark of lysine residues on both faces (left and right representations) of the enzyme (PBD code: 1BGL). From these representations, it appears that a great number of lysine residues are distributed all over the external area, suggesting that the grafting of the enzyme to the film can occur. β-Gal contains 80 lysine residues but only few lysine residues exposed to the outer surface are visible on this figure.*

## 4.4. Additional experiments

In order to determine if the structure of the enzymes present inside the multilayer films are influenced by the mechanical constraints applied to the material and so explaining the decrease of enzymatic activity observed under stretching, infrared and fluorescence measurements of the stretched and unstretched films were performed.

### 4.4.1. Infrared analysis

These experiments were done to detect shift in amide I band of enzymes known to be sensitive to secondary structures such as α-helix and β-sheets [23]. Thus conformational modifications of the proteins can be monitored by infrared spectroscopy [24]. In order to prevent protein denaturation by drying, all the manipulations were performed in liquid conditions in presence of $D_2O$ at room temperature. According to the literature, spectra acquisitions were performed between 1500 and 1700cm$^{-1}$, a characteristic domain of the amide I bands relative to the α-helix secondary structure [24, 25].

First of all, infrared measurements of the polyelectrolyte multilayer films without enzyme were performed in order to evaluate the contribution of PLL amide bonds (figure 4.6). These experiments were realized on typical films made of (PLL-S-TP/HA)$_{24}$ layers.
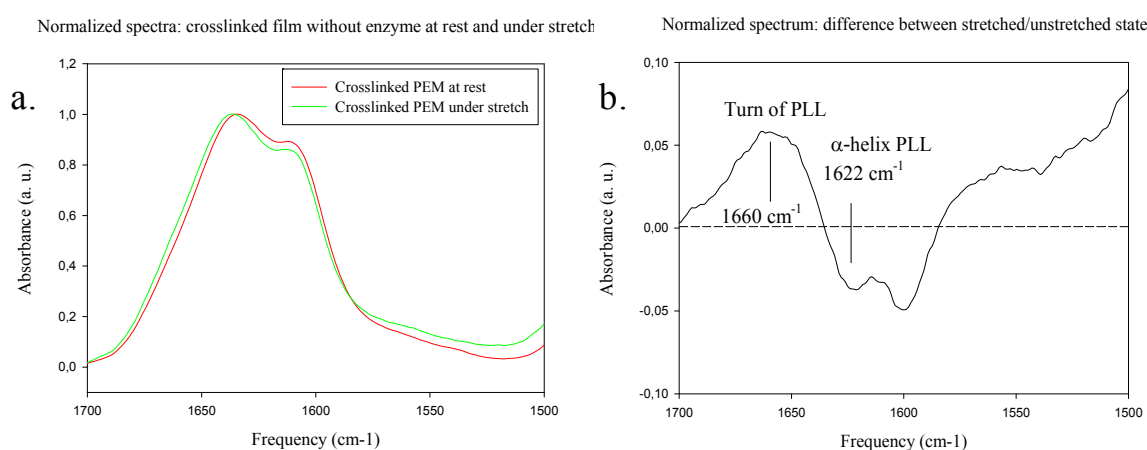


*Figure 4.6*: *(a) Infrared analysis of PEM structure at rest and under stretch; (b) Spectra difference*

Changes in polymeric matrix conformation are detected under stretch. Indeed in figure 4.6b. a diminution of the PLL α-helix secondary structure at 1622cm$^{-1}$ is observed in

agreement with an increase of the turns at $1660 cm^{-1}$. Once these results obtained, a comparison with a film containing reticulated enzymes was performed (figure 4.7).

Normalized spectra of crosslinked film with and without linked enzymes
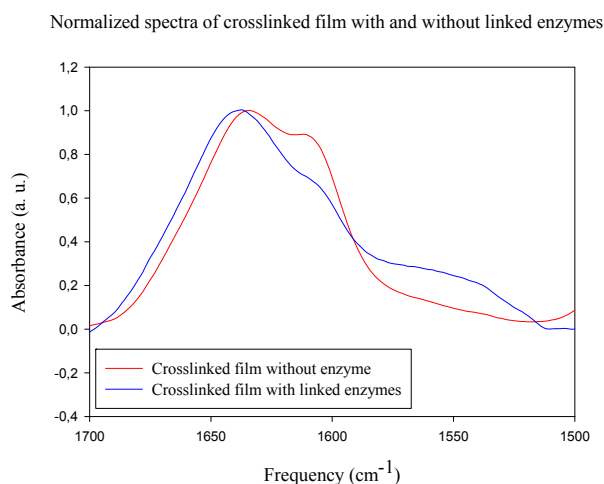


*Figure 4.7: Normalized spectra of crosslinked films with and without linked enzymes.*

After normalization, differences in the infrared spectrum between the native film and the one loaded with enzymes are observed confirming the presence of enzymes inside the matrix. Stretching experiments are finally studied and normalized spectra of the unstretched/stretched states are reported in figure 4.8a. Difference of the spectra is represented in figure 4.8b.
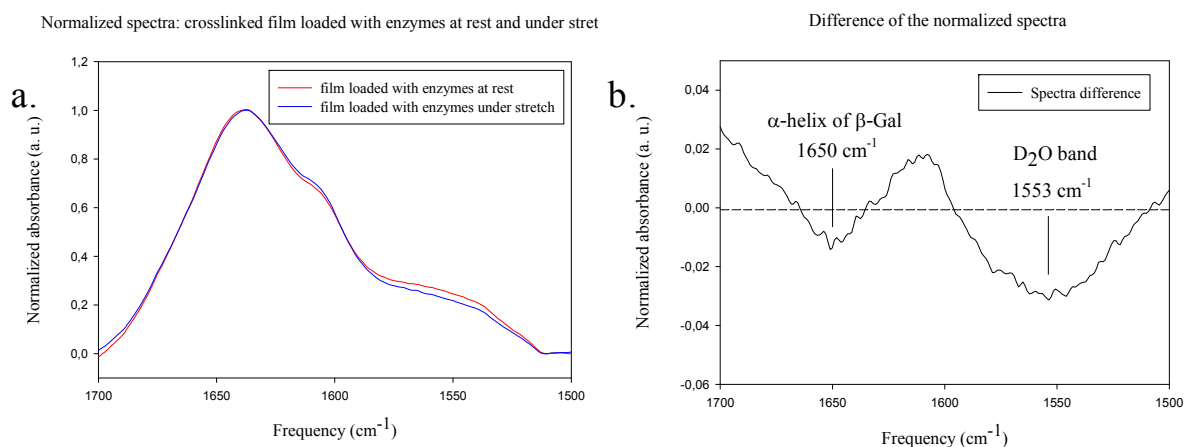


*Figure 4.8: (a) Normalized spectra of stretched/unstretched states of PEM containing enzymes; (b) Spectra difference.*

Although a slight shift in the amide I band characteristic of α-helixes is observed under stretching, the results observed aren't significant due to the impossibility to attribute the contributions coming from PLL and enzymes. Another way of characterization based on intrinsic fluorescence of protein was so experimented to prove the structural changes of the shape of the enzymes under stretching constraints.

### 4.4.2. Fluorescence measurements

In order to show beyond doubt that the decrease of catalytic activity of the films under stretch is due to enzymes conformational changes, additional fluorescent experiments were performed. Indeed, most proteins own an intrinsic fluorescence coming from the presence of specific aromatic amino-acids (tryptophan, tyrosine, phenylalanine) (figure 4.6) present in their sequences.
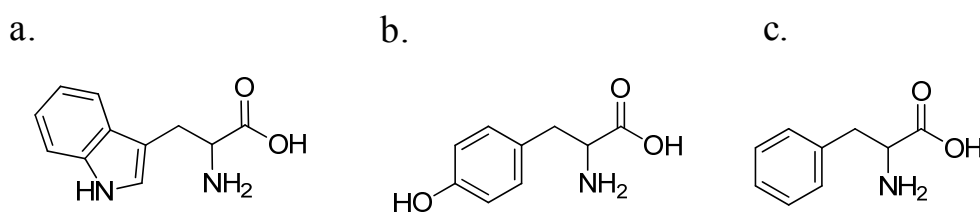


*Figure 4.9*: *Chemical structures of (a) tryptophan, (b) tyrosine and (c) phenylalanine amino-acids.*

Although the fluorescence of a folded protein is a mixture of the fluorescence from individual aromatic residues, it is essentially due to the contribution of tryptophan [26]. However, its fluorescence is influenced by various parameters. Thus tryptophan has a typically a maximum wavelength of adsorption at 280nm and an emission peak ranging from 300 to 350nm depending on the polarity of the local environment and the proximity of other residues [27, 28]. This property is used to study protein denaturation or conformational changes by monitoring the fluorescence response of the tryptophan [29] under various conditions. Thus, the aim of our experiments is to detect a change in fluorescence of the tryptophan when our material and so the enzymes are submitted to a stretching constraint modifying their structures.

However, first results aren't conclusive due to a too low signal-to-noise ratio and no shift or decrease of fluorescence was observed under mechanical constraint of the films.

Manipulations have so to be redone by using a more important quantity of enzyme by building a PEM with more bilayers for example.

## 4.5. Conclusion

After demonstrating the possibility inducing conformational changes of proteins by stretching their substrate in chapter 3, this study was focused on the elaboration of an enzymatic active material sensitive to mechanical constraints. To achieve this goal, a crosslinked polyelectrolyte multilayer film was in a first time elaborated then loaded with enzymes and finally submitted to stretching tests. A modification of 30% of the material enzymatic activity was observed and a partial reversibility of the system was obtained. This study is a proof of principle demonstrating the use of cross-linked enzyme containing PEM films to create chemo-mechano-responsive materials based on local modification of enzymatic conformation.

Although the direct proof of enzyme structure modification is not yet demonstrated, additional experiments are in progress in particular Raman spectroscopy and circular dichroism analysis.

## 4.6. References

1.    C.E. Diesendruck, B.D. Steinberg, N. Sugai, M.N. Silberstein, N.R. Sottos, S.R. White, P.V. Braun, and J.S. Moore, *Proton-coupled mechanochemical transduction: A mechanogenerated add.* Journal of the American Chemical Society, 2012. **134**: p. 12446-12449.

2.    V. Vogel, *Mechanotransduction involving multimodular proteins: Converting force into biochemical signals.* Annual Review of Biophysics and Biomolecular Structure, 2006. **35**: p. 459-488.

3.    R.M. Daniel, D.R. V, J.L. Finney, and S.J. C, *The role of dynamics in enzyme activity.* Annual Review of Biophysics and Biomolecular Structure, 2003. **32**: p. 69–92.

4.    A.M. Klibanov, G.P. Samokhin, K. Martinek, and I.V. Berezin, Biochim. Biophys. Acta 1976. **438**: p. 1-12.

5.    A.M. Klibanov, G.P. Samokhin, K. Martinek, and I.V. Berezin, Biotechnology and Bioengineering, 1977. **19**: p. 211-218.

6.    H. Gumpp, E.M. Puchner, J.L. Zimmermann, U. Gerland, H.E. Gaub, and K. Blank, *Triggering enzymatic activity with force.* Nano Lett., 2009. **9**: p. 3290-3295.

7.    C.Y. Tseng, A. Wang, and G. Zocchi, *Mechano-chemistry of the enzyme guanylate kinase.* EPL, 2010. **91**: p. Article Number: 18005.

8.    P.T. Hammond, *Form and function in multilayer assembly: New applications at the nanoscale.* Advanced Materials, 2004. **16**(15): p. 1271-1293.

9.    B.G. De Geest, G.B. Sukhorukov, and H. Mohwald, *The pros and cons of polyelectrolyte capsules in drug delivery.* Expert Opinion on Drug Delivery, 2009. **6**(6): p. 613-624.

10.   A.L. Becker, A.P.R. Johnston, and F. Caruso, *Layer-by-layer-assembled capsules and films for therapeutic delivery.* Small, 2010. **6**(17): p. 1836-1852.

11.   F. Lisdat, R. Dronov, H. Mohwald, F.W. Scheller, and D.G. Kurth, *Self-assembly of electro-active protein architectures on electrodes for the construction of biomimetic signal chains.* Chemical Communications, 2009(3): p. 274-283.

12.   D. Mertz, C. Vogt, J. Hemmerlé, J. Mutterer, V. Ball, J.-C. Voegel, P. Schaaf, and P. Lavalle, *Mechanotransductive surfaces for reversible biocatalysis activation.* Nat. Mat., 2009. **8**: p. 731-735.

13.   J. Früh, R. Köhler, H. Möhwald, and R. Krastev, *Changes of the molecular structure in polyelectrolyte multilayers under stress.* Langmuir, 2010. **26**: p. 15516-15522.

14.    R.H. Jacobson, X.J. Zhang, R.F. DuBose, and B.W. Matthews, *Three-dimensional structure of beta-galactosidase from e. Coli.* Nature, 1994. **369**: p. 761-766.

15.    D.H. Juers, R.J. Jacobson, D. Wigley, X.-H. Zhang, R.E. Huber, D.E. Tronrud, W. Brian, and B.W. Matthews, *High resolution refinement of b-galactosidase in a new crystal form reveals multiple metal-binding sites and provides a structural basis for a-complementation.* Protein Science, 2000. **9**: p. 1685-1699.

16.    . , Protein Data Bank, ID: 1BGL (see ref. 10).

17.    L. Richert, F. Boulmedais, P. Lavalle, J. Mutterer, E. Ferreux, G. Decher, P. Schaaf, J.C. Voegel, and C. Picart, *Improvement of stability and cell adhesion properties of polyelectrolyte multilayer films by chemical cross-linking.* Biomacromolecules, 2004. **5**(2): p. 284-294.

18.    J.N. Brantley, C.B. Bailey, J.R. Cannon, K.A. Clark, D.A. Vanden Bout, J.S. Brodbelt, A.T. Keatinge-Clay, and C.W. Bielawski, *Mechanically modulating the photophysical properties of fluorescent protein biocomposites for ratio- and intensiometric sensors.* Angewandte Chemie, International Edition in English, 2014. **53**(20): p. 5088-92.

19.    H.Z. Xie, O. Braha, L.Q. Gu, S. Cheley, and H. Bayley, *Single-molecule observation of the catalytic subunit of camp-dependent protein kinase binding to an inhibitor peptide.* Chemistry & Biology, 2005. **12**: p. 109-120.

20.    K. Thibaudeau, R. Léger, X.C. Huang, M. Robitaille, O. Quraishi, C. Soucy, N. Bousquet-Gagnon, P. van Wyk, V. Paradis, J.P. Castaigne, and D. Bridon, *Synthesis and evaluation of insulin-human serum albumin conjugates. .* Bioconjugate Chemistry, 2005. **16**: p. 1000-1008.

21.    P.K. Smith, R.I. Krohn, G.T. Hermanson, A.K. Mallia, F.H. Gartner, M.D. Provenzano, E.K. Fujimoto, N.M. Goeke, B.J. Olson, and D.C. Klenk, *Measurement of protein using bicinchoninic acid.* Analytical Biochemistry, 1985. **150**: p. 76-85.

22.    A. Habeeb, *Determination of free amino groups in proteins by trinitrobenzenesulphonic acid.* Analytical Biochemistry, 1966. **14**: p. 328-36.

23.    A. Barth, *Infrared spectroscopy of proteins.* Biochimica et Biophysica Acta (BBA) - Bioenergetics, 2007. **1767**(9): p. 1073-1101.

24.    J. Kong and S. Yu, *Fourier transform infrared spectroscopic analysis of protein secondary structures.* Acta Biochimica Et Biophysica Sinica, 2007. **39**(8): p. 549-559.

25.    J.L.R. Arrondo, A. Muga, J. Castresana, C. Bernabeu, and F.M. Goni, *An infrared spectroscopic study of beta-galactosidase structure in aqueous-solutions.* Febs Letters, 1989. **252**(1-2): p. 118-120.

26.    F.W. Teale and G. Weber, *Ultraviolet fluorescence of the aromatic amino acids.* The Biochemical journal, 1957. **65**(3): p. 476-82.

27.    A.S. Ladokhin, *Fluorescence spectroscopy in peptide and protein analysis.* Encyclopedia of Analytical Chemistry, 2006.

28.    J.T. Vivian and P.R. Callis, *Mechanisms of tryptophan fluorescence shifts in proteins.* Biophysical Journal, 2001. **80**(5): p. 2093-2109.

29.    J.R. Lakowicz, *Principles of fluorescence spectroscopy.* 2nd Edition ed. 1999

# Chapter 5

# Design of mechano-responsive materials based on multilayer films made from alginate-catechol and alkaline phosphatase

## Contents

## 5.1. Introduction

### 5.1.1. Enzymatically stable polymeric matrix

Confinement of enzymes on surfaces of lipid monolayers [1], in lipid vesicles [2, 3], in porous materials such as inverse opals,[4] in polyelectrolyte multilayer films [5-7]or in gels [8] offers many opportunities to confer biological activity to materials. To achieve the realization of a long term enzymatic activity without release, which is needed for the production of stable biosensors or materials meant to be manipulated, it is mandatory to control the immobilization mechanism of the enzymes. In the case of stable enzyme immobilization, the active moleculesshould be bound preferentially by means of covalent bonds, but without undergoing a significant conformational change to avoid its decrease or loss of activity [9-11]. In addition the immobilization matrix should be porous enough to allow access of the substrate to all the immobilized enzymes. It has been found that in the case of polyelectrolyte multilayer films produced by the alternated layer-by-layer deposition of chitosan and glucose oxidase (GOX), the sensitivity for glucose sensing was maximal when only the last layer pair contained GOX [12], implying that the enzymes embedded in the internal layers of the film remained either inaccessible to the substrate or underwent some severe denaturation. This last assumption seems however unlikely because it has been shown that many proteins have increased thermal stability when embedded in polyelectrolyte multilayered films [13, 14]. It is the aim of the present work to use the layer by layer deposition method of a polyelectrolyte and an enzyme to produce stable enzymatic active filmsin timewithout enzyme release, and modify their biological properties under mechanical constraints.

### 5.1.2. Project

Our idea is to create bio-active films stable in time and responding to mechanical stress by changing their enzymatic activity. This property is expected by changes of enzymes conformation upon stretching leading to modification of their catalytic activity (figure 5.1).
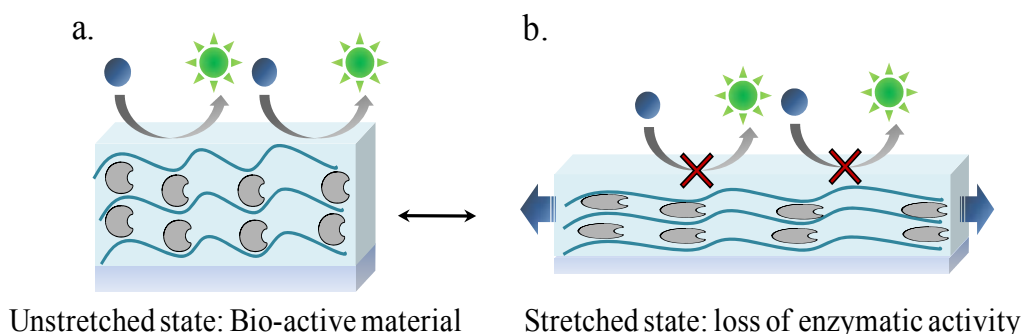
*Figure 5.1*: *Schematic representation of the mechano-responsive film. (a.) At rest enzymatic activity occurs. (b.)Under mechanical stress, enzyme structure is putting out of shape leading to a loss of activity.*

Such behavior is only possible with the covalently linking of enzymes into the material. In the previous chapter we presented a method to achieve this goal based on the diffusion of enzymes into a crosslinked polymeric matrix followed by their binding. Here we present one other method based on the elaboration of a polyelectrolytemultilayer film made of both polyelectrolytes and enzymes. In such structuresthe enzymes themselves are an integral part of the material and thus are hopefully more sensitive to its deformation.

This project was separated in different parts, beginning with the elaboration of the PEM, then its crosslinking by taking in account various constraints inherent to the use of biological macromolecules, and finally the investigation of the stretching influence on the enzymatic activity of the material (figure 5.2).
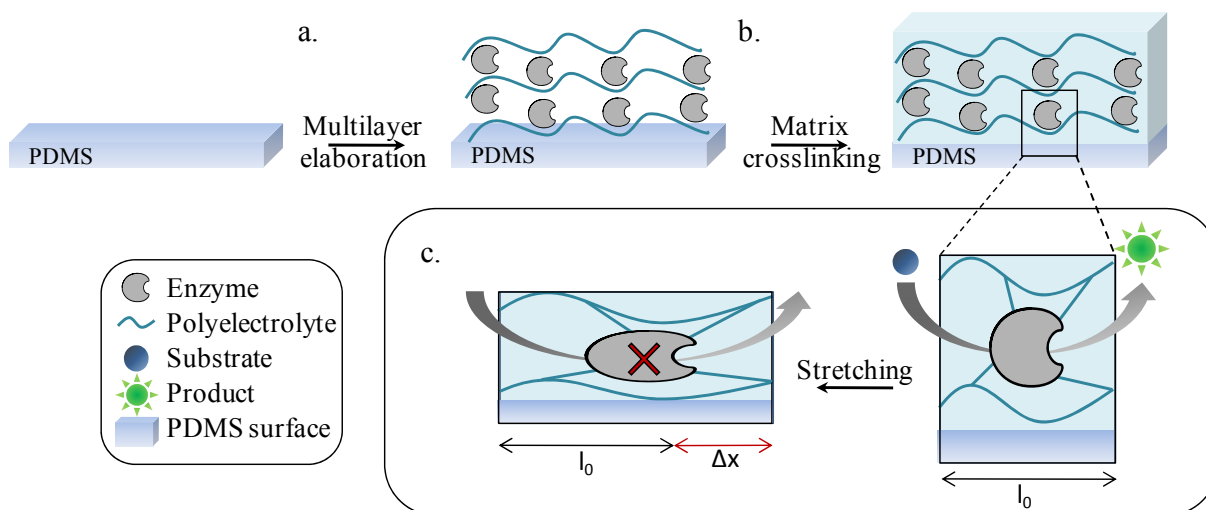


*Figure 5.2*: *Schematic representation of the different parts of the project corresponding to (a.) elaboration of the polyelectrolyte multilayer film; (b.) crosslinking of polymeric matrix without enzyme degradation and (c.) stretching experiments.*

## 5.2. Elaboration of the multilayer architecture

### 5.2.1. Layer-by-layer (LBL) method

Polyelectrolyte multilayer films are elaborate by the alternate adsorption on a surface of positively and negatively charged polymer chains respectively polycations and polyanions. This method called Layer-by-layer [15] is schematically represented on figure 5.3. The substrate generally negatively charged is immersed in a solution of polycations for a given time. Due to electrostatic interactions, positively charged chains adsorb on the surface of the material. Excess polymers are removed using a rinsing step. The substrate surface is then positively charged that allowed a new deposition of polyanions. This build-up process is pursued by the alternate depositions of polycations and polyanions leading to the multilayer films elaboration. The driving force of the construction is the charge overcompensation at the surface of the substrate.
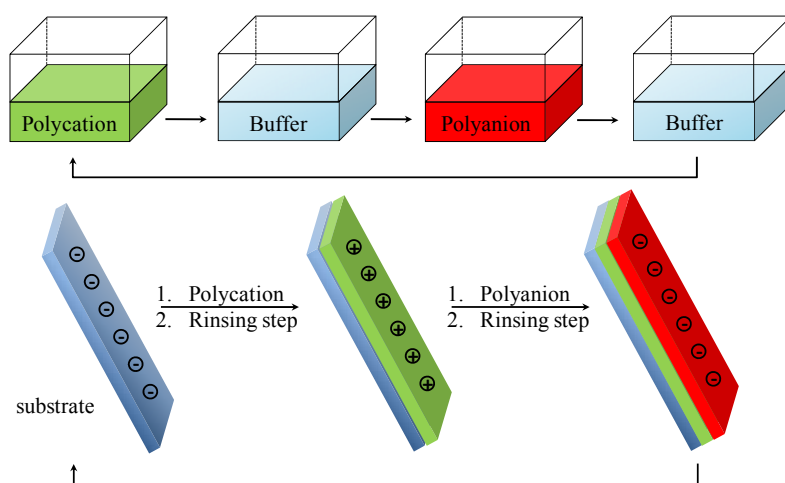


*Figure 5.3*: *Schematic representation of the polyelectrolyte multilayer films (PEM) elaboration. The substrate is alternatively immersed in polycations and polyanions solutions leading to the film build-up.*

In order to elaborate mixed structures, one of the polyelectrolyte used during the layer-by-layer film build-up is replaced by an enzyme.

### 5.2.2. Materials

### Nature of the polymer used to elaborate the PEM

In order to elaborate our polymeric matrix we selected a polyelectrolyte which is able to undergo gelation, and hence a high degree of swelling. Indeed it was a criterion to get highly porous and hydrated films allowing a fast diffusion process of the enzyme's substrate

in the whole film. To respect these constraints, we decided to use an anionic polysaccharide namely sodium alginate. This polymer extracted from cell walls of brown algae is well known for its use across a wide variety of application including food [16, 17], textile printing, pharmaceutical [18, 19] and tissue engineering [20]due to its biocompatibility and is able to absorb 200 to 300 times its own weight in water.

### Specific modification of the polyelectrolyte

This polyanion was also modified with catechol groups (figure 5.4) in order to crosslink the (AlgCat-enzyme)$_n$ multilayer films and thus increase their stability. The polymer was produced in our laboratory by Dr. T. Garnieraccording to protocol fromKastrup et al. [21]with a grafting ratio of 10%.



**Figure 5.4**: *alginate modified with catechol moieties (red).*

The use of catechol groups as adhesive and reactive moieties originates from biology[22]. Marine mussels, *MytilusEdulis*, secret protein material that initiate robust adhesion and energy dissipation for mitigating the impact of waves. Adhesive proteins in the mussel adhesive pads promote adhesion to virtually any type of organic or inorganic material [23]. Proteins found in this material contain a high level of a catecholic amino acid namely 3,4-dihydroxy-L-phenylalanine (L-DOPA). This amino acid has redox properties that allow oxidative cross-linking to form protein networks. Oxidative transition of the catechol group in

the L-DOPA to o-quinone triggered by alkaline pH results a highly reactive groups with primary amines (figure 5.5) and in catechol-catechol addicts [24].
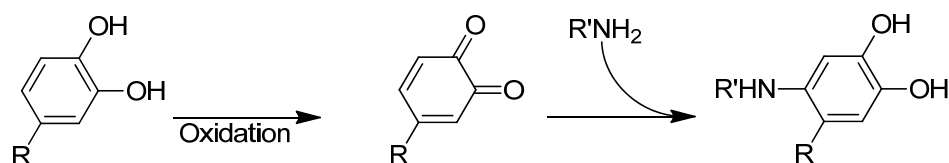


*Figure 5.5: Michael addition between catechol group and primary amine under oxidative conditions.*

Catechol modified alginate can be used to produce gels of tunable swelling ratios and elastic moduli without the use of divalent cations[25]. Gels made from L-DOPA containing proteins can easily be cross-linked using $Fe^{3+}$ as a complexing agent [26]. Subsequently the metallic cations undergo reduction whereas the catechol groups of L-DOPA are oxidized in quinone groups [27]. Sodium periodate can also be used as an oxidant to crosslink mussel inspired adhesive hydrogels [28]. Chitosan modified with catechols was blended with thiol terminated pluronic F-127 triblock copolymers to yield thermosensitivehydrogels whichgelate spontaneously at the body temperature. These gels are biocompatible and useful as hemostatic materials [29].In addition polyelectrolytes modified with catechol moieties have already been used to build up multilayer polyelectrolyte films in combination with clays allowing to produceultrastrong coatings after oxidation of the catechol moieties to create covalent bonds in the composite architecture [30]. Catechol modified polymers allow also to deposit polyelectrolyte multilayers on substrates which do not carry charged groups [31]owing to the strong and substrate independent adhesion strength provided by catechols in a reminiscent manner to the mechanism used by mussels to strongly adhere on solid substrates in a marine environment and under strong shear stresses [23, 32].

## Choice of the enzyme

First to verify if PEM films can be constructed and if the cross-linking by the oxidized catechols preserves the enzymatic activity, we used a model system composed of alginate-catechol and alkaline phosphatase (ALP) as enzyme.This enzyme was chosen according to its specific properties. Indeed, it ispositively charged in the conditions of the PEM elaboration, owns a robust structure allowing its binding without degradation and its activity can easily be monitored through UV absorbance by using paranitrophenyl phosphate (PNP) as substrate

which is transformed into paranitrophenolate and phosphate(see figure 5.6). Paranitrophenolate is then easily detected by UV absorbance at 405 nm.



*Figure 5.6*: *Transformation of para-nitrophenylphosphate in UV absorbantpara-nitrophenolate under alkaline phosphatase activity.*

### 5.2.3. Experimental conditions

We first investigated the buildup of Alg-Cat/ALP films by step-by-step deposition based on electrostatic interactions. The first deposition experiments were performed by dissolving Alg-Cat and ALP in 50mMTris buffer at pH 8.5. These experiments were performed in such conditions owing to the known pH sensitivity of the enzymatic activityof ALP [33], even if both ALP and Alg-Cat are negatively charged in these conditions, which is a priori not favorable for the deposition of polyelectrolyte multilayer films relying only on electrostatic interactions. Indeed, no noticeable film deposition was measured by means of QCM-D when both polyelectrolytes were dissolved at pH 8.5. For this reason, further deposition experiments were performed in the presence of 50 mM sodium acetate buffer at pH 5.0.in order to make the enzyme positively charged. It must be noticed that prior to these experiments, the stability of the enzyme at such pH was verified in liquid conditions.

## 5.3. Build-up monitoring and characterization of the films

In order to monitorand characterize the multilayer film build-up, different physico-chemical analysis techniques were performed such as QCM, FTIR and AFM.

### 5.3.1. Quartz crystal Microbalance (QCM)

The film buildup was in a first time followed by QCM-D.Figure 5.7a shows the evolution of the normalized frequency shifts of the different measured overtones. One

observes a regular film buildup. Yet, there is no superposition of the normalized frequency shifts of the different overtones, indicating that Sauerbrey's equation does not apply to determine the film's deposited mass. We thus used Voinova's model to treat our data [34]. Figure 5.7b shows the evolution of the mass of the film during film buildup determined by this data treatment. The mass increases fairly linearly with the number of deposition steps reaching $7\mu g.cm^{-2}$ after the deposition of 14 Alg-Cat/ALP bilayers. It must be noticed that this mass corresponds to a hydrated mass and thus includes the water bound to the protein[35]. When the film is brought in contact with a 3.3mM $CaCl_2$ solution during 10 min followed by cross-linking with 1mM $NaIO_4$ solution, a slight decrease of the mass of the film takes place.
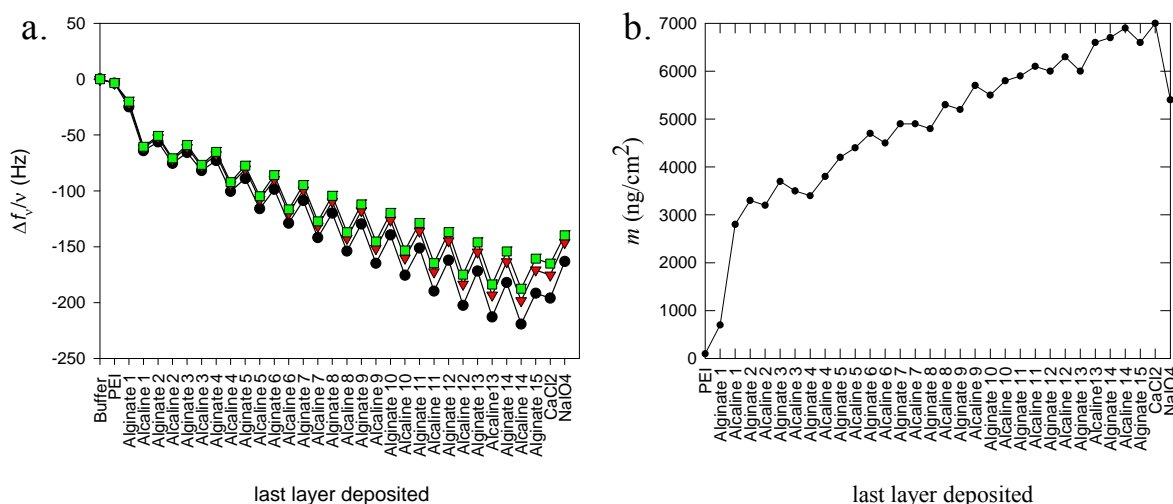


***Figure 5.7***: *(a) Evolution of the normalized frequency shifts observed by QCM experiments during the buildup of the Alg-Cat/ALP multilayer film buildup for v =3, 5 and 7 respectively black, red and green curves(b) evolution of the thickness of the film determined from the QCMD data by using Voinava's model[34].*

## 5.3.2. UV-Visible monitoring

In order to gain a better insight into the film buildup process it was followed by UV absorbance measurements at 280nm (figure 5.8). This wavelength is usually chosen to follow protein deposition. It is thus characteristic of the deposition of ALP. The film was deposited on a quartz crystal with a PEI precursor layer. Here too a regular enzyme deposition, which is in first approximation linear with the number of deposition steps, is observed.
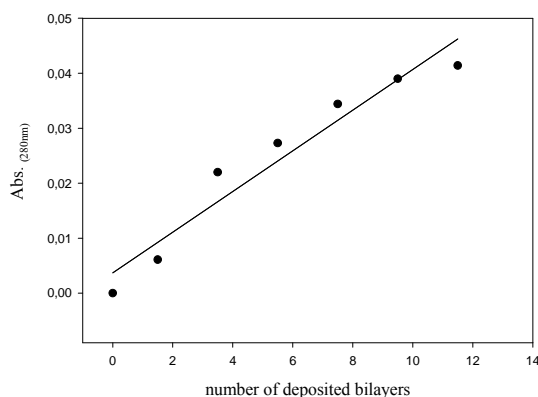
*Figure 5.8: evolution of the absorbance at 280 nm for an Alg-Cat/ALP multilayer as a function of the number of bilayers.*

### 5.3.3. Infrared monitoring

In order to evaluate the contribution of each component during the PEM elaboration, the build-up of the film is monitored using FTIR spectroscopy. The film is elaborated and characterized at each step *in-situ* on a germanium crystal. To prevent the signal of water contribution during the analyses, all the polymers, enzymes and buffer solutions were prepared shortly before the manipulation using $D_2O$. Monitoring of the (Alginate-Catechol/alkaline phosphatase)$_{8,5}$ film build-up is given in figure 5.9. In order to facilitate the graph understanding all the deposition steps aren't represented (only the steps 1; 3; 6 and 9 are reported on the figure 5.9). Specific bands are detailed thereafter.
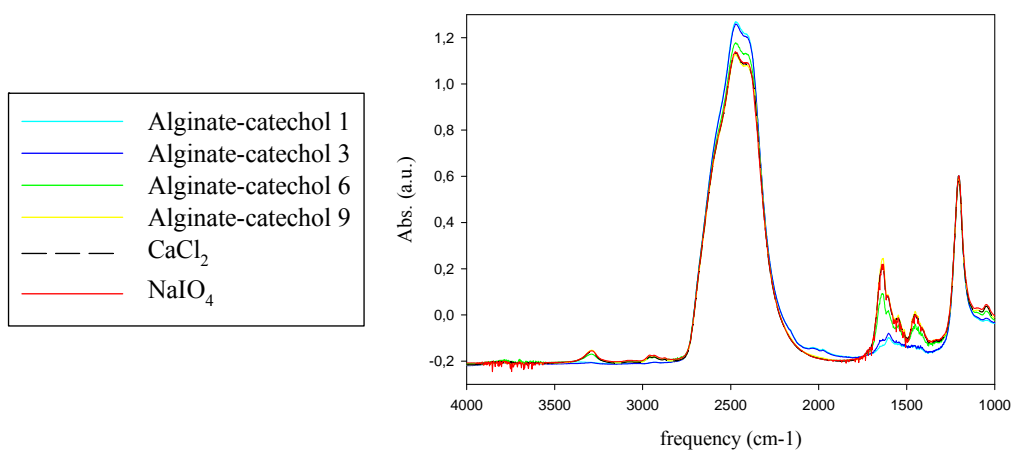


**Figure 5.9**: *Infrared monitoring of the (Alginate-Catechol/alkaline phosphatase)$_{8,5}$ film elaboration. Numbers next to the layer name are relative to the order of depositionof the successive bilayers.*

Typical spectra of Alg-Cat and ALP adsorbed on an ATR crystal are given in figure 5.10a and 5.10b. The evolution of the IR spectra taken in ATR mode during theAlg-Cat/ALP multilayer film buildup is shown in figure 5.9. One clearly observes the constant increase evolution of the vibration band intensity between 1300 and 1800cm$^{-1}$ indicating the increase of the mass of the film as it builds up. Yet, due to the fact that most bands observed in IR appear both for Alg-Cat and ALP, it is difficult to discriminate them. Nevertheless the band at 1540cm$^{-1}$ is strong for ALP [36] and the contribution of Alg-Cat at this wavelength is rather weak. This band corresponds to theamide II bond that results from the N-H bending vibrations and C-N stretching vibrations. The band at 1600cm$^{-1}$ can be attributed to carboxylate groups of alginate [37]and its contribution to ALP appears rather modest. We thus used these two bands to follow the evolution of deposited amount of Alg-Cat and ALP during the film buildup (figure 5.11). The intensity of both bands increases steadily during the film construction. At the end of the buildup, the film is brought in contact with the 3.3mM CaCl$_2$ solution.No decrease of either of the two bands is observed, indicating that the film remains stable during this step. When the film is then further brought in contact with the 10mM NaIO$_4$ solution one observes a decrease of the 1540cm$^{-1}$band. On the other hand the intensity of the 1600cm$^{-1}$band does not decrease after addition of NaIO$_4$. This indicates that cross-linking only affects the signal relative to the enzymes. The decrease of the intensity at 1540 cm$^{-1}$ band can have two origins: either the crosslinking of Alg-Cat with ALP modifies C-N bending vibrations or there is some leaching out of the enzymes from the film into the solution.
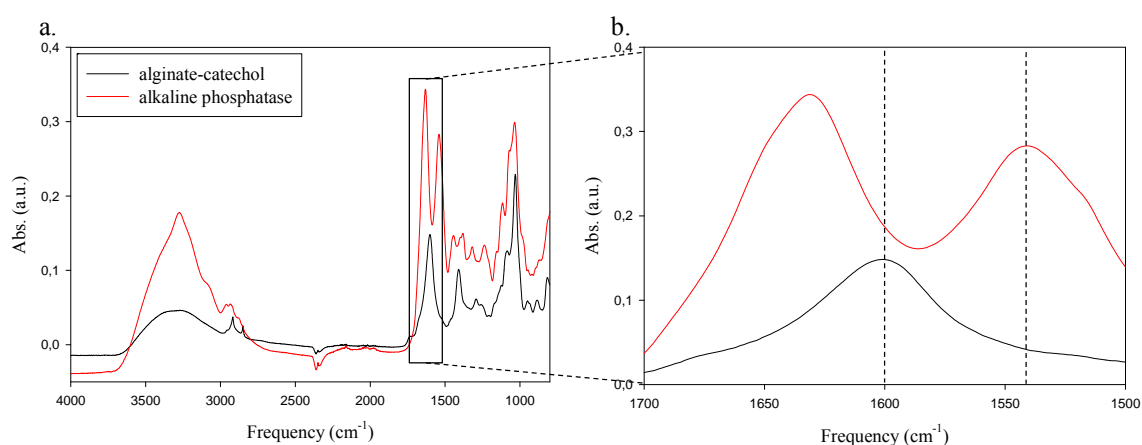


*Figure 5.10*: *(a.) IR spectra over the entire spectrum range of alginate-catechol (black) and alkaline phosphatase (red); (b.) detail of the spectrum between 1500cm$^{-1}$ and 1700 cm$^{-1}$. The absorbance at 1540 cm$^{-1}$ will mainly correspond to ALP while the absorbance at 1600 cm$^{-1}$.*
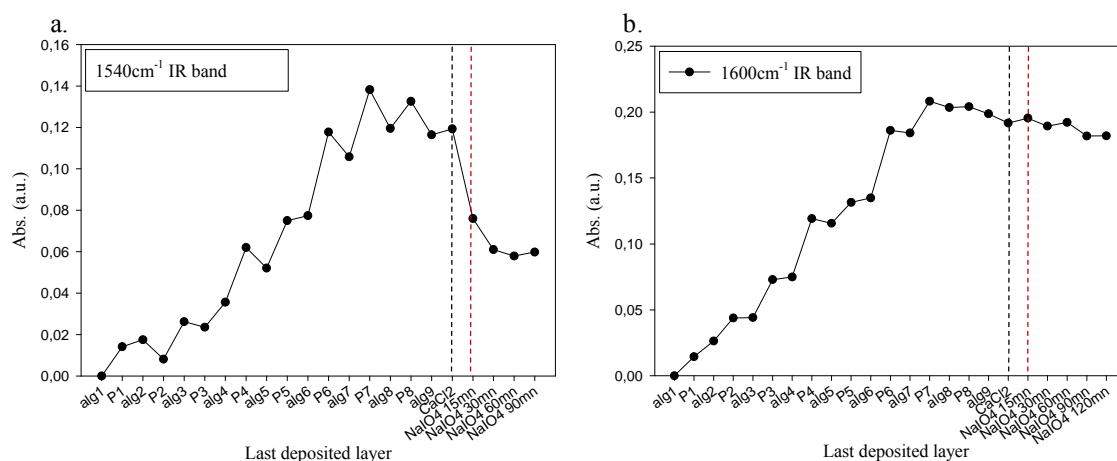
**Figure 5.11**: *Evolution of the band intensity (a.) at 1600 cm$^{-1}$ attributed to Alg-Cat and (b.) at 1540cm$^{-1}$ attributed to alkaline phosphatase. Black and red dotted lines corresponding respectively to the measurements after contact with CaCl$_2$ and NaIO$_4$.*

### 5.3.4. Atomic Force Microscopy (AFM) characterization

Next we determined if the film totally covers the surface and what is its thickness. To this aim, AFM imaging in contact mode under liquid conditions by scratching the film elaborate on a QCM quartz crystal was performed. Figure 5.12 shows a typical AFM image with the topography for a film constituted of 7.5Alg-Cat/ALP bilayers.
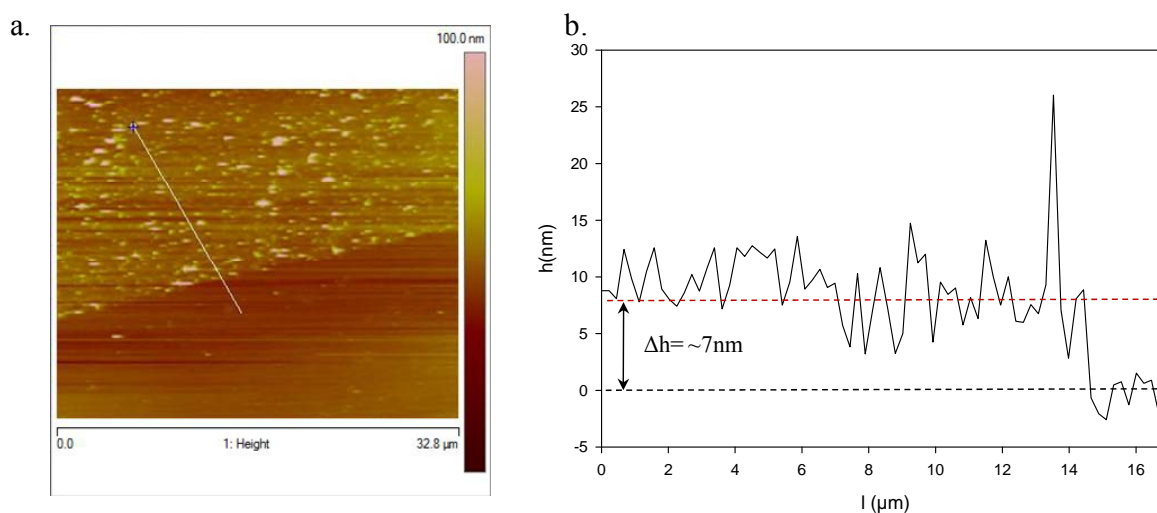


**Figure 5.12**: *(a.) Atomic Force Microscopy (AFM) scratch image of the multilayer film; (b.) scratch profile of the film.*

The AFM analysis shows that the film totally covers the surface but owns an important roughness (13.7nm) due to enzyme aggregates on its surface. Its thickness about 7nm is inferior to the expected one according to QCM-D experiments. This difference is directly linked to its important roughness increasing artificially the mass calculatedfrom the QCM results.

## 5.4. Enzymatic properties of the films

Next we analyzed the enzymatic activity of the films. As already stated, we used paranitrophenyl phosphate (PNP) as substrate and followed its transformation into paranitrophenol and phosphate through enzymatic activity.

### 5.4.1. Enzymatic release tests

We first investigated the release of the enzymes from the films into their contacting solution. This was done as follows: after buildup, the films were brought in contact with 30mL of a Tris buffer solution at pH 8.5 for different contact times (10, 30 and 120 min).After these contact times, the supernatant was removed from the film and its enzymatic activity was measured by supplementing it with a 10% PNP solution in TRIS 50mM buffer and by measuring the absorbance at 405 nm which correspond to the absorbance peak of paranitrophenol.
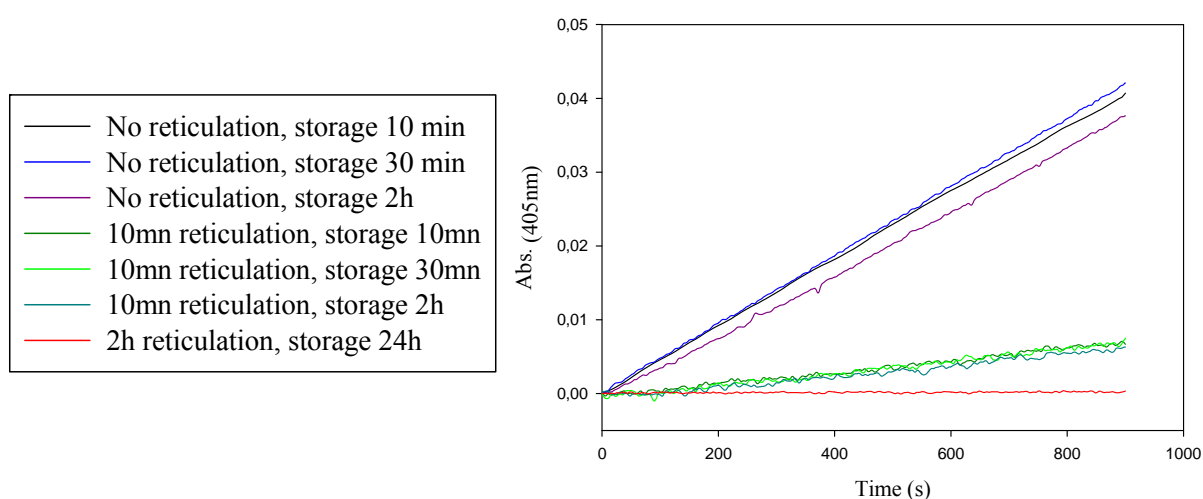


*Figure 5.13: Enzymatic activity of the supernatant monitored using UV Absorbance measurements over time.*

The enzymatic activity of the supernatant is strong for non-reticulated films, much reduced when the film was brought in contact with $NaIO_4$ for 10min and there is no enzymatic activity of the supernatant when the film was 2 hours in contact with $NaIO_4$(figure 5.13). Moreover, for films in contact during 10min with $NaIO_4$, one observes that the enzymatic activities of the supernatant solutionscontacting the film during 10min, 30min or 120min are almost identical. This indicates that for non-reticulated films and for films reticulated during 10min, there is a loss of enzymes from the film. Moreover this loss takes place during the first 10 minutes of contact with $NaIO_4$. This is in accordance with the observations done by IR by following the intensity of the band at 1540 $cm^{-1}$. When the film is in contact with the $NaIO_4$ solution for 2h, there is no loss anymore of enzymes from the film (at least during the investigated time scales).

Then we determined the enzymatic activity of the films themselves by bringing them in direct contact with a PNP solution for 2 hours after different storage times at 4°C in a Tris buffer solution at pH 8.5. The enzymatic activity was determined by following the absorbance at 405nm with time. The results of the enzymatic activities are summarized in figure 5.14. One observes that non-reticulated films lose almost all enzymatic activity after 25h of storage. This is in agreement with the strong desorption of enzymes from these films. Reticulated films lose also some activity during the first 25 storage hours, yet even over long storage times the films remain enzymatically active. The activity loss during these first 25 storage hours should be due to some slow enzyme release that was not detected in the experiments where the enzymatic activity of the supernatant was measured. This may be due to the fact that the release was too slow to be detectable. It is interesting to notice that even after 2h of contact with the $NaIO_4$ solution and thus oxidation, there is no effect on the enzymatic activity of the film indicating that the $NaIO_4$solution does not denature the enzymes (at least in such a way as to decrease their activity). In the following we always used 1hour of contact with the $NaIO_4$ solution (acetate buffer) followed by a rinsing step with TRIS buffer at pH 8.5.
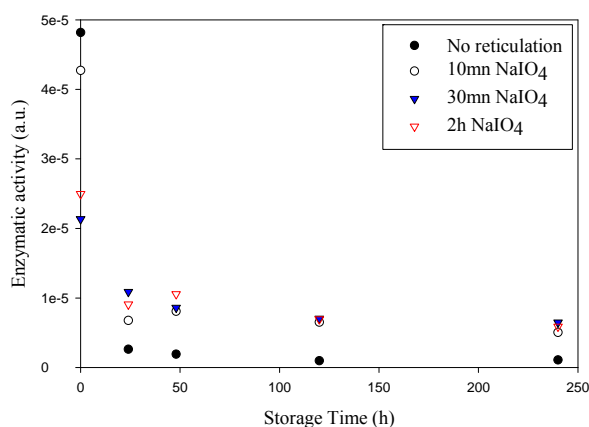
*Figure 5.14: Enzymatic activity of 7,5 bilayers films in function of the reticulation time.*

In a control experiment we checked that the catalysis of the PNP hydrolysis was indeed due to the enzyme and not to the catechol-quinone moieties present on the AlgCat polymer. For this aim, we deposited a PEI-(AlgCat-Lysozyme)$_{7.5}$ film on a quartz slide, performed the two crosslinking steps as for the films containing ALP and measured the hydrolysis rate of PNP. No detectable hydrolysis of PNP was found in this case.

### 5.4.2. Influence of the bilayers number on the film activity

Next we investigated the effect of the number of deposition steps on the film enzymatic activity. For this purpose the hydrolysis of PNP was measured for PEI-(AlgCat/ALP)$_n$ films deposited by changing the number of deposition cycles (5.5; 8.5 and 11.5), and hence the deposited mass (Figure 5.15a). The absorbance obtained after 2000s of PNP hydrolysis is proportional to the number of deposition cycles. Since the amount of deposited enzyme per unit area in a linear function of n (Figure 5.15b), this means that the enzymatic activity of the PEI-(AlgCat-ALP)$_n$ films can be precisely controlled by the number of deposition cycles and that the enzymes deposited during each deposition step are active and accessible to their substrate, PNP. This result is by far not obvious. Indeed, one finds in the literature examples of enzyme multilayer films whose activities increase with the number of layers constituting the films. This is for example the case for multilayers constituted of glucose oxidase with various polycations[38, 39]or of polyphenol oxidase/poly(allylamine) multilayers which were evaluated electrochemically towards different metabolically related catecholamine [40]. One also finds examples where the activity is confined to the outer layers.

In this case, after a first increase of the activity with the number of deposited bilayers, the activity becomes fairly independent of this number. This is for example the case for films obtained by alternating the deposition of (peroxidase/polystyrene sulfonate) complexes with poly(allylamine) whose activities level-off after the deposition of 7 bilayers [41]. It has also been observed for multilayers produced by the alternated deposition of chitosan and glucose oxidase. The sensitivity for glucose sensing levelled off after the deposition of 5 bilayers and was maximal when only the last layer pair contained glucose oxidase [12].
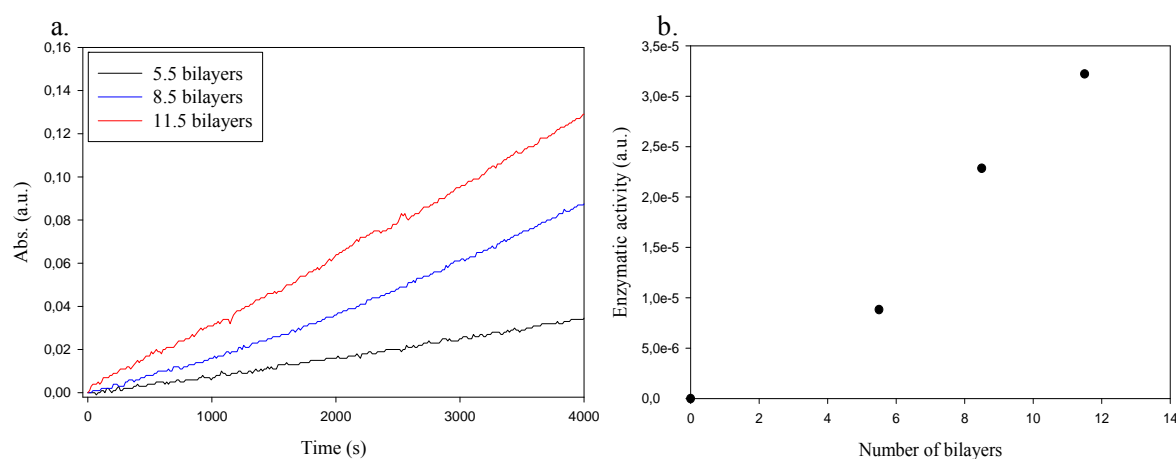


***Figure 5.15****: (a.) Evolution of the absorbance at 405 nm for films constituted of 4.5, 8.5 and 11.5 bilayers of (Alg-Cat/ALP); (b.) Absorbance increase per unit time as a function of the number of deposition steps.*

### 5.4.3. Storage of the film by freeze drying

Finally we investigated if PEI-(AlgCat-ALP)$_7$ films deposited on a substrate, freeze dried and stored at 4°C during 3 weeks before being rehydrated keep their enzymatic activity. We observed that indeed their activity was indistinguishable from that of the same film but estimated directly after its preparation (Figure 5.16).
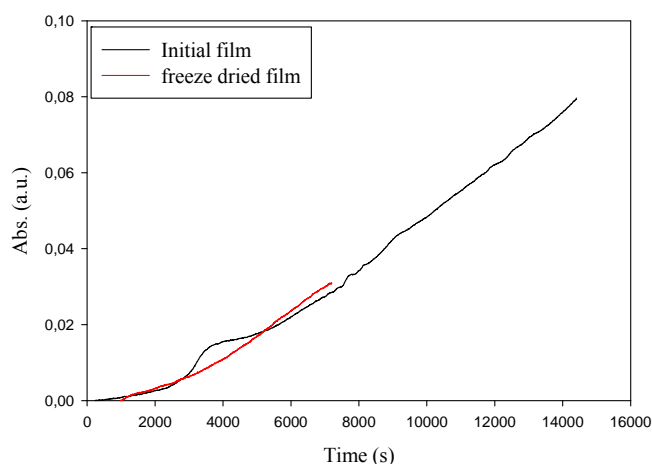
**Figure 5.16**: *Enzymatic activity of film after preparation and after a freeze-drying periode of 3 weeks.*

This shows that PEI-(AlgCat-ALP)$_n$ films can used in a totally preserved state after freeze drying. This result opens an avenue for the preparation of biosensors by layering Alg-Cat with enzymes presenting a real sensing ability like glucose oxidase, β-galactosidase etc. Indeed the preparation of such films using the layer-by-layer deposition method can be realized in an automatized manner using dipping robots and the obtained films can be stored safely before their use as a biosensor. In addition each sample can be used several times over a time duration of one or two weeks as shown in Figure 5.14 without significant loss of enzymatic activity.

## 5.5. Stretching experiments

### 5.5.1. Film elaboration on viscoelastic polydimethylsiloxane substrate

Our final goal was to create a mechano-responsive film. To this end, we deposited similar PEI-(Alg-Cat/ALP) multilayers on silicone substrates. Because the characterization techniques that we have are usually difficult to apply on silicone, we verified that the film builds up on this substrate by measuring its enzymatic activity as a function of the number of deposition steps. The resultisshown on figure 5.17.
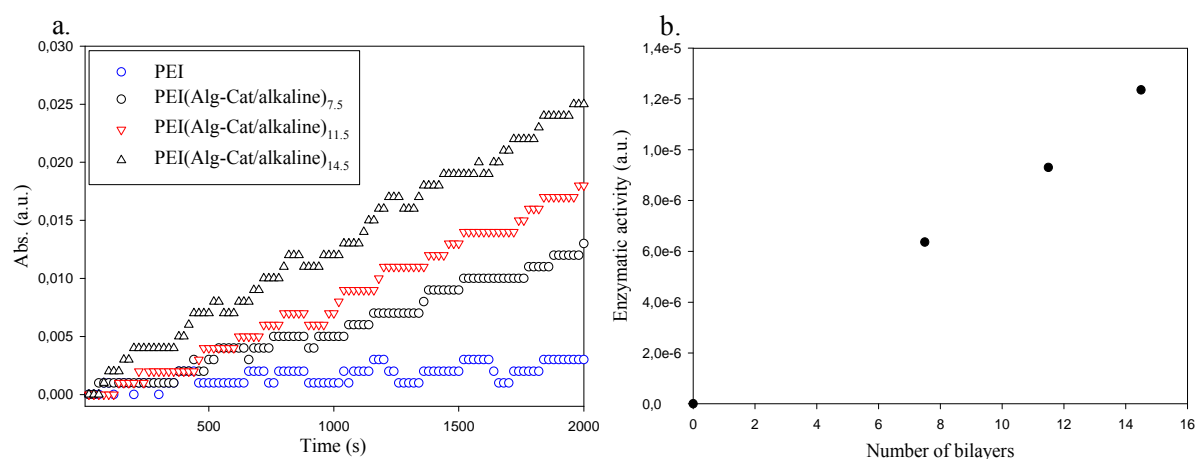
***Figure 5.17****: a.) Enzymatic acitivity of (PEI-(AlgCat/ALP)n films build on silicone sheets with n=7.5, 11.5 and 14.5 followed by UV absorbance at 405 nm; (b.) slope of the absorbance increase per unit time as a function of the number of deposited bilayers.*

The increase of the activity with the number of deposited layers indicates that film builds up on silicone.

## 5.5.2. Enzymatic activity of the films under stretching constraints

In order to have a better detection sensitivity of the film response during stretching/unstretching cycles, a fluorescent substrate was used instead of PNP. In presence of alkaline phosphatase, the fluorescein diphosphate initially colorless is transformed in fluorescein easily detectable (Ex=490nm/Emi=515nm)(figure 5.18).
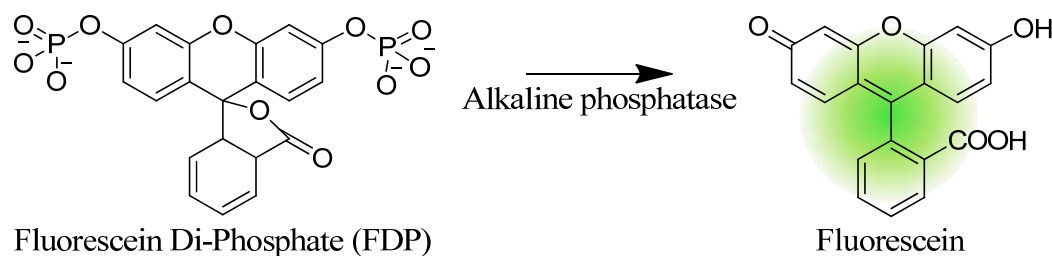


***Figure 5.18:****Transformation of fluorescein diphosphate in fluorescein under alkaline phosphatase activity.*

The PEM film was then submitted to stretching/unstretchingcyles and its enzymatic activity was monitored (figure 5.19). "SR" corresponding to the stretching ratio and the numbers in brackets are relative to the stretching/unstretching cycle performed.
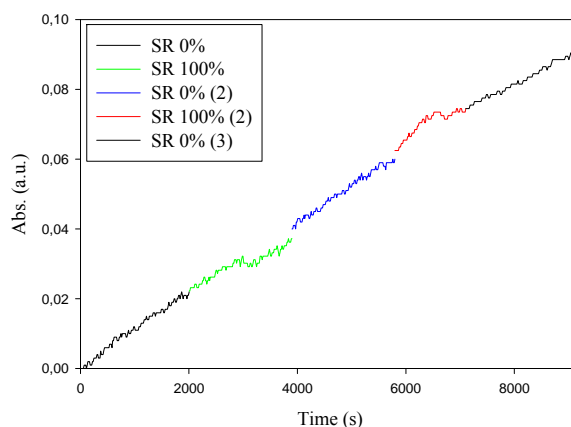
*Figure 5.19*: *Enzymatic activity of the film under stretching/unstretching cycles monitored by fluorescence measurements.*

A typical result is given in figure 5.19. One observes that there is no change of the film enzymatic activity when it is stretched at 100%. This result was verified three times. This indicates that, despite the fact that the ALP enzymes are covalently fixed into the cross-linked multilayer, their activity does not change upon stretching. This may be due to the fact that ALP is a particularly robust enzyme which is also difficult to denature even thermically.

## 5.6. Conclusion

We have shown the possibility to elaborate covalently cross-linked multilayer films that are enzymatically active by alternating AlgCat and alkaline phosphatase. These films can be constructed on various substrates such as quartz, glass and siliconeand stay active in time..however, it appears that stretching the film does not change its enzymatic activity. This may be due to the fact that alkaline phosphatase is too robust. In the future, this method has to be applied to other enzymes such as beta-galactosidase or chymotrypsin. An alternative method of film elaboration consisting of a crosslinking step after each bilayer deposition, preventing the important desorption of enzyme observed is also in development.

## 5.7. References

1.      L. Caseli, R.G. Oliveira, D.C. Masui, R.P.M. Furriel, F.A. Leone, B. Maggio, and M.E.D. Zaniquelli, *Effect of molecular surface packing on the enzymatic activity modulation of an anchored protein on phospholipid langmuir monolayers.* Langmuir, 2005. **21**(9): p. 4090-4095.

2.      P. Walde and S. Ichikawa, *Enzymes inside lipid vesicles: Preparation, reactivity and applications.* Biomolecular Engineering, 2001. **18**(4): p. 143-177.

3.      A. Grotzky, E. Atamura, J. Adamcik, P. Carrara, P. Stano, F. Mavelli, T. Nauser, R. Mezzenga, A.D. Schluter, and P. Walde, *Structure and enzymatic properties of molecular dendronized polymer-enzyme conjugates and their entrapment inside giant vesicles.* Langmuir, 2013. **29**(34): p. 10831-10840.

4.      D.B. Gornowich and G.J. Blanchard, *Enhancement of enzyme activity by confinement in an inverse opal structure.* Journal of Physical Chemistry C, 2012. **116**(22): p. 12165-12171.

5.      M. Onda, Y. Lvov, K. Ariga, and T. Kunitake, *Sequential actions of glucose oxidase and peroxidase in molecular films assembled by layer-by-layer alternate adsorption.* Biotechnology and Bioengineering, 1996. **51**(2): p. 163-167.

6.      L. Derbal, H. Lesot, J.C. Voegel, and V. Ball, *Incorporation of alkaline phosphatase into layer-by-layer polyelectrolyte films on the surface of affi-gel heparin beads: Physicochemical characterization and evaluation of the enzyme stability.* Biomacromolecules, 2003. **4**(5): p. 1255-1263.

7.      H.Q. Yao and N.F. Hu, *Ph-controllable on-off bioelectrocatalysis of bienzyme layer-by-layer films assembled by concanavalin a and glucoenzymes with an electroactive mediator.* Journal of Physical Chemistry B, 2010. **114**(30): p. 9926-9933.

8.      C.C. Huang, H. Bai, C. Li, and G.Q. Shi, *A graphene oxide/hemoglobin composite hydrogel for enzymatic catalysis in organic solvents.* Chemical Communications, 2011. **47**(17): p. 4962-4964.

9.      G. Kalnitsky, J.P. Hummel, H. Resnick, J.R. Carter, L.B. Barnett, and C. Dierks, *The relation of structure to enzymatic activity in ribonuclease.* Annals of the New York Academy of Sciences, 1959. **81**: p. 542-69.

10.     C.Y. Tseng, A. Wang, and G. Zocchi, *Mechano-chemistry of the enzyme guanylate kinase.* Epl, 2010. **91**(1): p. 6.

11.     H.S. Kim, S.H. Ha, L. Sethaphong, Y.M. Koo, and Y.G. Yingling, *The relationship between enhanced enzyme activity and structural dynamics in ionic liquids: A combined computational and experimental study.* Physical Chemistry Chemical Physics, 2014. **16**(7): p. 2944-2953.

12.     L. Caseli, D.S. dos Santos, M. Foschini, D. Goncalves, and O.N. Oliveira, *The effect of the layer structure on the activity of immobilized enzymes in ultrathin films.* Journal of Colloid and Interface Science, 2006. **303**(1): p. 326-331.

13.    P. Schwinte, J.C. Voegel, C. Picart, Y. Haikel, P. Schaaf, and B. Szalontai, *Stabilizing effects of various polyelectrolyte multilayer films on the structure of adsorbed/embedded fibrinogen molecules: An atr-ftir study.* Journal of Physical Chemistry B, 2001. **105**(47): p. 11906-11916.

14.    P. Schwinte, V. Ball, B. Szalontai, Y. Haikel, J.C. Voegel, and P. Schaaf, *Secondary structure of proteins adsorbed onto or embedded in polyelectrolyte multilayers.* Biomacromolecules, 2002. **3**(6): p. 1135-1143.

15.    G. Decher, *Fuzzy nanoassemblies: Toward layered polymeric multicomposites.* Science, 1997. **277**(5330): p. 1232-1237.

16.    B. Lupo, A. Maestro, M. Porras, J.M. Gutierrez, and C. Gonzalez, *Preparation of alginate microspheres by emulsification/internal gelation to encapsulate cocoa polyphenols.* Food Hydrocolloids, 2014. **38**: p. 56-65.

17.    D. El Khoury, H.D. Goff, S. Berengut, R. Kubant, and G.H. Anderson, *Effect of sodium alginate addition to chocolate milk on glycemia, insulin, appetite and food intake in healthy adult men.* European Journal of Clinical Nutrition, 2014. **68**(5): p. 613-618.

18.    S.G. Reddy and A.S. Pandit, *Controlled drug delivery studies of biological macromolecules: Sodium alginate and lignosulphonic acid films.* Journal of Applied Polymer Science, 2014. **131**(13): p. 6.

19.    J.U. Menon, P. Ravikumar, A. Pise, D. Gyawali, C.C.W. Hsia, and K.T. Nguyen, *Polymeric nanoparticles for pulmonary protein and DNA delivery.* Acta Biomaterialia, 2014. **10**(6): p. 2643-2652.

20.    A. Shapira, D.-H. Kim, and T. Dvir, *Advanced micro- and nanofabrication technologies for tissue engineering.* Biofabrication, 2014. **6**(2): p. 020301.

21.    C.J. Kastrup, M. Nahrendorf, J.L. Figueiredo, H. Lee, S. Kambhampati, T. Lee, S.W. Cho, R. Gorbatov, Y. Iwamoto, T.T. Dang, P. Dutta, J.H. Yeon, H. Cheng, C.D. Pritchard, A.J. Vegas, C.D. Siegel, S. MacDougall, M. Okonkwo, A. Thai, J.R. Stone, A.J. Coury, R. Weissleder, R. Langer, and D.G. Anderson, *Painting blood vessels and atherosclerotic plaques with an adhesive drug depot.* Proceedings of the National Academy of Sciences of the United States of America, 2012. **109**(52): p. 21444-21449.

22.    J.H. Waite and M.L. Tanzer, *Polyphenolic substance of mytilus-edulis - novel adhesive containing l-dopa and hydroxyproline.* Science, 1981. **212**(4498): p. 1038-1040.

23.    B.P. Lee, P.B. Messersmith, J.N. Israelachvili, and J.H. Waite, *Mussel-inspired adhesives and coatings*, in *Annual review of materials research, vol 41*, D.R. Clarke and P. Fratzl, Editors. 2011, Annual Reviews: Palo Alto. p. 99-132.

24.    H. Lee, S.M. Dellatore, W.M. Miller, and P.B. Messersmith, *Mussel-inspired surface chemistry for multifunctional coatings.* Science, 2007. **318**(5849): p. 426-430.

25.     C. Lee, J. Shin, J.S. Lee, E. Byun, J.H. Ryu, S.H. Um, D.I. Kim, H. Lee, and S.W. Cho, *Bioinspired, calcium-free alginate hydrogels with tunable physical and mechanical properties and improved biocompatibility.* Biomacromolecules, 2013. **14**(6): p. 2004-2013.

26.     E. Loizou, J.T. Weisser, A. Dundigalla, L. Porcar, G. Schmidt, and J.J. Wilker, *Structural effects of crosslinking a biopolymer hydrogel derived from marine mussel adhesive protein.* Macromolecular Bioscience, 2006. **6**(9): p. 711-718.

27.     M.J. Sever, J.T. Weisser, J. Monahan, S. Srinivasan, and J.J. Wilker, *Metal-mediated cross-linking in the generation of a marine-mussel adhesive.* Angewandte Chemie-International Edition, 2004. **43**(4): p. 448-450.

28.     C.E. Brubaker and P.B. Messersmith, *Enzymatically degradable mussel-inspired adhesive hydrogel.* Biomacromolecules, 2011. **12**(12): p. 4326-4334.

29.     J.H. Ryu, Y. Lee, W.H. Kong, T.G. Kim, T.G. Park, and H. Lee, *Catechol-functionalized chitosan/pluronic hydrogels for tissue adhesives and hemostatic materials.* Biomacromolecules, 2011. **12**(7): p. 2653-2659.

30.     P. Podsiadlo, Z.Q. Liu, D. Paterson, P.B. Messersmith, and N.A. Kotov, *Fusion of seashell nacre and marine bioadhesive analogs: High-strength nanocompoisite by layer-by-layer assembly of clay and l-3,4-dihydroxyphenylaianine polymer.* Advanced Materials, 2007. **19**(7): p. 949-+.

31.     H. Lee, Y. Lee, A.R. Statz, J. Rho, T.G. Park, and P.B. Messersmith, *Substrate-independent layer-by-layer assembly by using mussel-adhesive-inspired polymers.* Advanced Materials, 2008. **20**(9): p. 1619-+.

32.     J. Sedo, J. Saiz-Poseu, F. Busque, and D. Ruiz-Molina, *Catechol-based biomimetic functional materials.* Advanced Materials, 2013. **25**(5): p. 653-701.

33.     A. Garen and C. Levinthal, *A fine-structure genetic and chemical study of the enzyme alkaline phosphatase of e. Coli. I. Purification and characterization of alkaline phosphatase.* Biochimica et biophysica acta, 1960. **38**: p. 470-83.

34.     M.V. Voinova, M. Rodahl, M. Jonson, and B. Kasemo, *Viscoelastic acoustic response of layered polymer films at fluid-solid interfaces: Continuum mechanics approach.* Physica Scripta, 1999. **59**(5): p. 391-396.

35.     F. Hook, B. Kasemo, T. Nylander, C. Fant, K. Sott, and H. Elwing, *Variations in coupled water, viscoelastic properties, and film thickness of a mefp-1 protein film during adsorption and cross-linking: A quartz crystal microbalance with dissipation monitoring, ellipsometry, and surface plasmon resonance study.* Analytical Chemistry, 2001. **73**(24): p. 5796-5804.

36.     R. ISHIWATARI, *Infrared absorption band at 1540 cm -1 of humic acid from a recent lake sediment.* Geochemical Journal, 1967. **1**: p. 61-70.

37. J. Venkatesan, I. Bhatnagar, and S.K. Kim, *Chitosan-alginate biocomposite containing fucoidan for bone tissue engineering.* Marine Drugs, 2014. **12**(1): p. 300-316.

38. N. Ferreyra, L. Coche-Guerente, and P. Labbe, *Construction of layer-by-layer self-assemblies of glucose oxidase and cationic polyelectrolyte onto glassy carbon electrodes and electrochemical study of the redox-mediated enzymatic activity.* Electrochimica Acta, 2004. **49**(3): p. 477-484.

39. F. Caruso and C. Schuler, *Enzyme multilayers on colloid particles: Assembly, stability, and enzymatic activity.* Langmuir, 2000. **16**(24): p. 9595-9603.

40. E.S. Forzani, V.M. Solis, and E.J. Calvo, *Electrochemical behavior of polyphenol oxidase immobilized in self-assembled structures layer by layer with cationic polyallylamine.* Analytical Chemistry, 2000. **72**(21): p. 5300-5307.

41. A.M. Yu, Z.J. Liang, and F. Caruso, *Enzyme multilayer-modified porous membranes as biocatalysts.* Chemistry of Materials, 2005. **17**(1): p. 171-175.

# Conclusion and outlook

My thesis work was dedicated to the development of mechano-responsive materials based on protein conformational changes induced by stretching. We grafted proteins on a surface or embedded them in a matrix, expecting that the mechanical constraint applied to the material be transferred at a molecular scale, leading to the modification of three dimensional structure of the protein and so modulating its property. To achieve this goal, we elaborated different strategies based on polymeric structures coupled with proteins or enzymes allowing the conversion of a mechanical stress such as stretching in a bio-chemical response.

In the first part of this study (chapter 3), we designed a PDMS substrate specifically functionalized with Green Fluorescent Proteins (GFP) responding to external constraints by modulating its spectral properties. This strategy was based on the use of specifically bis-modified GFP byPr. Schillers group (Freiburg Universität) allowing its anchoring in the material and increasing its mechanical sensitivity. This project was divided in two main parts, beginning with the functionalization of the substrates and the stretching experiments. The modification of the PDMS was performed by UV-Ozone treatment followed with bis-isocyanate reaction to anchor chemically active functions at the top of its surface. Once this step was performed, alkyne terminated polyethylene glycol chains were grafted to the surface avoiding proteins adsorption and degradation. The specifically modified GFP was finally linked to the material through soft click chemistry conditions. This material was then submitted to stretching experiments and its fluorescence response was monitored. Under stretching constraint, the mechanical constraints applied to the material were transferred through the PEG chains to the grafted GFP leading to a decrease of its fluorescence emission. This was interpreted as a GFP conformational change resulting in a change of the fluorophore direct environment. Moreover, reversibility of these changes is observed when the surface is relaxed. With this material, we succeeded in making a proof of concept that the three dimensional structure of a protein can be affected by the application of stretching a substrate onto which the proteins are grafted.

In chapter 4, we developed a new strategy based on the loading and anchoring of a pre-crosslinked polymeric matrix with enzymes in order to elaborate a chemo-mechano-responsive film. We expected the catalytic activity of such films to decrease when the material is submitted to a stretching due to enzyme structural modifications. To achieve this goal, we used a crosslinked poly-L-lysine/hyaluronic acid multilayer film as a matrix functionalized with beta-galactosidase enzymes and then submitted it to stretching experiments. We succeeded in modulating the enzyme activity of the film under stretching/unstretching cycles. A modification of 30% of the enzymatic activity of the material was observed. Moreover, a partial reversibility of the system was obtained. According to the results obtained during this study, although the direct proof of enzyme structure modification could not yet be demonstrated, it seems to be the only explanation of such behavior of the films.

In order to increase the response of the material to stretching constraints, a new strategy based on the elaboration of a multilayer architectures composed of enzymes and polyelectrolytes was developed in chapter 5. By this way, the structure itself of the material is composed of enzymes, which are thus more sensitive to the material deformation. For this purpose, we elaborated a film according to the layer-by-layer method by using a positively charged enzyme, alkaline phosphatase and a specifically modified polyanion, alginate-catechol (Alg-Cat). Once the PEM built, the entire structure is crosslinked thanks to catechol chemistry then submitted to stretching constraints in order to modulate its properties. We developed a strategy to elaborate enzymatically active crosslinked multilayer films based on the alternated deposition of AlgCat and alkaline phosphatase. However, no modulation of the PEM enzymatic activity was observed under stretching constraints. This result can be explained by the robustness of the alkaline phosphatase. In the future, this method has to be applied to other enzymes such as beta-galactosidase previously demonstrated as more sensitive to external constraints.

This thesis work highlighted different constraints inherent to the work with biomacromolecules and in particularly enzymes. Thus, in order to elaborate stable biosensors or materials meant to be manipulated, it is mandatory to control the immobilization mechanism of the enzymes. In the case of stable enzyme immobilization, the active molecules should be bound preferentially by means of covalent bonds, but without undergoing a significant conformational change to avoid its decrease or loss of activity. In addition the immobilization matrix should be porous enough to allow access of the substrate to all the immobilized enzymes. In this context, the elaboration of a gel-like material made of both polymers and enzymes seems to be an

interesting approach. Indeed, such material should own a crosslinked structure but without strong constraints, and allows the diffusion of products and substrates. Essentially made of enzymes it should have a high catalytic activity and external constraints applied to the material should directly affect its structure and so the enzymes themselves. Thus important modifications in material enzymatic activity are expected under mechanical stress.

Since several years an increasing number of works based on the use of dopamine derivatives in biomaterials are reported. As shown in chapter 5, these components have a high reactivity allowing the formation of covalent bonds with numerous chemical functions under soft condition which is one of the principle constraints in the use of biomacromolecules. In this context a new strategy of material elaboration is being developed at the present time in our laboratory based on the use of enzymes linked together by the use of bis-catechol-functionalized linkers. By varying the size of the linker, it should be possible to control the physical properties of the material such as its rigidity. Moreover, polydopamine and its derivatives were reported to be high adherent to various substrates allowing its use as a "smart" coating in a lot of applications.

The development of mechano-sensitive coating is of high interest for biomedical applications, in particular implants which are submitted to various mechanical constraints when placed in the human body. These implants could be functionalized in an easy way by polymeric coating such as polyelectrolyte multilayers or polymer networks in order to give them mechano-sensitive properties. Once functionalized, they could become sensitive to biomechanical constraints existing in their neighborhood and adapt their responses by initiating for example biochemical reactions owning a therapeutic interest.

# Annexe 1

# Cyto-mechanoresponsive Polyelectrolyte Multilayer Films

# Cyto-mechanoresponsive polyelectrolyte multilayer films

Annexe 2

# Reversible biomechano-responsive surface based on genetically modified Green Fluorescent Protein

## COMMUNICATION

# Reversible biomechano-responsive surface based on genetically modified Green Fluorescent Protein

J. Longo,[a†] C.Yao,[b†] C. Rios[a], F. Boulmedais,[a,c,d] J. Hemmerlé,[e,f] P. Lavalle,[e,f] S. Schiller,[b*] P. Schaaf[a,c,d,e,f,g*] andL. Jierry[a,c,d]

**GFP has been genetically modified at two specific positions of its molecular architecture. These modifications allow its covalent graftingonto PEG brushes grafted on silicone surfaces.The stretching of this material leads to a reversible decrease of the fluorescence intensity due to the changing of conformation underwent by the biomacromolecule.**

Mechanotransduction processes can be defined as the transfer of information initiated by a mechanical force and resulting in a chemical signal.This topic is a rapidly growing field of study which covers biology, chemistry and more recently material science. Indeed, the design of mechano-responsive materials opens the gate to new developments in various fields such as drug delivery, detection of stress or biomaterials. From a chemical point of view there are clearly two possible approaches to tackle this subject: one way is to investigate the effect of a mechanical force on the behavior of covalent bondsto induce bond breaking or intramolecular reaction. This approach is the most widely used in the current field of smart material design. It is, for example,illustrated by the work of the groups of Moore and Sotos[1] who showed that a mechanical force can induce chemical modifications in materials contained "mechanophore" compounds, leading to acolour change in material regions of high mechanical strain.Currently, many more chemo-mechano-responsive materials based on an intramolecular reaction resulting in a color change of the material have been reported. A second approach is to mimic the mechanotransduction processes used by nature to transform a mechanical signal into a chemical one. Such processes are in particular used by cells which sense the mechanical properties of their environment with widespread consequence on their fate. There are at least two mechanisms used by cells to transform a mechanical force into a chemical signal: one is based on membrane channels whose properties change when the membrane is under the influence of a mechanical stress and the other is based on conformational changes of proteins that are submitted to a mechanical force.[2] One of the first examples of this type of protein that has been extensively studied is that of fibronectin, an adhesion protein present in the extracellular matrix.[3]Since the five last years, our group has developed different approaches to design mechano-responsive materials based on the hiding of ligand[4] or enzymes[5],

becoming accessible to their environment through a mechanical stretching.

Up to now, manycomputational simulation and single-molecule studies have demonstrated that a deformation of the ternary structure of biomacromoleculescan result from the application of a mechanical force.[6, 7]In particular, Green Fluorescent Protein (GFP) is a model of protein extensively studied because of its photophysical properties and used for biomolecule localization or expression. Its fluorescence emission is due to its particular folding where a chromophore is located in the centre of a β-barrel structure.Thus, mechanical stresses applied to this β-barrel alter the resulting fluorescence.

Herein, we report the design of a biomechano-responsive material based on a mechanical force directly underwent by GFPand leading to a fluorescence change of the material.GFP has been specifically modified on two points of its three dimensional structure to be covalently grafted onto functionalized silicone substrate. A uniaxial stress strain of this material at various proportions of its initial length is applied to affect the conformation of the GFP resulting in fluorescence emission changes.

The green fluorescent protein (GFP) from *Aequorea Victoria*is a protein composed of 238aminoacids residues (26.9 kDa) forming an eleven-stranded β-barrel structure with an α-helix running through the center of the barrel[8]. Along it central helix, inside the hydrophobiccore, a*para*-hydroxybenzylideneimidazolidonechromophore (HBI) takes place. This chromophoreis formed from an internal cyclisation of Ser65, Tyr66 and Gly67 into a conjugated structure. Single-molecule measurements have shown that the three dimensional deformation response of the GFP varies with the direction of the force applied. In particular, a minimal force-extension is required along the direction of the amino acid positions 3 and 212 to unfold partially the GFP, compared to others directions of stress tested.[6]Truncated GFP mutant has been produced by Saeger et *al.* to mimic GFP elongated along roughly the same direction (3, 212). The authors observed a decrease of the fluorescence intensity but no shift of the maxima of fluorescence.[7]Therefore, we decided to introduce unnatural amino acids in the spatial regions around these two positions of the primary structure of the GFP.[9] Two tyrosines, Tyr39 and Tyr182, present in the GFP wild type (wt) sequence appeared as good candidates. Both amino acids do not have any role in the folding of the protein, and

furthermore, they are accessible from outside of the structure. *Para*-azidophenylalanin(*p*AzF) was chosen to take place of Tyr39 and Tyr182. Indeed, *p*AzFis an unnatural amino acid having the same chemical structure as tyrosine except that an azido group in *para* position of the aromatic ring replaces the natural phenolic hydroxyl.This chemical group allows to click further the GFP through Copper(I)-catalyzed Azide-Alkyne Cycloaddition (CuAAC) onto a silicone surface modified beforehand in a suitable way. Representation of the molecular structure of GFP (wt) and GFP mutants (N$_3$-GFP (39) and N$_3$-GFP-N$_3$ (39, 182) are shown in Figure 1a and all details concerning their preparationsare given in the Part 1 of the Electronic Supporting Information (ESI).

Covalent grafting of azide containing GFP mutants onto a substrate required the modification of its surface by the introduction of alkyne groups. The elastomer chosen was the polydimethylsiloxane (PDMS) named Sylgard-184, prepared from starting precursors provided by Dow Corning (Part 2, ESI). This PDMS is a filler-free elastomer, transparent but chemically inert. The modification method mainly used to functionalize PDMS surface is based on oxygen plasma treatment. This process allows the introduction of hydroxyl groups all over the surface but propagates also the oxidation deep into the material, leading to the formation of a thin brittle silica layer. Thus, manipulations of such an oxidized material generate cracks on its surface, which must be obviously avoided in case ofa mechano-responsive materialdesign. Genzer et al. have developed a milderand efficient method of PDMS oxidation based on UV irradiations and ozone treatment (UVO).[10]This treatment generates the formation of silanol groups on the surface in a controlled way. We investigated this method of PDMS oxidation to start the modification of the silicone before the ultimate grafting step of azide-containing GFP mutants. The three steps of silicone treatment are illustrated in Figure 1:(*i*) once the UVO oxidation is realized, (*ii*) the introduction of an homobifunctionnal linker such as the 4,4'-methylenebis(phenyl)isocyanate (MDI) can be done. This linker, generally used for the modification of polyurethane, is covalently anchored on silicone surface andallows to have free and reactive isocyanate groups. (*iii*) Nucleophilic addition between these groups and amine-ended PEG chains lead to PEG brushes surfaces. The presence of alkyne groups on the other end side of the PEG chains is necessary for the further GFP grafting.
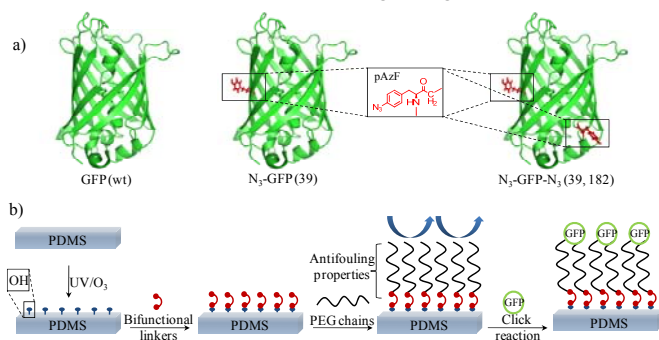


**Figure 1:(a)** Molecular structureof the GFP (wt),N$_3$-GFP (39) and N$_3$-GFP-N$_3$ (39, 182); (**b**)Schematic representation of the three modification steps of the PDMS surface required beforehand to graft covalently the GFP mutants, N$_3$-GFP (39) and N$_3$-GFP-N$_3$ (39, 182) through CuAAC click reaction.

One hour of UVO exposition of a 30% stretchedPDMS leads to a hydrophilic surface. Stretching of the substrate was done using a home-made device (Figure S-1) and thus allows higher density of polar groups grafted onto the PDMS, as reported in the literature. Water contact angle measurements reveals a value of 71° compared to the 110° of the native silicone sheet (Part 3.1in SI). The presence

of the hydroxyl groups (silanol) all over the surface is confirmed by ATR FTIR spectroscopy. Then, this highly hydroxylated surface is quickly brought in contact with 0.2 mg/mL of MDI in acetone solution during two hours. The contact angle of the so-modified surface increases up to 90°. PEG chains having 3000 kDa of molecular weight (Mw), and ended with amine on one side and alkyne on the other side, are brought in contact with the silicone surface. Nucleophilic addition of the amino-PEG chains provides a highly hydrophilic surface with 5° of water contact angle. Thus, the silicone has tobe modified to allow the covalent grafting of GFP mutants through CuAAC click chemistry in presence of copper(II) sulfate and sodium ascorbate.

Proteins are fragile biomacromolecules that need to be handled in adapted environment to keep their whole structural and functional integrity. In particular, it is known that copper salts have to be avoided because of their ability to denature proteins due to complexation reactions and induction of redox processes. Indeed, in primary tests, our GFP (wt) was brought in contact with a low concentration of Cu(II) and the reductive agent sodium ascorbate: in few minutes we observed a complete loss of the characteristic fluorescence emission. Since the last decade, many procedures allowing to click biomacromoleculesin mild conditions have been developed. In 2009, Hong et al. described the preparation and use of tris(3-hydroxypropyltriazolylmethyl)amine (THPTA), an hydrosoluble ligand of Cu(I).[11]This ligand complexes Cu(I) and thus avoids side-reactions from Cu(II) and increases the click reaction rate. Click reaction between GFPwt or mutants, N$_3$-GFP (39) and N$_3$-GFP-N$_3$ (39, 182), onto the modified silicone substrate were realized in presence of copper sulfate, sodium ascorbate and THPTA in buffered solution (pH 7.4), 25°C during 60 minutes. Fluorescence emission pictures are shown in Figure 2.



**Figure 2:** Fluorescence microscopy images taking from modified silicone surface after contact with (**a**) GFP wt, (**b**) N$_3$-GFP (39) and (**c**) N$_3$-GFP-N$_3$ (39, 182). The values written in white is the quantification of the fluorescence evaluated in arbitrary unity (a.u.) by using ImageJ software but comparable one to each other.

As expected, the substrate is fully antifouling against GFP (wt) because of the presence of the PEG brushes on the surface and the absence of azide along the GFP (Fig 2a). GFP mutantsN$_3$-GFP (39) and N$_3$-GFP-N$_3$ (39, 182), lead to almost similar fluorescenceemission surface due to the occurring of the click reaction between the PEG-ended alkyne and the free azide along both GFP mutants(Fig 2b and 2c).Then, the modified PDMS surface with the mono-azide mutant N$_3$-GFP (39) was stretched in a uniaxial direction and the fluorescence intensity measured at different stretching ratio: 10%, 20% and 30%. Beyond 30% of stretching, we observed tearing of the substrate. We thus limited our study to this maxima of elongation. A linear decrease of the fluorescence intensity is measured due to a "dilution effect" (see Figure 3a): a decrease of fluorescence intensity of 8%, 15% and 22% is measured when the substrate is stretched at 10%, 20% and 30% respectively. When the substrate is stretched in one direction, the density of grafted GFP decreases only partially because a contraction of the material occurs in the direction perpendicular to the stretching. This contraction contributes to limit the reduction of the GFP density. When the material is returned at rest (the initial length is restored), the initial density of GFP anchored onto the surface is recovered.The

behavior of the so-prepared surface is repeatable at great number of times (Figure 3b). Stretching of the PDMS surface modified with the $N_3$-GFP-$N_3$ (39, 182) leads also to a linear decrease of the fluorescence intensity but with a more important slope: 23%, 42% and 60% decrease of the initial fluorescencewhen the PDMS is stretched at 10%, 20% and 30% respectively. In addition to the "dilution effect" due to the uniaxial stretching, when the GFP is anchored to the surface at two opposite positions, the mechanical force imposed to the material is transferred to the biomacromolecule whosethe three dimensional structure is deformed. This deformation leads to a decrease of fluorescence intensity, in agreement with single molecule measurement and simulations works previously reported.[6,7]A full restoration of the initial fluorescence emission is measured when the material is returned at 0% of stretching. Furthermore, three cycles of stretching-release show that the influence of the stretching on the fluorescence emission is highly reversible (Figure 3c).
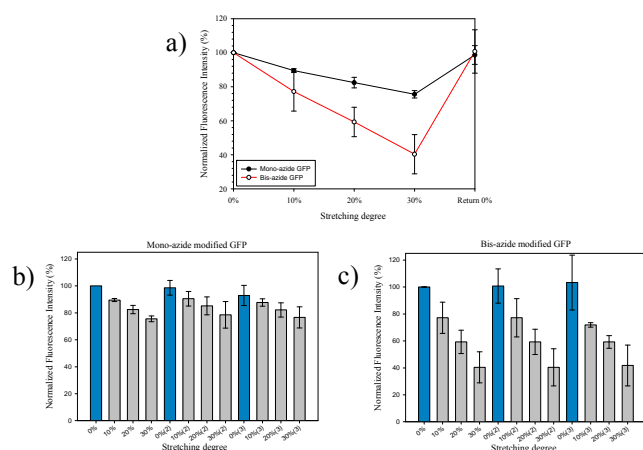


**Figure 3:(a)** Normalized fluorescence intensity measured by fluorescence microscopy in function of the stretching degree of the modified PDMS by $N_3$-GFP (39) and $N_3$-GFP-$N_3$ (39, 182); Normalized fluorescence intensity measured onto the PDMS surface modified with theGFP mutants **(b)** $N_3$-GFP (39) and **(c)** $N_3$-GFP-$N_3$ (39, 182). The measured fluorescence emission corresponds to means ± standarddeviations from at least three independent experiments. The stretching ratio is defined as the ratio of the lengths ofsubstrate after and before stretching x 100.

Mechano-responsive materials based on biomacromolecules are rare. Very recently, Brantley et al. have described the development of biocomposite materials including GFP modified by site-selective mutagenesis.[12] This material exhibits a decrease of fluorescence when the compression force is increasing. A gradual deformation of the three dimensional structure of the GFP explains this effect. When reaching 40 MPa, a non-reversible quenching of the fluorescence is observed.Herein, we report the first example of system where a GFP changes its fluorescence due to a uniaxial stretching and in a reversible way.

## Conclusions

To sum up, we designed a biomechano-responsive surface based on conveniently functionalized silicon substrate and genetically modified GFP. Position of the unnatural aminoacids introduced into the primary sequence of GFP has been selected on the basis of simulation and single-molecule works reported. When stretching is applied to our system in a uniaxial direction, we observe a linear decrease of the fluorescence intensity up to 60% (when stretched up to 30%). Return at rest allows to fully restore the initial fluorescence which is a crucial point in the future development of stress-strain mechano-responsive materials.

## Notes and references

[a] Institut Charles Sadron (UPR22-CNRS), 23 rue du Loess, BP 84047, 67034, Strasbourg Cedex 2, France.

[b]Universität Freiburg (FRIAS), Albertstrasse 19, Freiburg im Breisgau, Deutschland.

[c]Université de Strasbourg, International Center for Frontier Research in Chemistry (icFRC), 8 allée Gaspard Monge, 67083 Strasbourg, France.

[d] Institut d'Etudes Avancées de l'Université de Strasbourg (USIAS), 5 allée du Général Rouvillois, 67083 Strasbourg, France.

[e] INSERM, UMR-S 1121, 11 rue Humann, 67085 Strasbourg Cedex, France.

[f] Université de Strasbourg, Faculté de Chirurgie Dentaire, 8 rue Sainte Elisabeth, 67000, Strasbourg, France.

[g] Institut Universitaire de France (IUF), 103 boulevard Saint-Michel, 75005 Paris, France.

† Both first authors have contributed equally to this work.

Electronic Supplementary Information (ESI) available: [Material and methods, preparation and characterization of GFP wt and mutants, PDMS preparation and surface modifications]. See DOI: 10.1039/c000000x/

1 D. A. Davis, A. Hamilton, J. L. Yang, L. D. Cremar, D. Van Gough, S. L. Potisek, M. T. Ong, P. V. Braun, T. J. Martinez, S. R. White, J. S. Moore, N. R. Sottos, *Nature* 2009, **459**, 68.

2 V. Vogel, M. Sheetz, *Nat. Rev. Mol. Cell Biol.* 2006, **7**, 265.

3 V. Vogel, in *Annual Review of Biophysics and Biomolecular Structure, Vol. 35*, Annual Reviews, Palo Alto, 2006, pp. 459.

4 J. Davila, A. Chassepot, J. Longo, F. Boulmedais, A. Reisch, B. Frisch, F. Meyer, J. C. Voegel, P. J. Mesini, B. Senger, M. H. Metz-Boutigue, J. Hemmerle, P. Lavalle, P. Schaaf, L. Jierry, *J. Am. Chem. Soc.* 2012, **134**, 83 ; J. Bacharouche, F. Badique, A. Fahs, M. A. Spanedda, A. Geissler, J.-P.Malval, M.-F. Vallat, K. Anselme, G. Francius, B. Frisch, J. Hemmerlé, P. Schaaf, V. Roucoules, *ACS Nano*, 2013, **7**, 3457.

5 D. Mertz, C. Vogt, J. Hemmerle, J. Mutterer, V. Ball, J. C. Voegel, P. Schaaf, P. Lavalle, *Nat. Mater.* 2009, **8**, 731.

6 H. Dietz, F. Berkemeir, M. Bertz, M. Rief, *Proc. Nat. Acad. Sci*, 2006, **103**, 12724.

7 J. Saeger, V. P. Hytönen, E. Klotzsch, V. Vogel, PLOSone, 2012, **7**, e46962.

8 J. J. van Thor, *Chem. Soc. Rev.*, 2009. **38**, 2935.

9 C. J. Noren, S. J. Anthony-Cahill, M. C. Griffith, P. G. Schultz, *Science*, 1989, **244**, 182.

10 K. Efimenko, W.E. Wallace, J. Genzer, *J. ColloidInterface Sci.*, 2002,**254**, 306.

11 V. Hong, S. I. Presolski, C. Ma, M. G. Finn, *Angew.Chem.Int. Ed.*, 2009,**48**, 9879.

12 J. N. Brantley, C. B. Bailey, J. R. Cannon, K. A. Clark, D. A. Vande Bout, J. S. Brodbelt, A. T. Keatinge-Clay, C. W. Bielawski, *Angew. Chem. Int. Ed.*, 2014, **53**, 5088.

# Supporting Information

## Biomechano-responsive surface based on genetically modified Green Fluorescent Protein

J. Longo, C. Yao, C. Rios, F. Boulmedais, J. Hemmerlé, P. Lavalle, S. Schiller*, P.  Schaaf* and L. Jierry
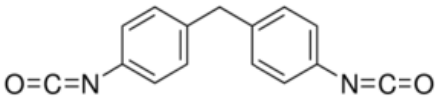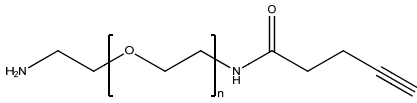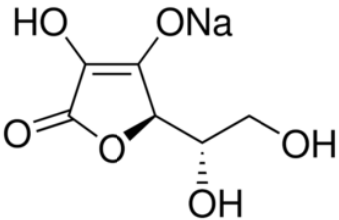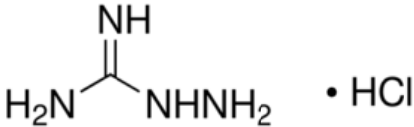
## Summary

# Material and methods

### 1. List of chemicals

All chemicals used in this work are gathered in the following table.

| Name and Acronyme | Molecular structure | Mw (g.mol$^{-1}$) | Supplier | CAS number |
|---|---|---|---|---|
| 4,4'-Methylenebis(phenyl isocyanate) <br><br> MDI |  | 250.25 | Sigma-Aldrich | 101-68-8 |
| alpha-Amino-omega-propargylacetamido poly(ethylene glycol) |  | 3000 | Iris-Biotech | -- |
| Copper sulfate pentahydrate | CuSO$_4$.5H$_2$O | 249.69 | Sigma-Aldrich | 7758-99-8 |
| (+)-Sodium L-ascorbate |  | 198.11 | Sigma-Aldrich | 134-03-2 |
| Aminoguanidine hydrochloride |  | 110.55 | Sigma-Aldrich | 1937-19-5 |
| Ampicillin |  | 403.45 | AppliChem | 7177-48-2 |

| | | | | |
|---|---|---|---|---|
| Chloramphenicol |  | 323.13 | Roth | 56-75-7 |
| L-(+)-Arabinose |  | 150.13 | Roth | 5328-37-0 |
| Isopropyl β-D-1-thiogalactopyranoside |  | 238.30 | Gerbu | 367-93-1 |
| p-azidophenylalanin (pAzF) |  | 206.20 | BACHEM | 33173-53-4 |
| 1-dodecanthiol | $CH_3(CH_2)_{10}CH_2S$ | 202.40 | Sigma-Aldrich | 112-55-0 |
| Sodium dodecyl sulfate |  | 288.37 | Roth | 151-21-3 |
| Imidazole |  | 68.08 | AppliChem | 288-32-4 |
| Acrylamide-solution | | | AppliChem | |

## 2. UVO set-up

Oxidation treatments of the PDMS surface was done by using a "UV-Ozone ProCleaner™ Plus" purchased from Bioforce-Nanosciences.

## 3. Contact angle measurements

Contact angle measurements were performed with a DIGIDROP-GBX® coupled with a camera by using 6uL pure water droplets. Values result from the average of three independent measurements done at different area of the PDMS surface studied.

## 4. Infrared spectroscopy

All the experiments were performed by using an FTIR spectrometer (Vertex 70, Bruker, Billerca, MA, USA) equipped with a deuterated triglycine sulfate (DTGS) detector. Total reflectance ATR germanium crystal accessory was used for IR measurements. All spectra acquisitions were performed at $2cm^{-1}$ resolution over 20 scans within the range $4000-800cm^{-1}$. This analytical method was performed the observed the hydroxyl group formation (silanol groups) onto the PDMS surface at various UVO exposition time. Immediately after the UVO treatment, the oxidized PDMS was analyzed by IR: the surface of the surface was directly brought in contact with the ATR diamond crystal, and the spectra recorded.

## 5. Fluorescence microscopy

The fluorescence measurements described in this work were performed by using an inverted light microscope (Nikon Microphot-FXA, Japan) equipped with a mercury lamp and operating between 470nm and 490nm for excitation and above 500nm for detection. The image analyses were performed by using ImageJ software (Raspband, W. S, ImageJ, U.S. National institutes of Health, Bethesda, USA).The measured fluorescence emission corresponds to means ± standard deviations from at least three independent experiments.

## 6. Elecstrospray mass spectrosocopy

Mass spectrometric measurements were performed on an LTQ Orbitrap XL mass spectrometer (Thermo Fisher Scientific, Bremen, Germany) coupled to an Agilent 1200 nanoflow-HPLC (Agilent Technologies GmbH, Waldbronn, Germany). Samples were applied directly onto the column without pre-column. A gradient of A [0.5% acetic acid in water] and B [0.5% acetic acid in 80% ACN/water] with increasing organic proportion was used for

peptide separation. The flow rate was 250nl/min and for sample application 500nl/min. The mass spectrometer was operated in the data-dependent mode and switched automatically between MS (max. of 1 x106 ions) and MS/MS. For MS/MS, wideband activation was enabled. The mass range for MS was m/z = 350 to 2,000 and signal threshold was 1,000. The resolution was set to 60,000. Data analysis was performed using Mascot.

## 7. Stretching devices

A homemade stretching device was designed and elaborated in our group (Figure S-1). It permits to stretch surface-modified PDMS substrates in a uniaxial direction up to 100% elongation.



**Figure S-1:** Picture of the stretching devices. The silicone sheets are placed between the two clamps**.**

The stretching degree is defined as:

$$\alpha = \frac{(l - l_0)}{l_0} \cdot 100$$

With $l_0$ and $l$ correspond respectively to the initial and the stretched length of the silicone substrate. All the stretching experiments were performed at room temperature and with PDMS surface kept always wet (never dried).

## 8. SDS-PAGE

**Gel preparation**

Solutions to get gels were prepared according to Laemmli et *al*.[1] The separating gel was 15%, the stacking gel was 6%. The electrophorese was performed in a Mini-Protean Tetra

Cell (Bio-Rad Laboratories). The gel mixures were gently pourred in the casting modules. The separating gel was firstly filled in, and carefully overlaid with isopropanol to allow a flat surface. After Polymerization, the alcohol was removed. The stacking gel was prepared and pourred until the top of the plate, the desired comb was inserted. After polymerisation, the comb was removed and the wells were washed with running buffer.

**Sample preparation**

Protein solution was prepared by adding 5 X SDS sample buffer (225 mM Tris-HCl pH6.8, 250 mM 1,4-Dithiothreitol, 50% Glycerin, 5% SDS, 0.05% Bromphenolblau) and heated at 99% for 3 min, centrifuged and stored at -20°C until analysis.

**Run conditions**

Electrophoresis was performed at room temperature with voltage 120 V for 1h until the tracking dye reached the bottom of the gel.

**Staining and destaining**

After ending electrophoresis, gel was removed from the plate and placed in a preheated staining solution containing 50% Ethanol, 10% acetic acid and 0.1% Coomassie Brillant Blue R250 for 30 min. Destaing of gel was accomplished by replacing the gel in a preheated destaining solution containing 30% Ethanol and 10% acetic acid for 30 min. The destaining procedure was repeated for 2-3 times.

**Gel scanning**

Scanning the gels were performed by using a Image System (Image Reader LAS-4000, Fujifilm) and saving in a graphic files in TIFF format.

[1] Laemmli. U. K. (1970) Cleavage of structural proteins during the assemly of the head of bacteriophage T4. *Nature***227**, 680-685.

## Part 1: Preparation and characterization of GFP wild type (wt) and N₃-GFP(39) and N₃-GFP-N₃(39, 182)

Plasmid pET21a/GFPY39TAG or pET21a/GFP-Y39TAG-Y182TAG (plasmid pET21a/GFP was from Group Suzuki, Saitama University Japan; pET21a/GFPY39TAG and pET21a/GFP-Y39TAG-Y182TAG were made for this work), which contain *gfp* gene (with amber mutation at codon 39 or, 39 and 182), and plasmid pEVOL/*p*AzF (Group Schultz, The Scripps Research Institute, USA) which contain *M. jannaschii* tyrosyl-RS/ tRNA$_{CUA}^{Tyr}$ gene were cotransformed into *E.coli* BL21 (DE3). Cells were amplified in 2xYT that contained ampicillin (50 mg L$^{-1}$) and chloramphenicol (34 mg L$^{-1}$) at 37°C. Protein expression was induced at an optical density of 0.8-1.0 at 600 nm by addition of Arabinose (0.02%) and isopropyl β-D-1-thiogalactopyranoside (1 mM), *p*-azidophenylalanin (*p*AzF) 2 mM (in case of one amber codon) or 4 mM (in case oft two amber codons) were added. After induction, cells were grown at 30°C for overnight. Cells were harvested by centrifugation before lysis by sonication using PBS buffer (pH 8). GFP-Y39*p*AzF or GFP-Y39*p*AzF-Y182*p*AzF were purified by virtue of the presence of a C-terminal hexahistinine residue by using PerfectPro Ni-NTA Agarose (5 PRIME) according to the manufacturers instruction. The purified proteins were determined with SDS-PAGE (Figure S-2).



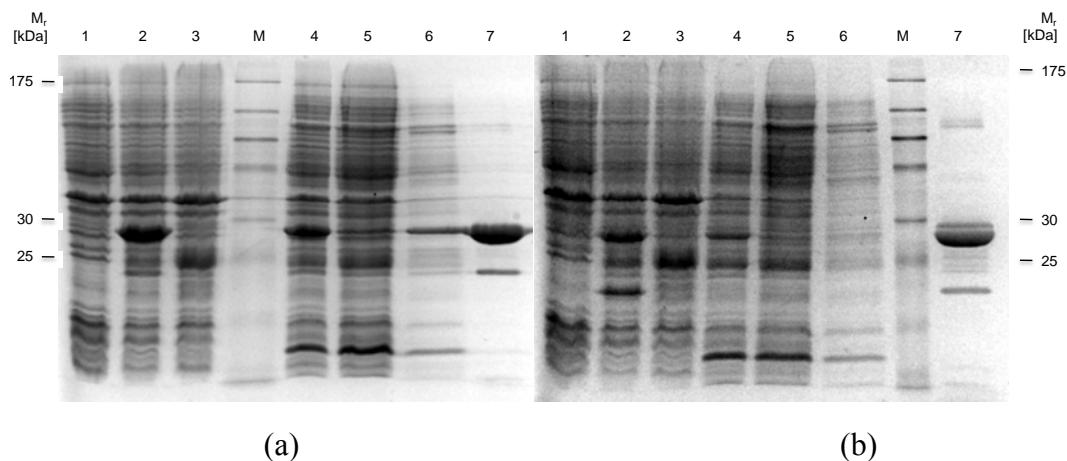(a)                                                    (b)

**Figure S-2**: SDS-PAGE analysis of the purification-pathway. (a) show purification of N₃-GFP(39) and (b) show purification of N₃-GFP-N₃(39,182). Lane M: prestained protein marker, 7-175 kDa; lane 1: no-induced cell expression; lane 2: induced cell expression by presence of *p*AzF; lane 3: induced cell expression by absence of *p*AzF; lane 4: cytosolic

proteins after sonication and centrifugation; lane 5: flow-through fraction; lane 6: wash fraction; lane 7: purified mutant GFP fraction.

The modified GFP's, $N_3$-GFP(39) and $N_3$-GFP-$N_3$(39,182), were characterized with ESI-MS (Table S-1). The Proteins were firstly enzymatically digested into small peptide fragments. The peptide fragment (aminoacids 27-41), which contain the first incorporated $p$AzF at position 39 was detected in both samples. The peptide fragment, which contain the second incorporated $p$AzF at position 182 could not be detected. Nevertheless, an expression test showed the evidences: 1) no fulllength GFP protein was producible by absence of $p$AzF; 2) a truncated mutant $N_3$-GFP(39)-Y182STOP was obtained by presence of $p$AzF. That means, the produced fulllength protein can only be the mutant $N_3$-GFP-$N_3$(39,182).

| Protein | Sequence (26-42) | M (cal.) | M (found) |
|---|---|---|---|
| GFP | K.FSVSGEGEGDATYGK.L | 1502,6525 | 1502,6525 |
| GFP-Y39$p$AzF | K.FSVSGEGEGDATY*GK.L | 1502,6525 | 1527,6620 |
| GFP-Y39$p$AzF-Y182$p$AzF | K.FSVSGEGEGDATY*GK.L | 1502,6525 | 1527,6620 |

**Table S-1**. Estimation of incorporation efficiency analyzed by ESI-MS. Peptide fragment (aminoacid 27-41, FSVSGEGEGDATY*GK, Y* = incorporation of $p$AzF) was obtained.

## Part 2: Preparation of the PDMS-Sylgard 184

Poly(dimethylsiloxane) PDMS Sylgard-184 is prepared by using a mixture composed of a "base" and a "curing agent" in a ratio of 10:1, both purchased from Dow Corning. After mixing the two components together, this mixture is degased for 1h under reduced pressure to remove all bubbles formed during the mixing step. Then, this bubble-free solution is melt into PMMA molds and cured overnight at 90°C at 254 mmHg. PDMS substrates are then unmold and washed, first with a solution of n-heptane and 1-dodecanethiol (0.01 %) for 1 h and then two times with n-heptane for 1h each time. These washing steps are performed in order to remove the remaining unreacted chains and the Pt catalyst from the material. The silicone sheets are then dried in two steps, first, under pressure at room temperature during 1h, and finally in the oven at 60°C overnight. The PDMS substrate so obtained is transparent and display elastic property. Prior to the manipulations, PDMS substrates with a defined size of 2x1cm are prepared and cleaned with water and intensively rinsed with milli-Q water to remove possible dust adsorption.

## Part 3: Chemical modification and characterization of the PDMS surface

*Part 3.1: UVO treatment and characterization*

PDMS substrates are first activated under UV-Ozone for 60mn. Immediately after, the substrates are immersed in a di-isocyanate solution for 1h at room temperature under slow agitation. After this reaction the surfaces are rinsed with acetone then with milli-Q water and immersed in a 1mg.mL$^{-1}$ PEG-amine solution in milli-Q water at room temperature overnight. After rinsing with milli-Q water the samples are kept in a PBS buffer until use.
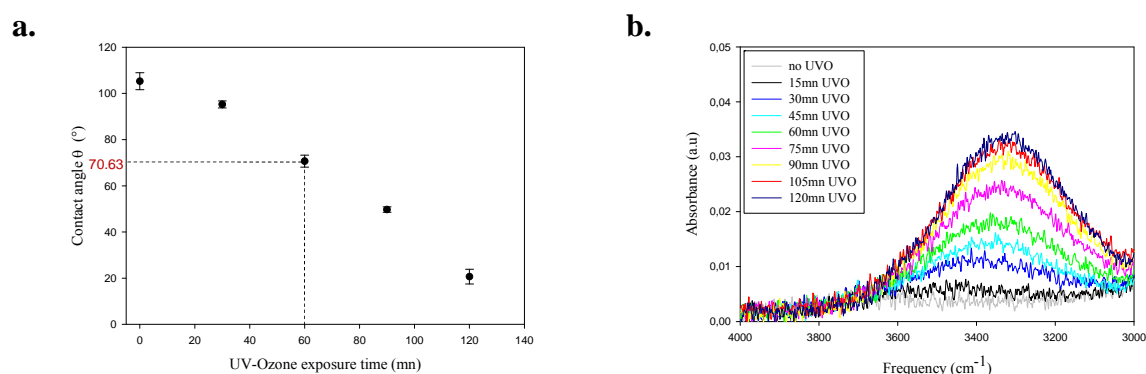
**a.**

**b.**



**Figure S-2:(a)** Contact angle measurements on PDMS substrate exposed to different times of UVO exposition. These measurements were performed with a DIGIDROP-GBX® coupled with a camera by using 6uL pure water droplets. Series of three measures were performed and averaged for each treatment; **(b)** Evolution of the O-H stretching vibration band observed at 3370 cm$^{-1}$, due to silanol group's formation when exposed to increasing UVO exposition time.

*Part 3.2: Introduction of MDI*

In order to modify our PDMS substrate, different bi-functional linkers were used. PDIT and MDI were solved at 2mg.ml$^{-1}$ in anhydrous acetone solution while DIDS is solved at 1mg.mL$^{-1}$ in milli-Q water.

*Part 3.3: Preparation of PEG-brushes silicone surface*

1 Once the PDMS surface functionalized with alkine groups, the reaction between the modified GFP and the alkyne-terminated PEG was performed following an optimized Copper(I)-catalyzed Azide-Alkyne Cycloaddition (CuAAC) protocol for

bioconjugation developed by Finn and coworkers (V. Hong, S. I. Presolski, C. Ma, M. G. Finn, *Angew. Chem. Int. Ed.*, 2009, **48**, 9879). For this reaction, all the reagents were mixed in a specific order to prevent degradation of the proteins. It must be noted that all the compounds except the GFP are solubilized in milli-Q water.

The reagents are added in a 2mL eppendorf tube according to the following order:

- 432µl of a 3.35 µg.mL$^{-1}$ GFP solution in phosphate buffer (PBS, 0.1M, pH 7.4)
- 7.5µL of a premixed solution of CuSO$_4$ / THPTA. 2.5µL of a 20mM CuSO$_4$ solution is mixed to 5µL of a 50mM THPTA solution.
- 25µL of 100mM aminoguanidine solution.
- 25µL of 100mM sodium ascorbate solution.

The solution is then quickly homogeneised and put in contact with functionalized PDMS for one hour. Once the reaction occurred, the surfaces were washed then stored in a phosphate buffer solution (PBS, 0.1M, pH 7.4) until analyze.

# Johan LONGO

Design of biomechanocatalytic surfaces: Modulations of enzymatic
activity through macromolecular conformational changes

**Résumé:** Depuis plusieurs années, une nouvelle génération de matériaux appelés "matériaux intelligents" et définis par leur capacité d'adaptation à leur environement, est intensément développée. Des systèmes sensibles à différents stimuli tels que le pH, la lumière, ou encore une force mécanique, impliquée dans un grand nombre de processus naturels, comme l'adhésion et la prolifération cellulaire, ont été rapportés.

Ce travail de thèse a ainsi été dédié au développement de matériaux mécano-sensibles. Plus précisément de matériaux transformant une contrainte mécanique en un signal chimique, en mimant le processus physique utilisé par la nature, à savoir des changements conformationnels de protéines. Nous avons donc cherché à atteindre ce but en greffant covalemment des protéines ou des enzymes sur un substrat élastomère. Etirer le substrat devant induire des modifications de structure des protéines, conduisant ainsi à des modulations de leurs propriétés.

**Mots-clés:** polyélectrolyte, couche-par-couche, mécano-transduction, surface bioactive, biosenseur, couplage protéique

**Summary:** Since many years, a new generation of materials called « smart materials » and defined by their capacity to adapt to their environment is intensively developed. Systems sensitive to different stimuli such as pH, light or ionic strength have been reported. One of these stimuli can also be a mechanical force which is involved in many reactions in nature such as, cells adhesion and proliferation, tissues growing or even plants developments.

The aim of my thesis was dedicated to the elaboration of mechano-responsive materials. More precisely, materials that transform a stretching constraint into a chemical signal by mimicking the physical processes used by nature, namely protein conformational changes. We planned to achieve this goal by covalently grafting proteins or enzymes onto a stretchable substrate or incorporating them into cross-linked polymer networks. Stretching these materials should induce protein conformational changes leading to modifications of their properties.

**Keywords:** Polyelectrolytes, layer-by-layer (LbL), mechano-transduction, bioactive surface, surface functionalization, biosensor